Iowa State University Bulletin

Joint Publication
Bulletin No. 188
Iowa Engineering Experiment Station
Bulletin No. 17
Iowa Highway Research Board

DYNAMICS OF HIGHWAY BRIDGES

by
D. A. Linger
C. L. Hulsbos

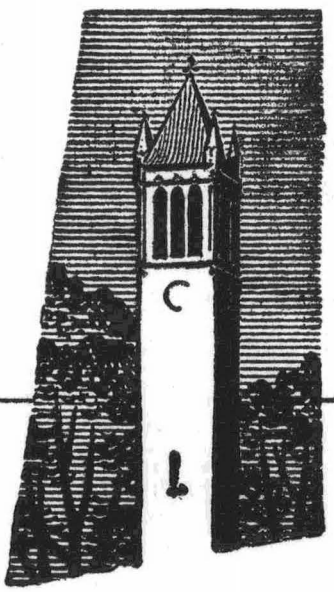

IOWA ENGINEERING EXPERIMENT STATION

Iowa State University
Ames, Iowa

THE IOWA ENGINEERING EXPERIMENT STATION

The Iowa Engineering Experiment Station, first of its kind in the country, was organized in 1904 for the purpose of providing organized research of the character needed to foster and develop the industries of the State.

This research is carried on through experimental programs and investigations in a wide variety of areas and is intended to encourage the development of raw materials and natural resources of the State, to increase the utilities of agricultural products, to aid in the establishment of additional industries within the State, and to solve engineering problems arising in municipal, county, and state administrations. Current research projects include studies in the fields of architectural, agricultural, aero-space, ceramic, chemical, civil, electrical, industrial, mechanical, and nuclear engineering, and in engineering mechanics.

The cooperation and facilities of the Station are offered to industries within and without the State in furtherance of the objective.

For additional information address,

THE IOWA ENGINEERING EXPERIMENT STATION
IOWA STATE UNIVERSITY
of Science and Technology
AMES, IOWA

GEORGE R. TOWN, *Director*
DAVID R. BOYLAN, *Associate Director*
JOHN H. BOLTON, *Editor*

DYNAMICS OF HIGHWAY BRIDGES

by

D. A. Linger, Associate Professor, Civil Engineering,
New Mexico State University

and

C. L. Hulsbos, Professor, Civil Engineering,
Lehigh University

JOINT PUBLICATION

Bulletin No. 188
of the
Iowa Engineering Experiment Station

and

Bulletin No. 17
Iowa Highway Research Board
The Iowa State Highway Commission

Price: $2.00

THE IOWA STATE UNIVERSITY BULLETIN
Ames, Iowa

Vol. LIX | November 2, 1960 | No. 23

Published weekly by Iowa State University of Science and Technology, Ames, Iowa. Entered as second-class matter at the Post Office at Ames, Iowa, under the Act of August 24, 1912.

CONTENTS

Dynamics of Highway Bridges

Part I. Forced Vibration of Continuous Highway Bridges

In the design of highway bridges, the static live load is multiplied by a factor to compensate for the dynamic effect of moving vehicles. This factor, commonly referred to as an impact factor, is intended to provide for the dynamic response of the bridge to moving loads and suddenly applied forces. Many investigators have published research which contradicts the current impact formula [1, 4, 17]. Some investigators feel that the problem of impact deals not only with the increase in over-all static live load but that it is an integral part of a dynamic load distribution problem[23].

The current expanded highway program with the large number of bridge structures required emphasizes the need for investigating some of the dynamic behavior problems which have been generally ignored by highway engineers. These problems generally result from the inability of a designer to predict the dynamic response of a bridge structure. Many different investigations have been made of particular portions of the overall dynamic problem. The results of these varied investigations are inevitably followed by a number of unanswered questions. Ironically, many of the unanswered questions are those which are of immediate concern in the design of highway bridges, and this emphasizes the need for additional research on the problem of impact.

Nature of the Investigation

This investigation is a study of the dynamic magnification of static load, commonly referred to as impact, resulting from the vibrations produced by a vehicle traversing the length of the bridge. More specifically, the purpose of this investigation is to correlate the response of actual continuous highway bridges under the effects of moving vehicles with vibration theory. The problem is then to determine by means of experimental

data, the important parameters affecting bridge vibration and to develop thereby a theoretical correlation of these parameters.

Theoretical. The fundamental problem of vibration is the determination of the natural modes and frequencies of a given vibrating system and the characteristics of the forcing function. Since the natural frequency depends on the restoring force and mass of the system, it is evident then that the size, stiffness, and initial conditions will determine the natural mode of transverse vibratory motion of a beam. The vehicle, which causes the forcing function, is partly a sprung mass and partly an unsprung mass. The actual vehicle is a very complicated vibratory system, but in this study its effect has been simplified as much as possible. The effect of the vehicle which has been assumed to predominate as the forcing function for the vibration of bridges is the cyclical repetition of the axles. This cyclical repetition is defined as the frequency of passage of the axles determined by the ratio of the velocity of the vehicle to the axle spacing.

Experimental. The experimental investigation was designed to determine if the simplications made in the theoretical impact analysis are justified in the application of this theory to actual structures. In this experimental work the impact was determined at midspan of a single span highway bridge and in the outer and inner spans and at the interior supports for three types of continuous four span highway bridges. The bridge structures investigated are as follows:

1. A simple span bridge with six postensioned prestressed concrete beams 100 ft long constructed to act compositely with a reinforced concrete roadway. The roadway is 30 ft wide with a 3 ft safety curb on both sides.

2. A fully continuous structure, 220 ft long with four aluminum stringers constructed to act compositely with a reinforced concrete roadway. The roadway is 30 ft wide with a 3 ft safety curb on both sides.

3. A fully continuous composite structure 240 ft long and very similar to the previous bridge but with four steel wide flange stringers. The reinforced concrete roadway is 28 ft wide with a 3 ft safety curb on both sides.

4. A continuous reinforced concrete roadway 24 ft wide with a 2 ft safety curb on both sides supported by six pretensioned prestressed concrete beams in each of the four spans. The ends of the simple span beams were encased by a cast-in-place diaphragm at the piers. The continuous roadway slab, constructed to act compositely with the stringers, and the pier diaphragm result in a relatively continuous 198.75 ft bridge.

The types of bridges chosen give a wide range of the various parameters involved in vibration. The aluminum stringer bridge is outstanding in that it allows a comparison of the effect of a lighter material with

a smaller elastic modulus in a structure similar in its other aspects to the steel stringer bridge. The continuous pretensioned prestressed concrete bridge resembles the other continuous bridges except that it is only partially continuous in its action.

The mass per unit length is nearly equal for the three continuous bridges. To investigate the effect of a variation in the mass per unit length, the much heavier postensioned prestressed concrete bridge was studied. Also these bridges provide a number of variables in their structural qualities which may affect structural damping. This characteristic, the damping, is important theoretically since it provides an upper limit for the amplitude of forced vibration and might determine the maximum amount of impact for that structure.

DEFINITIONS AND NOTATIONS

Definitions

Impact factor. The impact factor used herein, is the ratio of the difference between the dynamic and static effect of a vehicle to the static effect. It is therefore the fractional increase in the static live load, in this case the vehicle, which is required for the static live load to produce an effect equivalent to that of the dynamically applied live load.

Free vibration. Free vibration is that periodic motion which takes place when an elastic system moves under the action of no external forces or damping. The forces acting on the system during its motion are dependent only on the motion itself.

Natural frequency. The frequency of a free vibration is called the natural frequency of the elastic system. The elastic system used herein is the bridge structure itself.

Loaded natural frequency. The loaded natural frequency is the frequency of free vibration of a system, in this case the loaded bridge structure, when the mass of the loading vehicle is included in the system. This frequency is a function of the position of the vehicle.

Forcing function. The forcing function is an externally applied time-dependent disturbance acting on the structure to produce a time-dependent motion.

Forced vibration. When the vibration results from the application of an external time-dependent disturbance it is called a forced vibration.

Modes of vibration. An elastic system can generally perform vibrations of different modes. The mode of vibration is the shape of the vibrating beam and is classified by the number of nodes subdividing the length of the beam.

Resonance. When an elastic system is acted upon by an external

periodic forcing function having the same frequency as a natural frequency of the system, it is in a state of resonance.

Notations

A, B, C, D, F, H	Constants; evaluated by initial conditions
E	Modulus of elasticity
f	Natural frequency in cycles per unit of time
^{f}L	Loaded natural frequency in cycles per unit of time
f(x, t)	A function of position and time
g	Acceleration due to gravity
I	Moment of inertia
K	Frequency parameter, $\sqrt[4]{p^2m/EI}$
KE	Kinetic energy
$\overline{k}$	Ratio of span stiffnesses, $E_2I_2L_1/E_1I_1L_2$
L	Length of span
M	Mass of the load
m	Mass per unit length of span
N	Number of cycles
n	Any whole number
^{n}b	Damping coefficient
P	Oscillating load effect of a smoothly rolling load
PE	Potential energy
$\overline{p}$	Natural circular frequency of undamped vibration
^{p}L	Natural circular frequency of undamped vibration of the loaded structure
r	Ratio of the horizontal coordinate to the length of the span, x/L
s	Spacing of the vehicle axles
S	Stress
t	Time
T	A function of time
v	Velocity
W	Weight of the load
w	Frequency of the forcing function
x	Horizontal coordinate; a distance measured in the direction of the length of the span
X	A function of the horizontal coordinate
y	Vertical ordinate; deflected displacement due to the static live load
^{y}d	Vertical ordinate; deflected displacement due to the dynamic live load
a	Phase angle
ϕ	(coth KL-cot KL)
ψ	(cosech KL - cosec KL)

PREVIOUS INVESTIGATION

Bridge Vibration

The problem of bridge vibration came of age when heavy loads and high speeds became prevalent in railway transportation. In 1847 a British Royal Committee was appointed to inquire into the conditions to be observed by engineers in the use of iron in structures exposed to violent concussions and vibrations. The committee conducted an extensive series of laboratory tests at the Portsmouth dockyards[23]. A member of the committee, Professor R. Willis, attempted to simplify the analytical work by omitting the inertia of the bridge and considering only the mass of the moving load. This allowed Professor Willis to consider the deflection of the beam to be proportional to the force exerted on the beam by the moving load. The deflection could then be calculated by the equation of static deflection:

$$y = \frac{Rx^2(L-x)^2}{3EIL} \tag{1}$$

where the force R exerted by the moving load is

$$R = P - \frac{P}{g}\frac{d^2y}{dt^2}. \tag{2}$$

The equation of the path of the point of contact of the rolling load with the beam becomes

$$y_d = P\left(1 - \frac{v^2}{g}\frac{d^2y}{dx^2}\right)\left(\frac{x^2(L-x)^2}{3EIL}\right) \tag{3}$$

An exact solution of this equation was obtained by G. G. Stokes[19] by means of a power series. However, an approximate solution can be obtained by putting the equation of static deflection at zero velocity into the right hand side of this equation. Accordingly, the dynamic deflection is

$$y_d = y\left(1 + \frac{v^2}{g}\frac{PL}{3EI}\right) \tag{4}$$

where the additional term in the parentheses is the impact factor and is usually very small. Therefore the dynamic effect in this case is negligible.

The next theoretical approach was made by considering the mass of the bridge and disregarding the mass of the traversing load. This was investigated by A. N. Kryloff[12] in 1905 as the problem of a constant force traversing a single span beam with a constant velocity. In 1922, the problem of a pulsating force was investigated by Professor S. P. Timoshenko[21], and the same result was later reached by a somewhat different method by C. E. Inglis[10].

The first published solution considering the mass of the load and the mass of the bridge was by H. H. Jeffcott in 1929[11]. The general equation was written

$$EI\frac{d^4y}{dx^4} + m\frac{d^2y}{dt^2} = f(x,t) - \frac{f(x,t)}{g}\frac{d^2y'}{dt^2} \tag{5}$$

where y′ is the deflection under the load. An iteration procedure was used to obtain a solution in which it is implied that the effect of the acceleration force is always small compared with that of the applied load. The first approximation is found by disregarding the acceleration term and solving the equation. The next step is to substitute the first solution into the original equation in the previously disregarded term and solve the resulting equation. This process is shown to converge to the exact solution for a particular case. However, the general convergence of the method was not discussed. Since then H. Steuding[18] has shown that in some cases the iteration method used by Jeffcott does not converge.

A very comprehensive study was presented by Professor C. E. Inglis[10] in 1934 entitled "A Mathematical Treatise on the Vibrations in Railway Bridges". This study, supported by experiments, considers the various types of railway loadings on simple span bridges. The traversing load is expressed in the form of a harmonic series. The convergence of the series is discussed and it is found that only the first two or three components have any real practical importance.

Using the differential equation of motion

$$EI\frac{d^4y}{dx^4} + m\frac{d^2y}{dt^2} = f(x,t). \tag{6}$$

Professor Inglis uses the forcing function

$$f(x,t) = \frac{2W}{L}\sum_{i=1}^{i=00}\sin\frac{i\pi vt}{L}\sin\frac{i\pi x}{L} \tag{7}$$

for the case of a moving force of constant speed and magnitude. This function is equivalent to a series of stationary but alternating sinusoidal loads. The solution of the differential equation for this forcing function is

$$y = \frac{2WL^3}{\pi^4 EI}\sum_{i=1}^{i=00}\sin\frac{i\pi x}{L}\left(\frac{\sin\frac{i\pi x}{L}}{i^4-i^2\mu^2} - \frac{\mu}{1}\frac{\sin\frac{i^2\pi^2 at}{L^2}}{i^4-i^2\mu^2}\right) \tag{8}$$

where $a = \sqrt{\frac{EI}{m}}$

and $\mu = \frac{vL}{a\pi}$.

The solution was also found for a moving alternating force and a moving alternating force associated with a moving mass. A solution of the type

$$y = f(t) \sin \frac{\pi x}{L} \tag{9}$$

was used in all cases. Furthermore a harmonic series was used to represent the loads in all the solutions and in some solutions only the primary component of the harmonic series was considered. These simplifications in the analytical work were justified by Inglis [10, p. ix] because ". . . the main object of this treatise is the analysis of the oscillations due to hammer-blows and the evolution of formulae for computing dynamic deflections and the bending-moments and shearing-forces induced thereby". This treatise marks a turning point in the engineering approach to the problem of impact.

In 1937, A. Schallenkamp[16] presented a rigorous solution of the problem of bridge vibration considering the mass of both beam and load. The lateral vibration produced by the external disturbing forces are represented by a series, which for a beam with simply supported ends becomes

$$y(x, t) = \sum_{i=1}^{i=00} q_i(t) \sin \frac{i\pi x}{L}. \tag{10}$$

Using the expressions for potential and kinetic energy together with the equations of Lagrange, Schallenkamp obtained a nonhomogeneous second order linear differential equation in terms of $q_i(t)$ $(i = 1, 2, \ldots)$. The solution of this problem seems to indicate that the contribution of the mass is of relatively little importance in bridge vibration.

In 1955, the problem of bridge vibration was studied by H. S. Suer[20], who assumed that the bridge, again a simple span, could be represented by a single degree of freedom system. He therefore considered only the first mode behavior of the bridge. In addition, the vehicle was treated as a single degree of freedom system for which a solution was obtained in the form of two simultaneous differential equations in terms of the deflection of the bridge and the absolute position of the sprung mass and their derivatives. These equations were then solved by a digital computer. Excellent experimental correlation of this solution was obtained by choosing the initial position and velocity of the mathematical model of the vehicle to agree with the experimental load variation curves of the actual vehicle.

The forced vibration of a continuous two span beam has been investigated by G. Ford[5]. The load traversing the beam was simplified by ne-

glecting its mass. To idealize the assumptions made in the analysis, a model was built which had negligible damping, complete freedom to rotate at the supports, and a uniform cross section. The main purpose of the investigation was to determine the number of natural modes which must be considered in a theoretical study in order to obtain a fair agreement with observed results. The analytical procedures of Timoshenko[21] and Schallenkamp[16] were used and the shape functions were obtained for the various individual modes of vibration. The summation of these components for all possible modes was then considered on the basis of superposition, and the experimental correlation was made.

Many experimental studies have been made in attempting to correlate the dynamic action of a bridge with theory or to try and isolate the most significant parameters in this action. A very important contribution in this respect is the Highway Research Board Bulletin 124. In this bulletin Biggs and Suer[1] have reported some of the experimental tests which provided a basis for the analytical work of Suer[20] described previously. The significance of the various dynamic effects on the vibrations of highway bridges was investigated by Professor C. F. Scheffey[17]. Again the effect of the smoothly rolling mass was found to be negligible. Scheffey [17, p. 29] concluded that ". . . the effects of the oscillating single load was found to become more and more pronounced as the frequency of the span approaches the frequency of the vehicle", and that ". . . the superposition of the effects of a number of axles in phase is a most difficult problem to treat quantitatively on the basis of presently available data". A comparison of the measured deflections and stresses in two continuous plate girder bridges was reported by R. C. Edgerton and G. W. Beecroft[4]. This experimental investigation concluded that the effect of the roughness of the bridge deck greatly influenced the measured impact. J. M. Hayes and J. A. Sbarounis[8] studied the vibration of a three span continuous I-beam highway bridge. The effect of the load on the natural frequency of the bridge and the effect of the composite action of the I-beams are presented in this study. The various vehicles used in this experimental program had quite a varied axle spacing. The recorded amplitude of vibration seemed to correlate very well with this parameter. The correlation was made, assuming the bridge to have a single degree of freedom, with impact as a function of the amplification factor normally associated with forced vibrations. G. M. Foster and L. T. Oehler[6] attempted to correlate the dynamic deflection with the stringer depth to span ratio for a number of simple span roller-beam and plate-girder bridges. The damping coefficients of these bridges and of a continuous plate girder bridge are presented. A review of the analytical and experimental model studies on the highway bridge impact problem at the University of Illinois was presented by T. P. Tung, L. E. Goodman, T. Y. Chen, and N. M. Newmark[22]. The analytical study was made by a numerical step-by-step integration of the equations of motion. The study made by Tung *et al.* includes the effect of the road-

way uneveness and camber and also the unsprung part of the load. The dimensionless parameters which directly influence the calculations were reduced by some simplifications to five.

Weight Parameters:

$$R_1 = \frac{\text{Wt. of unsprung part of vehicle}}{\text{Wt. of bridge}}$$

$$R_2 = \frac{\text{Wt. of sprung part of vehicle}}{\text{Wt. of bridge}}$$

$$R = \frac{\text{Wt. of vehicle}}{\text{Wt. of bridge}}$$

Stiffness Parameter

$$\mu = \frac{\text{Natural frequency of vehicle}}{\text{Natural frequency of bridge}}$$

Speed Parameter

$$a = \frac{\text{Velocity of vehicle}}{2(\text{Length of span})\ (\text{Natural frequency of bridge})}$$

A good correlation was made of the model study results of a single axle vehicle traversing a single span bridge with the analytical solution obtained by a digital computer. A. Hillerborg[9] has shown that using only two of the five dimensionless parameters considered by Tung *et al.*, the third weight parameter R and speed parameter a, the impact of an idealized unsprung single concentrated mass can be predicted by method of Inglis[10]. The theoretical dynamic increment or impact is shown for both moment and deflection, but the experimental correlation is shown only for moment.

It is interesting to note that of the many facets to the problem of bridge vibration, the damping constant of the bridge is nearly always neglected in the simplifications of the analytical solutions. This is done even though the effect of damping will limit the maximum amplitude of stress or impact when the resonance condition is obtained between the forcing function and the structure. For a continuous bridge this resonance condition might be obtainable by a single unsprung mass traveling at a speed in which the application of the load in each span corresponds to the natural frequency of the structure. A condition of resonance is certain to occur when the mass is mounted on springs. This may not occur often in practice because of the difference in natural frequencies, but the situation should not be overlooked. A condition of resonance is also obtainable when the frequency of passage of the axles of a vehicle correspond to the resonant vibratory motion of the structure. This problem does not readily lend itself to analysis by the Inglis[10] method for moving loads of constant

magnitude, and yet the problem is not one of a moving alternating load. This is the problem for which a theoretical analysis has been derived in this investigation and correlated with experimental results.

Impact Factors

In 1859 August Wohler began a series of tests in which steel and iron specimens were subjected to alternating or varying stresses. It was found that failure occurred at a much lower stress than would have been observed for a static test. This emphasizes the problems inherent in dynamic loading. These results started the subject of the fatigue of metals. The first of the fatigue stress formulas was devised to fit the experimental data of Wohler. This rule was given by the formula[7]

$$\text{Failure stress} = S_e \left[1 + \left(\frac{S_u + S_e}{S_e} \right) \frac{\text{Minimum stress in member}}{\text{Maximum stress in member}} \right] \quad (11)$$

where S_e = endurance limit and S_u = static ultimate stress of the material. The endurance limit was considered as the maximum tensile stress for which the material could resist an indefinite number of repetitions. The results of Wohler's tests were used by bridge engineers to formulate the allowable stresses in members subjected to varying stresses. The resulting formulas were intended to reduce the allowable stresses to account for the effect of fatigue. The actual formulas used were derived from this rule by substituting a value for S_e and S_u and incorporating a suitable factor of safety. The formula was intended to reduce the allowable working stress as the stress range over which the material is worked increases. Thus the important part of this type of formula is the controlling variable which is the ratio of the live load stress to dead load stress. Because the reduction of stress using this type of formula involves a trial-and-error procedure in the design of members, a simplification was evolved which applies the controlling variable to the loadings. Therefore instead of reducing the stress to account for the effect of fatigue, the loading was increased. This was done by first simplifying the controlling effect as a percentage based on a ratio of live load stress to the live load plus dead load stress, or

$$\frac{S_L}{S_L + S_D}$$

where S_L is the live load stress and S_D is the dead load stress. This can be rewritten as

$$\frac{1}{1 + S_D/S_L}$$

where the ratio S_D/S_L is considered a function of the length for similar types of structures. This formula, with a value of L/300 for the function

of length, was introduced in 1894 and was used in the United States, Canada, Great Britain, and India to increase the static load and consequently account for the fatigue effect of the variation of stress due to repeated loads. The repeated load provision has since become accepted as a method of providing for live load impact and is called an impact factor. This error in terminology has resulted in abuse and confusion by engineers of a rule intended as a precaution against fatigue failures. In this investigation, the impact factor refers only to the effect of the load and is specifically a function of the amplitude of forced vibration of the bridge.

THEORETICAL INVESTIGATION

Free Vibration

General theory. One important parameter in the response of an elastic system to the action of a forcing function is the ratio of the frequency of the forcing function to the natural frequency of free vibration of the system. Therefore, in this study of the forced vibration of highway bridges, the natural frequencies and their corresponding modes of vibration will be considered first.

The differential equation governing the free vibration of a beam of constant E, I, and m is found by using the elementary theory of mechanics. This equation is

$$EI\frac{\partial^4 y}{\partial x^4} = -\text{force per unit length} \tag{12}$$

where the force in this case results from the inertial forces and is a function of both x and t. Then, using d'Alembert's principle for the loading

$$\text{force per unit length} = m\frac{\partial^2 y}{\partial t^2}. \tag{13}$$

Combining these results, the differential equation of motion for the lateral vibration of a beam becomes

$$EI\frac{\partial^4 y}{\partial x^4} + m\frac{\partial^2 y}{\partial t^2} = 0 \tag{14}$$

which must be satisfied at all points along the beam. The solution of this partial differential equation may be assumed to be of the form

$$y = X(x)T(t). \tag{15}$$

Then equation 14 can be written as

$$\frac{EI}{mX}\frac{d^4X}{dx^4} = \frac{-1}{T}\frac{d^2T}{dt^2}. \tag{16}$$

Since X is only a function of the position and T is only a function of time.

the left hand side of equation 16 can be equal to the right hand side if and only if they are both equal to the same constant. For T to be harmonic, the constant must be positive, say $+p^2$. Therefore the ordinary differential equations in X and T are

$$\frac{d^4X}{dx^4} - K^4X = 0 \tag{17}$$

$$\frac{d^2T}{dt^2} + p^2T = 0 \tag{18}$$

where the frequency parameter $K = 4\sqrt{\frac{mp^2}{EI}}$. The natural frequency of vibration in cycles per unit of time is obtained by dividing the natural circular frequency $p = K^2\sqrt{\frac{EI}{m}}$ by two pi. In terms of the frequency parameter K, the natural frequency is

$$f = \frac{p}{2\pi} = \frac{K^2}{2\pi}\sqrt{\frac{EI}{m}}. \tag{19}$$

The value of K is determined from the solution of the shape function X which in turn depends on the conditions for the span.

The general solutions of equations 17 and 18 are of the form

$$X = F \sin Kx + C \cos Kx + H \sinh Kx + D \cosh Kx \tag{20}$$

$$T = A \sin pt + B \cos pt \tag{21}$$

where C, D, F, H are constants to be determined by the geometrical boundary conditions and A and B are constants to be determined by the initial conditions.

Continuous beams with constant E, I, and m. The method used here in the general theory of the lateral vibration of continuous beams is an extension of the original work of E. R. Darnley[2] on the vibration of rotating shafts.

The determination of the natural frequency of multi-span beams is found by using equations 20 and 21 with the conditions at the ends and at the supported intermediate points. The boundary conditions on X result in a shape function for each span and the initial conditions result in a time function T which is the same for all spans. The conditions at the ends and at the intermediate supports of the continuous beams are the following:

1. At the simply supported end, the deflection and the bending moment are zero; $y = 0$, and $EI\frac{d^2y}{dx^2} = 0$.

2. At an intermediate support the deflection is zero, and the slope and the bending moment are continuous; $y = 0$, and $\frac{dy}{dx}$ and $EI\frac{d^2y}{dx^2}$ are continuous.

Taking the origin of coordinates at the left end of each span, the general equation giving the value of the shape function for the n^{th} span, considering the deflection at the left end equal to zero, will be of the form

$$X_n = C_n(\cos Kx_n - \cosh Kx_n) + F_n \sin Kx_n + H_n \sinh Kx_n . \quad (22)$$

The equations expressing the end condition of a zero deflection and the continuity conditions of slope and moment at the interior supports are respectively,

$$C_n(\cos KL_n - \cosh KL_n) + F_n \sin KL_n + H_n \sinh KL_n = 0 \quad (23)$$

$$-C_n(\sin KL_n + \sinh KL_n) + F_n \cos KL_n + H_n \cosh KL_n = F_{n+1} + H_{n+1} \quad (24)$$

$$C_n(\cos KL_n + \cosh KL_n) + F_n \sin KL_n - H_n \sinh KL_n = 2C_{n+1} \quad (25)$$

Adding equations 23 and 25 results in

$$C_n \cos KL_n + F_n \sin KL_n = C_{n+1} \quad (26)$$

and subtracting these equations results in

$$C_n \cosh KL_n - H_n \sinh KL_n = C_{n+1} . \quad (27)$$

Dividing by the coefficients of F_n and H_n and subtracting equation 26 from equation 27 gives

$$F_n + H_n = C_n(\coth KL_n - \cot KL_n) - C_{n+1}(\operatorname{cosech} KL_n - \operatorname{cosec} KL_n) \quad (28)$$

This operation assumes that sinh KL and sin KL are not zero. This is important in applying the following results, because the fundamental frequency of a simple span or a continuous beam of equal span length is $KL = \pi$, in which case sin KL is zero.

Using the notation:

$$\coth KL_n - \cot KL_n = \phi_n \quad (29)$$

$$\operatorname{cosech} KL_n - \operatorname{cosec} KL_n = \psi_n \quad (30)$$

the following equation is obtained:

$$F_n + H_n = C_n\phi_n - C_{n+1}\psi_n . \quad (31)$$

In a similar manner, the equation for the next intermediate support can be written

$$F_{n+1} + H_{n+1} = C_{n+1}\phi_{n+1} - C_n + 2\psi_{n+1} . \quad (32)$$

Combining equation 32 and equations 26 and 27 in terms of F_n and H_n, respectively, gives

$$-C_n(\sin KL + \sinh KL_n) + \frac{C_{n+1} - C_n \cos KL_n}{\sin KL_n} \cos KL_n$$

$$+ \frac{-C_{n+1} + C_n \cosh KL_n}{\sinh KL_n} \cosh KL_n = C_{n+1}\phi_{n+1} - C_{n+2}\psi_{n+1}. \quad (33)$$

Using the notation given in equations 29 and 30 and simplifying gives the general solution for the differential equation of the shape function for the $_{n+1}$ interior support. This equation can be written as

$$C_n \psi_n - C_{n+1} (\phi_n + \phi_{n+1}) + C_{n+2}\psi_{n+1} = 0 \quad (34)$$

for each intermediate support, thus giving a system of equations for a continuous beam of n spans. The frequency equation may be found, as shown below, by forming a determinant of the coefficients.

Three span bridge. The determinant for the three span continuous bridge is given below and evaluated.

$$\begin{bmatrix} \phi_1 + \phi_2 & \psi_2 \\ \psi_2 & \phi_2 + \phi_3 \end{bmatrix}$$

or

$$= (\phi_1 + \phi_2)(\phi_2 + \phi_3) - \psi_2^2 = 0. \quad (35)$$

For the case of equal end spans, this reduces to

$$\phi_1 + \phi_2 = \pm \psi_2. \quad (36)$$

The first root of this transcendental equation was determined for various ratios of lengths and the results are shown in figure 1. The curves shown in figure 1 can be used to find the value of K, the frequency parameter, for determining the first mode of natural frequency for a three span structure with equal end spans. Caution should be used, however, because extrapolation beyond the limits of the graph could be erroneous. Further, it should be pointed out that the relationship expressed in the figure is not linear as some writers seem to indicate[15]. Moreover, if the ratio of L_1/L_2 becomes less than 0.5, that is, if the middle span length exceeds twice the outer span length, the possibility of this mode of vibration occurring decreases, and instead a higher mode with a nodal point at the middle of the center span probably would occur.

Four span bridges. The continuous bridges studied experimentally have four spans. The application of this theory to four span bridges will be studied for application later to the experimental data. The determinant for a four span bridge is given below and evaluated.

$$\begin{bmatrix} \phi_1 + \phi_2 & \psi_2 & 0 \\ \psi_2 & \phi_2 + \phi_3 & \psi_3 \\ 0 & \psi_3 & \phi_3 + \phi_4 \end{bmatrix} = (\phi_1 + \phi_2)(\phi_2 + \phi_3)(\phi_3 + \phi_4)$$

$$+ \psi_3^2 (\phi_1 + \phi_2) + \psi_2^2 (\phi_3 + \phi_3^4) = 0. \quad (37)$$

Once again considering a symmetrical structure in which the span lengths

are simplified by $L_1 = L_4$ and $L_2 = L_3$ as generally used to help optimize the distribution of bending moments in highway bridges, the frequency equation degenerates to

$$\phi_1 + \phi_2 = 0 \tag{38}$$

and

$$(\phi_1 + \phi_2)\ \phi_2 - \psi_2^2 = 0. \tag{39}$$

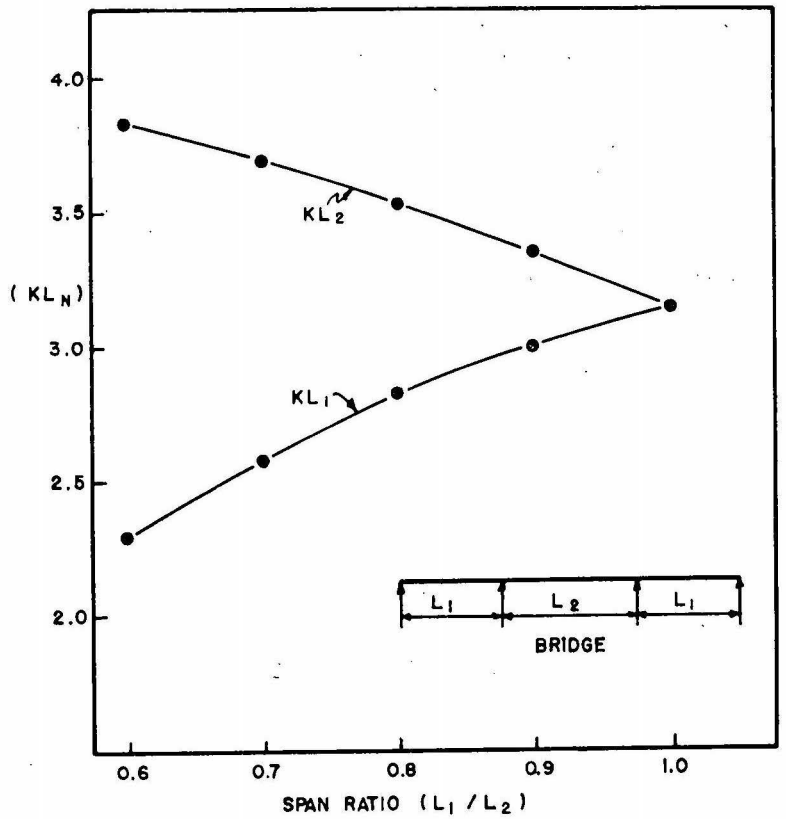

Fig. 1. The effect of the span ratio on the first root of the frequency equation of a three span bridge.

Equation 38 represents a mode of vibration of a four span bridge which is antisymmetrical about the center support, and the roots of this equation give the odd modes of vibration of the structure. Equation 39 represents a mode of vibration of a four span bridge which is symmetrical about the center support, and the roots of this equation give the even modes of vibration of the structure. In general, for an interior span of a continuous bridge, the odd modes correspond to the modes of vibration of a simply supported beam, and the even modes correspond to the modes of vibration of a fixed end beam. For the end spans of the continuous beam, the odd

modes are as before, but the even modes of vibration correspond with the modes of vibration of a beam with one end fixed and the other end simply supported. The first root of equation 38 has been determined for various ratios of lengths (figure 2). By means of figure 2 the value of KL and hence the first mode of natural frequency can be obtained for any ratio of lengths, within the limits of the curve.

The roots of the frequency equations are obtained in the form of KL, where L is the span length. In general, as in figures 1 and 2 which consider only span ratios, it is more convenient to determine the natural frequency by

$$f = \frac{(KL_n)^2}{2\pi L^2_n} \sqrt{\frac{EI}{m}} \qquad (40)$$

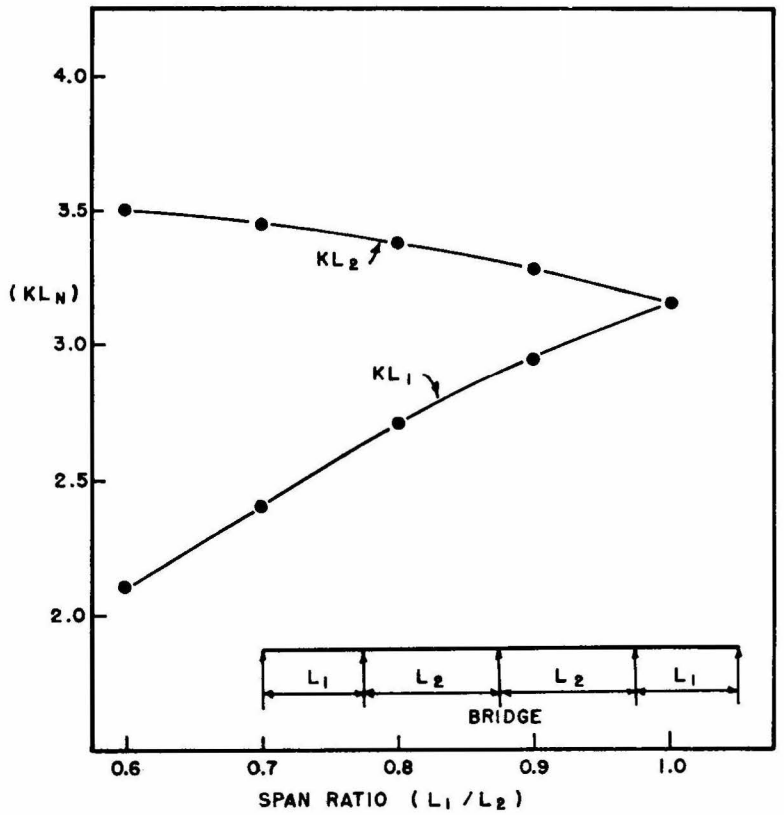

Fig. 2. The effect of the span ratio on the first root of the frequency equation for a four span bridge.

where KL is a root of a frequency equation. The value of KL can be obtained from figures 1 or 2, depending on the number of spans in the structure. The curves shown in each figure give identical values of K, since

each value must be divided by the respective length L. An observation can be made here using the first mode of natural frequency curves in figures 1 and 2. Reducing the ratio of lengths has the effect of reducing the value of K if the sum of the lengths remains the same. Therefore, for any given total length, considering E, I, and m constant, the more irregular the span lengths are, the lower the natural frequency of the structure becomes.

Continuous beams with variable E, I, and m. The previous analytical work has been carried out under the assumption that E, I, and m are constant throughout the length of the bridge. However, this may not be true. In the usual continuous highway bridge structure the section of the longitudinal stringers is increased by the composite action at the middle of the spans and by the cover plates at the interior supports. In this type of highway bridge the moment of inertia of the stringers and cover plates at the interior supports is approximately the same as the moment of inertia of the composite slab and stringer at the middle of the spans. This leads to simplified analysis of live load effects which assumes that the moment of inertia is constant throughout the length of the bridge. This assumption, however, has been shown to be incorrect for the few continuous highway bridge structures comprehensively studied experimentally[15]. Moreover, the variation in the moment of inertia depends on the unknown amount of composite action exhibited by the slab and stringer. For this reason, variations in the moment of inerita along the length of the bridge, due primarily to cover plates at the interior supports, will be disregarded and the moment of inertia at the center of the spans will be used in the analytical work. This simplification has some merit because of the way in which the inertial forces and the fundamental mode of vibration occur.

In the lateral vibration of a beam, the largest inertia forces occur near the center of the span. Moreover, when the continuous bridge is vibrating at its first mode of vibration it has a point of conterflexure at or near the supports. Therefore, the effect of the difference in the moment of inertia, as a measure of the stiffness, at or near the supports would have a very slight effect on the restoring force of the bridge. The variations in the moments of inertia near the supports, therefore, will have a minor effect on the first mode of vibration.

The preceding concerns the variation in the moment of inertia in any particular span. If, however, the variation from span to span is due to a changing slab thickness or changing stringer size, the restoring force in each span might be very much affected. This problem usually results from an abrupt change in the rolled section at a splice or an abrupt change in the size of flange of a built-up plate girder.

This problem will be studied analytically by assuming a constant but different moment of inertia and mass per unit length in each span. The

mathematical model will be set up with the origins at each end and at the center of a symmetrical four span bridge. The problem reduces to the solution of equation 20 for each span and equation 21 for the entire structure. The value of p which yields the natural frequency will be the same for both spans, however the parameter K will differ for each span. Therefore the frequency parameters are written

$$K^4_1 = \frac{m_1 p^2}{E_1 I_1} \tag{41}$$

and

$$K^4_2 = \frac{m_2 p^2}{E_2 I_2}. \tag{42}$$

The general solutions of the shape function equations for each span are

$$X_1 = F_1 \sin K_1 x_1 + C_1 \cos K_1 x_1 + H_1 \sinh K_1 x_1 + D_1 \cosh K_1 x_1 \tag{43}$$

$$X_2 = F_2 \sin K_2 x_2 + C_2 \cos K_2 x_2 + H_2 \sinh K_2 x_2 + D_2 \cosh K_2 x_2 \tag{44}$$

Applying the conditions that the ordinate is zero at the origins, equations 43 and 44 give

$$X_1 = C'_1 \sin K_1 L_1 \left[\frac{\sin K_1 x_1}{\sin K_1 L_1} - \frac{\sinh K_1 x_1}{\sinh K_1 L_1} \right] \tag{45}$$

$$X_2 = C'_2 \sin K_2 L_2 \left[\frac{\sin K_2 x_2}{\sin K_2 L_2} - \frac{\sinh K_2 x_2}{\sinh K_2 L_2} \right] \tag{46}$$

The continuity conditions of bending moment and slope are, $E_1 I_1 \frac{d^2 X_1}{dx^2_1} = E_2 I_2 \frac{d^2 X_2}{dx^2_2}$ and $\frac{dX_2}{dx_2} = \frac{dX_1}{dx_1}$. Applying the equality of bending moments gives

$$\left[\frac{\sin K_1 L_1}{\sin K_1 L_1} + \frac{\sinh K_1 L_1}{\sinh K_1 L_1} \right] = \frac{E_2 I_2 K^2_2 C'_2 \sin K_2 L_2}{E_1 I_1 K^2_1 C'_1 \sin K_1 L_1} \left[\frac{\sin K_2 L_2}{\sin K_2 L_2} + \frac{\sinh K_2 L_2}{\sinh K_2 L_2} \right]$$

or

$$E_1 I_1 K^2_1 C'_1 \sin K_1 L_1 = E_2 I_2 K^2_2 C'_2 \sin K_2 L_2. \tag{47}$$

Then equating the slopes and substituting for C'_2 from equation 47 yields the equation

$$\left[\frac{\cos K_1 L_1}{\sin K_1 L_1} - \frac{\cosh K_1 L_1}{\sinh K_1 L_1} \right] = \frac{-E_1 I_1 K_1}{E_2 I_2 K_2} \left[\frac{\cos K_2 L_2}{\sin K_2 L_2} - \frac{\cosh K_2 L_2}{\sinh K_2 L_2} \right] \tag{48}$$

By reducing and using the previous notation in equations 29 and 30, this equation becomes very similar to the previous frequency equation for a symmetrical four span bridge. This equation becomes

$$\phi_1 = - \frac{E_1 I_1 K_1}{E_2 I_2 K_2} \phi_2 . \tag{49}$$

Substituting the value of K_1 and K_2 from equation 41 and 42 into equation 49, yields

$$\phi_1 = - 4 \sqrt{\frac{m_1 E^3{}_1 I^3{}_1}{m_2 E^3{}_2 I^3{}_2}} \phi_2 . \tag{50}$$

If the span stiffnesses and masses per unit length are the same, the factor

$$4 \sqrt{\frac{m_1 E^3{}_1 I^3{}_1}{m_2 E^3{}_2 I^3{}_2}}$$

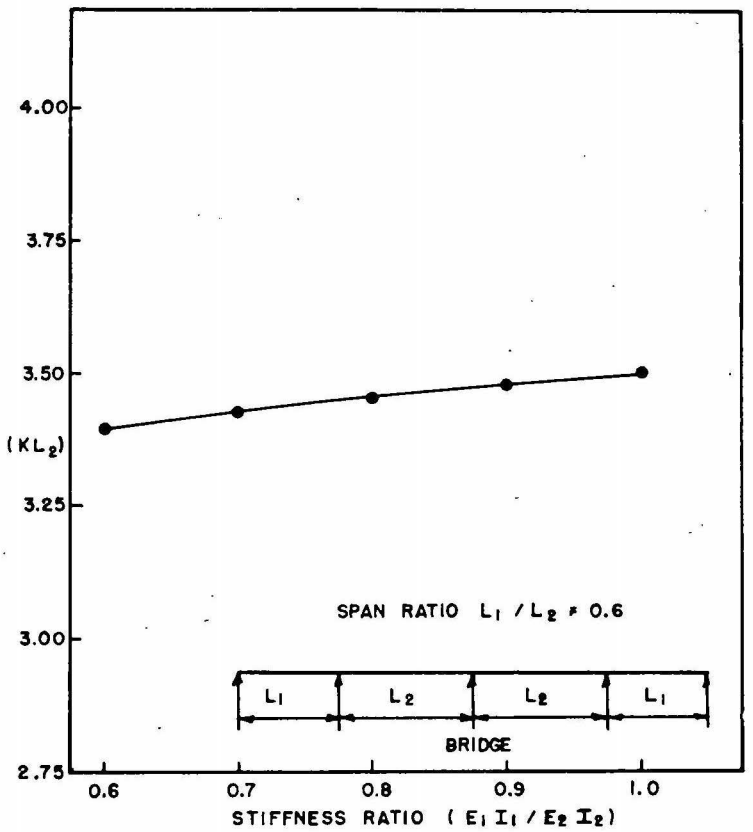

Fig. 3. The effect of span stiffness on the first root of the frequency equation of a four span bridge.

reduces to unity and this equation becomes exactly like the previous frequency equation 38.

$$\phi_1 = \phi_2 . \tag{51}$$

It is seen therefore that the frequency equation derived, which includes the effect of a constant but different E, I, and m in adjacent spans, is applicable only to the odd modes of vibration. This, of course, includes the most important which is the first mode.

Since relatively small differences in the mass per unit length of adjacent spans are usually found in practice and because the mass ratio only affects the factor by the fourth root, this effect will probably be very small. Thus the mass ratio was taken as unity, and the effect on the natural frequency of the different stiffness ratios of the outer and inner spans of a symmetrical four span bridge was obtained. The effect is shown by plotting the frequency parameter against the ratio of stiffness (figure 3).

Live load effect on natural frequency. The natural frequency of vibration varies as the position of the mass of the live load changes in each span. The effect of adding this concentrated mass is a reduction in the natural frequency of the structure by an amount depending on the position of the mass. This change in natural frequency results in a variation in the coincidence of the frequency of the forcing function and the frequency of the bridge.

It is important, therefore, to study this change in frequency by a procedure in which the effect of the position of the vehicle can be easily determined. A method well adapted to this type of study is the energy method. This method is based on the law of conservation of energy which requires that, provided damping is negligible, the sum of the kinetic energy KE and the potential energy PE must be a constant. Thus

$$\underline{\mathrm{KE}} + \mathrm{PE} = \text{constant}. \tag{52}$$

Because of the periodicity of vibratory motion, the displacement will be a maximum when the velocity is zero, and the displacement will be zero when the velocity is a maximum. Since the sum of the energies is a constant, equation 52 can be written

$$\underline{\mathrm{KE}}_{\text{max}} = \underline{\mathrm{PE}}_{\text{max}} \qquad \underline{\mathrm{KE}}_{\text{max}} = \underline{\mathrm{PE}}_{\text{max}} \tag{53}$$

In a flexural vibratory system with simple harmonic motion the maximum potential energy of the system is given by

$$\underline{\mathrm{PE}}_{\text{max}} = (1/2) \int_0^L \mathrm{EI} \left(\frac{d^2X}{dx^2} \right)^2 dx \tag{54}$$

and the maximum kinetic energy of the system is given by

$$\underset{\text{max}}{KE} = \tfrac{1}{2}\, p^2 \int_0^L m(X)^2 dx \tag{55}$$

where the simple harmonic motion is defined by

$$y = X \sin(pt - a). \tag{56}$$

By equating the maximum kinetic and potential energies, the resulting energy equation for the natural frequency is

$$p^2 = \frac{\int_0^L E\, I \left(\frac{d^2X}{dx^2}\right)^2 dx}{\int_0^L m\, X^2\, dx} \tag{57}$$

When the vibratory system includes a number of spans, the kinetic and potential energies are determined for the entire structure. The resulting energy equation for the natural frequency of vibration becomes

$$p^2 = \frac{\int_0^{L_1} E_1 I_1 \left(\frac{d^2X}{dx^2}\right)_1 dx_1 + \int_0^{L_2} E_2 I_2 \left(\frac{d^2X}{dx^2}\right)_2 dx_2 + \ldots}{\int_0^{L_1} m_1 X^2_1\, dx_1 + \int_0^{L_2} m_2 X^2_2\, dx_2 + \ldots}$$

where the subscript denotes the span for which the function applies.

The application of this relationship is made by assuming a configuration of the vibratory system. This configuration is then used to determine the kinetic energy and potential energy of the system and therefore to find the natural frequency of vibration.

The solution obtained by this method will always be higher than the exact solution. That is, as the assumed shape of the vibratory deflection curve approaches the actual shape of the vibratory deflection curve, the value of the natural frequency will decrease as it approaches the exact value. For this reason the energy solution is called an upper bound solution.

The approximate shape of the vibratory deflection curve is often assumed to be the same as the dead load deflection curve. The application of this assumption to an indeterminate structure might be erroneous. This would result because the static effect of the dead load of a continuous beam causes a downward deflection in all the spans. However, vibratory motion, alternating deflections of the spans will occur for the fundamental mode of vibration. If the live load deflection curve is used instead of the dead load curve, the curve becomes different for each position of the load. This complicates the analysis and does not increase the accuracy of the solution, since the effect of the mass of the beams has been omitted. To

overcome the lack of a known vibratory deflection curve, an arbitrary polynominal solution could be used with the degree of the polynominal depending on the conditions available for the determination of the constants. This procedure has been applied to the vibration of symmetrical single span rigid frames[14]. This can also be extended for the effect of a concentrated mass at the center of a symmetrical three span continuous beam.

Using a similar procedure for a symmetrical four span continuous structure, the general polynomial deflection curves, in terms of the shape function X, assumed for the outer and inner spans are respectively,

$$X_1 = L_1(A + Br + Cr^2 + Dr^3 + Fr^4) \tag{59}$$

$$X_2 = L_2(A' + B'r + C'r^2 + D'r^3) \tag{60}$$

where r is taken as the dimensionless ratio x_1/L_1 for the first span and x_2/L_2 for the second span. Then the following conditions are used for the evaluation of the constants. The notation y_1 (1) is the deflection in the first span at r = 1 and a prime indicates a derivative with respect to x.

Deflection conditions:

$$y_1(0) = 0;\ y_1(1) = 0;\ y_2(0) = 0;\quad y_2(1) = 0;\ y_2(2) = 0.$$

Continuity conditions:

$$y'_1(1) = y'_2(0);\ EI_1y''_1\ (1) = EI_2y''_2\ (0);\ EI_1y''_1\ (0) = 0.$$

Symmetry conditions:

$$y'_2(0) = y'_2\ (2).$$

These conditions will restrict the vibratory deflection curve to an alternating movement in adjacent spans which is antisymmetrical about the center of the structure. The symmetry conditions imposed on the interior span could have been

$$EI_2y''_2\ (1) = 0,$$

and a similar result would have been obtained.

The application of the end conditions to the polynomial for the first span yields the following equations:

$y_1(0) = 0$	$A = 0$
$EI_1y''_1\ (0) = 0$	$C = 0$
$y_1(1) = 0$	$B + D + E = 0$

Applying the conditions on the polynomial assumed for the second span gives:

$y_2(0) = 0$	$A' = 0$
$y_2(1) = 0$	$B' + C' + D' = 0$
$y_2(2) = 0$	$2B' + 4C' + 8D' = 0$

The continuity conditions give the following:

$$y'_1(1) = y'_2(0) \qquad B + 3D + 4E = B'$$
$$y'_2(0) = y'_2(2) \qquad 4C' + 12D' = 0$$
$$E_1I_1y''_1(1) = E_2I_2y''_2(0) \qquad 3D + 6E - kC' = 0$$

where

$$k = \frac{E_2I_2L_1}{E_1I_1L_2}.$$

All the coefficients were found in terms of D'. The resulting vibratory deflection equations have the arbitrary amplitude constant D' taken as unity. These equations are

$$X_1 = L_1 \left[-(2+k)r + (4+3k)r^3 - (2k+2)r^4\right] \tag{61}$$

$$X_2 = L_2 \left[2r - 3r^2 + r^3\right] \tag{62}$$

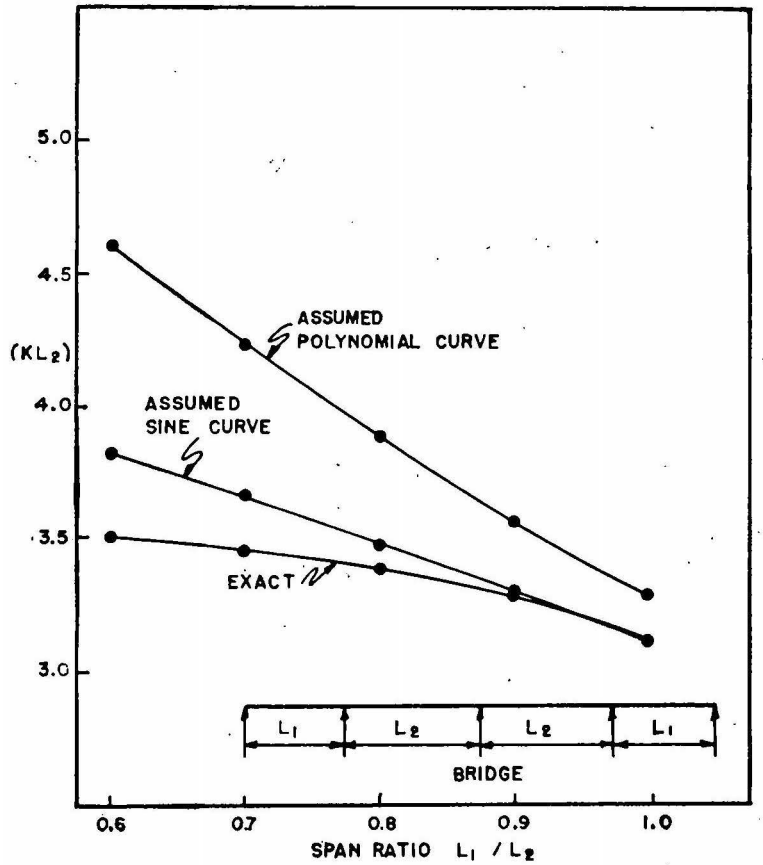

Fig. 4. A comparison of the effect of the span ratio on the first root of the frequency equation by approximate and exact methods.

Substituting these equations and their derivatives into the energy frequency equations gives

$$p^2 = 7560 \frac{E_2 I_2}{m_2 L^4_2} \left[\frac{\frac{1.6}{k} + 1.2 + 0.6k = 1}{\frac{m_1 L^3_1}{m_2 L^3_2} (124 + 95k + 19k^2) + 48} \right] \quad (63)$$

The natural frequency can be obtained by dividing the natural circular frequency p, from equation 63, by two pi. In this operation only the energy of the structure was considered, therefore the solution should approach the natural frequency with no live load.

Comparing the values of natural frequency obtained from equation 63, for different ratios of lengths, with those of the exact method (figure 4) suggests that a better assumption for the deflection curve might be made. Obtaining a better polynomial solution is doubtful because the elimination of the coefficients depends on the number of conditions imposed on the vibrating structure, and a minimum number of conditions were used on the previous polynomials. If a higher degree polynomial is used, the greater number of conditions required for the determination of the coefficients would, in general, restrict the deflection curve even more, thus increasing the error in the solution. For this reason a different type of dynamic deflection curve might not only improve the accuracy of the natural frequency but also provide an insight into some types of forced vibration analysis which require assumptions as to the shape of the deflection curve. The second deflection curve chosen for this case is a sine function. The equations are

$$X_1 = A \sin n_1 x_1 \quad (64)$$

$$X_2 = B \sin n_2 x_2 \quad (65)$$

Taking the origins of coordinates at the left end of each span, the constants are evaluated using the following conditions:

Deflection conditions:

$y_1(0) = 0$; $y_2(0) = 0$; $y_1(L_1) = 0$; $y_2(L_2) = 0$.

Continuity conditions:

$y'_1(L_1) = y'_2(0)$; $E_1 I_1 y''_1(L_1) = E_2 I_2 y''_2(0)$.

The application of these conditions gives the following equations:

$y_1(L_1) = 0$ $\qquad$ $n_1 = \pi / L_1$

$y_2(L_2) = 0$ $\qquad$ $n_2 = \pi / L_2$

$y'_1(L_1) = y'_2(0)$ $\qquad$ $A = -(L_1/L_2) B$.

Using these results the vibratory deflection equations with the amplitude constant B taken as unity become

$$X_1 = -(L_1/L_2)\ \sin\frac{\pi X_1}{L_1} \tag{66}$$

$$X_2 = \sin\frac{\pi X_2}{L_2} \tag{67}$$

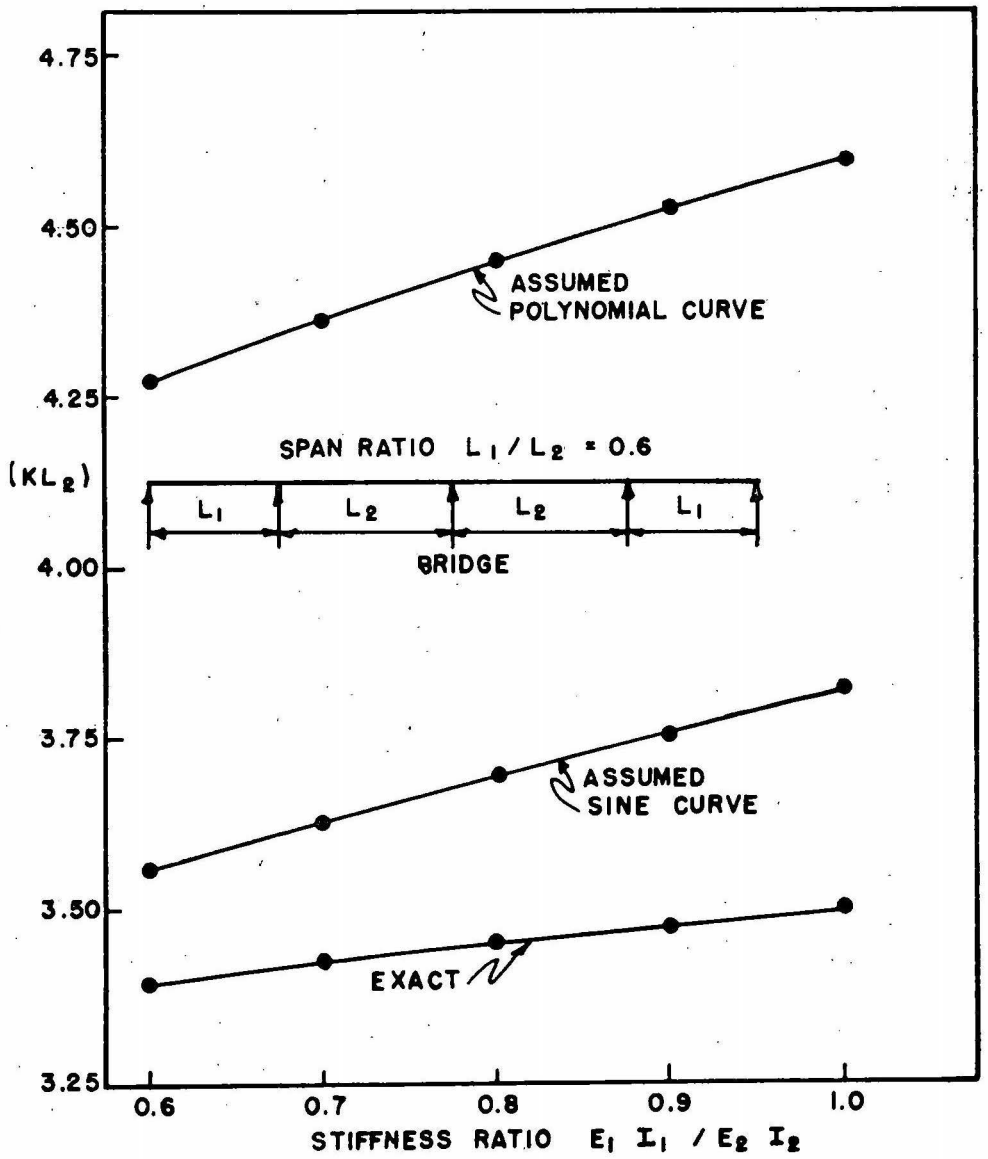

Fig. 5. A comparison of the effect of the stiffness ratio on the first root of the frequency equation by approximate and exact methods.

Substituting these results obtained from an assumed sine curve and their derivatives into the energy equation gives

$$p^2 = \pi^4 \frac{E_2 I_2}{m_2 L_2^4} \left[\frac{\dfrac{E_1 I_1 L_2}{E_2 I_2 L_1} + 1}{\left(\dfrac{L_1}{L_2}\right)^3 \dfrac{m_1}{m_2} + 1} \right] \tag{68}$$

From this equation the natural frequency can be found as previously noted. A comparison of the natural frequency as determined by the exact solution and by both energy methods, the polynomial solution and the sine function, are shown in figure 4 for various ratios of lengths but constant stiffness and mass.

A comparison of the effect of the variation in stiffness from span to span as determined by the exact equation and by two energy equations is shown in figure 5. The ratio of mass was taken as unity.

It has been found that the deflection curves derived from the sine function give good results for the unloaded natural frequency even when the ratio of lengths becomes irregular. The sine curves also have a tendency to give an even better answer when the stiffness of the longer span increases in proportion to the stiffness of the smaller span for the more irregular lengths. This correlation indicates that the assumed sine curve should give better results than the polynomial curve when the live load is placed on the span. This is especially true if the mass of the live load is small compared with the mass of the bridge. In the usual highway bridge this is often true as shown by the bridges tested in this study.

The effect of the live load mass is easily accounted for in the energy frequency equation. The equation was found by equating the maximum potential energy to the maximum kinetic energy. The maximum potential energy is a function only of the deflection curve and therefore the additional live load mass does not change the numerator of the equation. The maximum kinetic energy, however, will change considerably as the maximum velocity of the live load mass changes. The velocity of this mass depends on the position of the mass in the span and on the deflection curve. Thus, for any one deflection curve the denominator of the frequency equation will change, for the addition of live load, by the term

$$M\bar{y}^2$$

where $\bar{y}$ is the deflection under mass M. The frequency solution for the structure including live load mass then has the general form

$$p^2_L = \frac{\int_0^{L_1} E_1 I_1 \frac{d^2X}{dx^2 1}\, dx_1 + \ldots}{M\,\overline{X}^2 + \int_0^{L_1} m_1(X_1^2)\, dx_1 + \ldots} \tag{69}$$

The subscript denotes the span for which the function applies and $\overline{X}$ is a function of the position of the mass M.

Using the vibratory deflection curves obtained from the sine functions, the frequency equations for the mass of the load in the outer and inner spans respectively of a symmetrical four span bridge are

$$P^2_{L_1} = \pi^4 \frac{E_2 I_2}{m_2 L_2^4} \left[\frac{\frac{E_1 I_1 L_2}{E_2 I_2 L_1} + 1}{\frac{m_1}{m_2}\left(\frac{L_1}{L_2}\right)^3 + 1 + \left(\frac{L_1}{L_2}\right)^2 \frac{M}{m_2 L_2} \sin^2 \frac{\pi x_1}{L_1}} \right] \tag{70}$$

and

$$P^2_{L_2} = \pi^4 \frac{E_2 I_2}{m_2 L_2^4} \left[\frac{\frac{E_1 I_1 L_2}{E_2 I_2 L_1} + 1}{\frac{m_1}{m_2}\left(\frac{L_1}{L_2}\right)^3 + 1 + \frac{M}{m_2 L_2} \sin^2 \frac{\pi x_2}{L_2}} \right] \tag{71}$$

It is interesting to note that the form of the energy frequency equation suggests that the effect of a number of live load masses at different positions on the structure can be superimposed by adding the inverse square of the circular frequency of each

$$\frac{1}{p_L^2} = \frac{1}{p_1^2} + \frac{1}{p_2^2} + \frac{1}{p_3^2} + \frac{1}{p_4^2} + \ldots \frac{1}{p_n^2} \tag{72}$$

where p_n^2 is the circular frequency of the n^{th} load. This procedure has a limitation in its accuracy due to the original assumption that the dynamic deflection curve does not change due to the live load. Therefore, there is an increase in error as the amount of live load increases.

The reduction in natural frequency for use in the correlation of the experimental data was determined by first computing the ratio of the loaded frequency to the unloaded natural frequency using the energy frequency equations 68, 70 and 71. This gives the equation

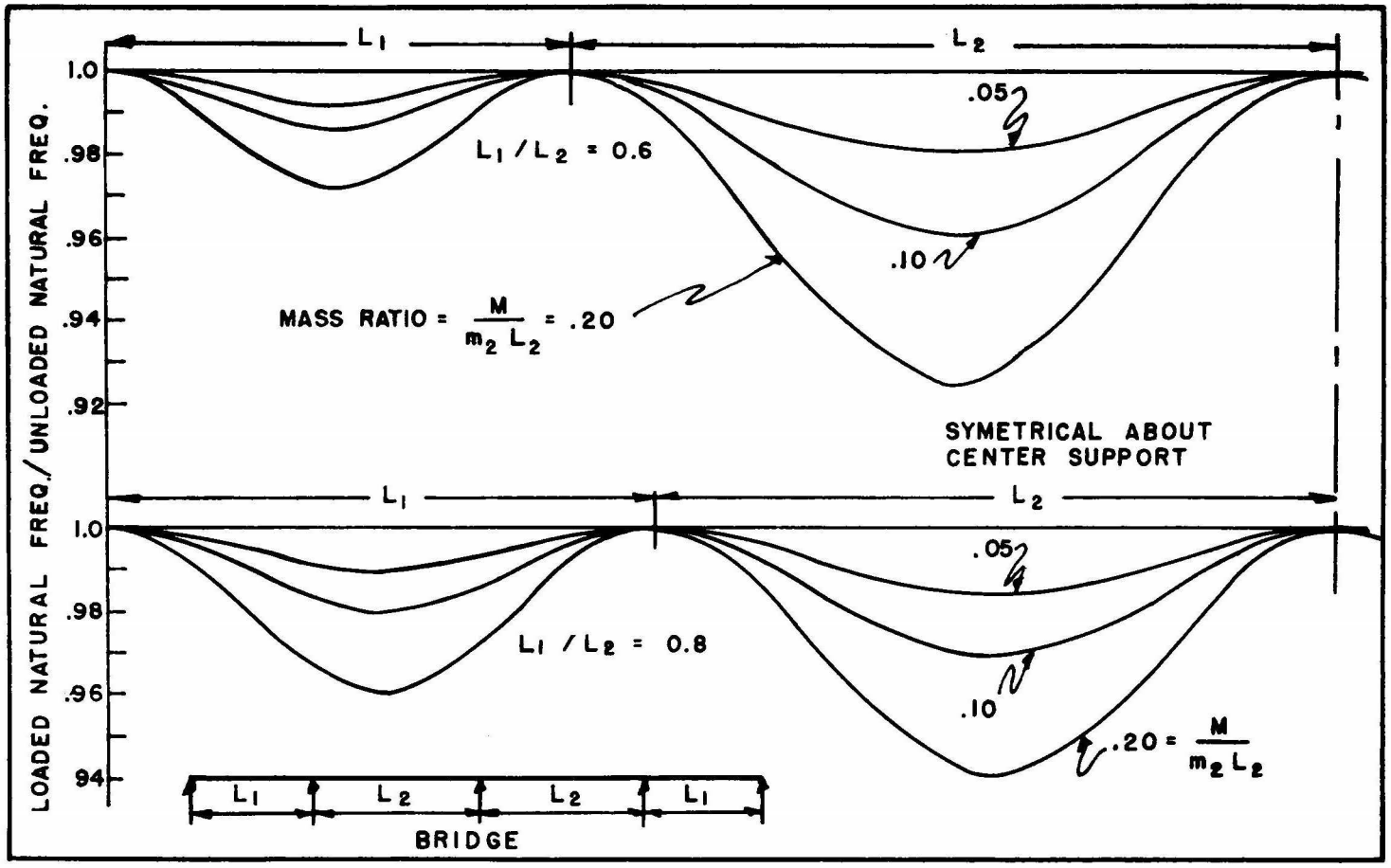

Fig. 6. Influence of a concentrated mass M on the natural frequency of a four span bridge.

$$\frac{f_L}{f} = \frac{p_L}{p} = \sqrt{\frac{\left(\frac{L_1}{L_2}\right)^3 \frac{m_1}{m_2} + 1}{\frac{m_1}{m_2}\left(\frac{L_1}{L_2}\right)^3 + 1 + \left(\frac{L_1}{L_2}\right)^2 \frac{M}{m_2 L_2} \sin^2 \frac{\pi x_1}{L_1}}} \tag{73}$$

for the mass of the load in the outer span of a four span continuous highway bridge in which the outer and inner spans are equal respectively, that is $L_1 = L_4$ and $L_2 = L_3$. This also gives the equation

$$\frac{f_L}{f} = \frac{p_L}{p} = \sqrt{\frac{\left(\frac{L_1}{L_2}\right)^3 \frac{m_1}{m_2} + 1}{\frac{m_1}{m_2}\left(\frac{L_1}{L_2}\right)^3 + 1 + \frac{M}{m_2 L_2} \sin^2 \frac{\pi x_2}{L_2}}} \tag{74}$$

for the mass of the load in the inner span of the same symmetrical four span continuous highway bridge, the ratio thus found was then applied to the theoretical natural frequency as determined by the exact solution previously derived. The results of this procedure make the best use of the two methods of vibration analysis presented herein.

For the simple span the substitution of an assumed sine deflection curve into the energy frequency equation and the subsequent ratio of the reduction in the natural frequency is used by Inglis[10] and has the form

$$\frac{f_L}{f} = \frac{p_L}{p} = \sqrt{\frac{1}{1 + \frac{2M}{mL} \sin^2 \frac{\pi x}{L}}} \tag{75}$$

Equations 73 and 74 were used to determine the change in the natural frequency of continuous bridges with different span ratios for various positions of the live load mass, and this reduction in frequency is shown in figure 6. The mass ratio shown is the ratio of live load mass to the dead load mass of the entire inner span.

Forced Vibration

Assumptions and discussion. The analytical solution of the equations of motion for the forced vibration of an elastic system depends on the type of forcing function causing the motion. The assumptions made concerning the type of forcing function representing a moving vehicle on a highway bridge generally result in the use of a moving force or mass freely mounted on springs or harmonically oscillating as it traverses the bridge. Usually a single load with one degree of freedom is used when the force or mass is spring mounted. A more complicated loading assumption is made by

considering both the sprung mass, made up of the vehicle body, and the unsprung mass of the axles and springs.

A vehicle is a complex system made up of a chassis suspended on springs and connected to either the front or rear axles, which are mounted on balloon tires. The compressibility of the balloon tires might allow the axles to be considered as sprung masses also. Thus a vehicle can be considered as three separate masses, each with six degrees of freedom. This system could be simplified by using only the most important motions, but the primary quantities governing the simplest of motions can vary considerably from vehicle to vehicle. Some investigators have shown that the random vibration of the vehicle often coincides with the harmonic vibration of the bridges, even though this vibration is not a resonant frequency of the vehicle[15]. Other researchers indicate that the force required to initiate springing action in the vehicle is great enough that only the springing of the tires needs to be considered over most of the span[17]. A very complete analytical study has been made using a computer for a step-by-step solution of the equations of motion for a series of smoothly rolling loads on simple spans[13]. This research added a great deal of qualitative data for interpreting the effect of the various parameters on bridge vibration. It was found that at certain speeds the effect of the individual axles would accumulate and at other speeds would interfere with each other, thus varying considerably the impact caused by the group of axles. These results mark a significant change in the concept of highway bridge impact. A very significant change, however, is in the assumptions required for the analytical solution of this problem. The solutions of Inglis[10], for example, which found the effect of the smoothly rolling forces and masses to be insignificantly small, considered the loading as a sine series in which usually only the first term is used. It would be difficult to study the effect of two relatively closely spaced axle loads when each load is represented mathematically by a sine curve extended over the length of the span. Thus the primary problem in this analytical study is the determination of a forcing function which will form a series of impulses representing the repetitive action of a series of axles rolling across a bridge.

The two significant parameters of this forcing function are the magnitude and the frequency of the forcing function. The magnitude of the forcing function is assumed herein to be a function of the oscillation in the structure resulting from the response of the structure to a smoothly rolling load of constant magnitude. The frequency of the forcing function is assumed to be the frequency of repetition of the axles of a vehicle traversing the bridge.

The analytical work of Inglis, although it does not touch on this problem, does offer a great deal of insight into a solution.

General theory

Inglis incorporates the use of a Fourier sine series for the representation of the various loadings. A concentrated load W at section x=a, is expressed in the form

$$\frac{2W}{L} \sum_{i=1}^{i=\infty} \sin \frac{i\pi a}{L} \sin \frac{i\pi x}{L} \tag{76}$$

The deflection resulting from this load function provides a basis for some simplification of this load function. The static deflection can be determined by using elementary mechanics. The deflection curve must satisfy the relationship

$$EI \frac{d^4y}{dx^4} = \frac{2W}{L} \sum_{i=1}^{i=\infty} \sin \frac{i\pi a}{L} \sin \frac{i\pi x}{L} \tag{77}$$

When the load is near the center of a simple span, the static center line deflection is obtained approximately by using only the first harmonic component of the load series. The resulting static deflection is

$$y = \frac{2WL^3}{\pi^4 EI} \; 1 \; = \frac{2WL^3}{\pi^4 EI} = \frac{WL^3}{48.7EI} \tag{78}$$

Therefore, by using only the first harmonic component of the 1°ad, a very close approximation to the exact values of $WL^3/48EI$ is obtained. Thus, only the first harmonic component was used by Inglis for most of the solution.

The above calculation for deflection was made with the assumption that the elastic curve of the beam is free to rotate at the support, which is the elastic curve of a simply supported beam. The exactness of this solution for deflection is a result of the small difference between the simple beam deflection curve for a concentrated load and the deflection resulting from the first component of the harmonic representation of load, a sine curve. Therefore the type of solution which results in a sine deflection curve is applicable to a simply supported beam, but it requires some justification before it can be applied to a continuous beam. However, to do this it is only necessary to consider the computations for natural frequency by the energy method. It has been shown in figure 5 that the assumed sine deflection curve gives a very good approximation in determining the first mode natural frequency. This indicates the closeness of the sine curve to

the exact theoretical first mode of vibration curve of a continuous beam. In addition, the reduction in natural frequency resulting from the mass of the loading vehicle on the bridge, figure 6, seems to agree with the experimental reduction. Therefore, the type of first mode does not change appreciably due to the live load mass. Therefore, in the analysis of the forced vibration, the shape function X will be represented by a sinusoidal curve. The solution of the partial differential equations of motion may then be taken as

$$y = T(t) \sin \frac{\pi x}{L}. \tag{79}$$

To represent a moving load, the distance that the load travels is taken as vt, where v is the velocity of the load and t is the time required for the load to traverse the distance a. The series representing the moving load of constant magnitude then takes the form

$$\frac{2W}{L} \sum_{i=1}^{i=} \sin \frac{i\pi vt}{L} \sin \frac{i\pi x}{L} \tag{80}$$

A more revealing form of this series can be made by making the substitution $z = \frac{v}{2L}$, resulting in

$$\frac{2W}{L} \sum_{i=1}^{i=\infty} \sin i2\pi zt \sin \frac{i\pi x}{L}. \tag{81}$$

This form of the series indicates that the effect of a moving concentrated load is equivalent to a series of stationary but alternating loads whose forcing frequency is z.

Moving loads of constant magnitude

The oscillations produced in a beam by a moving load of constant magnitude is found by solving the differential equation of motion, equation 6, with the proper forcing function equation 7 or 81. The solution of this problem by Inglis[10, p. 27] is shown in equation 8. Using only the primary component of the load function, this equation becomes

$$y_d = \frac{2WL^3}{\pi^4 EI}\left[\frac{\sin\frac{\pi x}{L}}{1-\left(\frac{v}{2Lf}\right)^2}\left(\sin 2\pi zt - \left(\frac{v}{2Lf}\right)\sin 2\pi ft\right)\right] \tag{82}$$

Due to the practical limitations of speed, the term $\frac{v}{2Lf}$ in the denominator is negligible in comparison with unity and can be ignored. Therefore the equation for this motion can be written

$$y_d = \frac{2WL^3}{\pi^4 EI}\left[\sin\frac{\pi x}{L}\sin 2\pi zt - \left(\frac{v}{2Lf}\right)\sin 2\pi ft \sin\frac{\pi x}{L}\right] \tag{83}$$

Using the first term in the parenthesis with z replaced by its value of v/2L and the distance vt taken as L/2, the static deflection is obtained. The second term then is the amplitude of oscillation of the beam which is superimposed on the static deflection curve, and can be written

$$\frac{2WL^3}{\pi^4 EI}\left(\frac{v}{2Lf}\right)\sin 2\pi ft \sin\frac{\pi x}{L} \tag{84}$$

The maximum variation or oscillation in the beam deflection is therefore

$$\frac{y_d - y}{y} = \frac{v}{2Lf} \tag{85}$$

The right hand side of equation 85 is equivalent to a variation in a stationary load W of

$$\frac{P}{W} \tag{86}$$

The use of this equivalence allows the repetitive motion of a series of axles to be represented by a stationary load whose frequency of application is determined by the repetition of the axles and whose magnitude of oscillation is v/2Lf or P/W.

Repetition of axles

The frequency of the impulses representing the passage of axles is given by

$$w = \frac{v}{s} \tag{87}$$

where s is the spacing of the axles and v is the velocity of the vehicle. The

harmonic oscillation which is assumed to represent the repetition of axles is then taken as

$$P \sin 2\pi wt. \tag{88}$$

The differential equation of motion used in the forced vibration analysis will include the effect of damping. The damping effect will be taken as a resistance to the transverse vibration per unit length of bridge equal to

$$4\pi n_b m \frac{dy}{dt}.$$

The differential equation of motion including damping is then expressed by

$$EI \frac{\partial^4 y}{\partial x^4} + 4\pi n_b m \frac{\partial y}{\partial t} + m \frac{\partial^2 y}{\partial t^2} = f(x, t) \tag{89}$$

The harmonic forcing function $f(x, t)$ for the repetition of axle impulses is represented by the first harmonic component of the load series and includes the effect of the mass of the load. The forcing function is written

$$f(x, t) = \frac{2}{L}\left[P \sin 2\pi wt - M \frac{\partial^2 \bar{y}}{\partial t^2} \right] \sin \frac{\pi x}{L} \tag{90}$$

where $\bar{y}$ is the vertical deflection of the mass. As discussed previously, the solution of this partial differential equation may be taken, as shown in equation 79, as

$$y = T(t) \sin \frac{\pi x}{L}. \tag{91}$$

Moreover, since the loading is equivalent to a stationary but harmonically alternating load, the vertical deflection of the mass is considered only a function of time, therefore

$$\bar{y} = T(t). \tag{92}$$

Applying equations 91 and 92 to the partial differential equation of motion for this case and rearranging, results in the equation

$$\frac{EIL\pi^4}{L^4} T + 4\pi n_b Lm \frac{dT}{dt} + (Lm + 2M)\frac{d^2T}{dt^2} = 2P \sin 2\pi wt. \tag{93}$$

Further rearranging of this equation yields

$$\frac{d^2T}{dt^2} + 4\pi n_b \left[\frac{1}{1 + \frac{2M}{mL}} \right] \frac{dT}{dt} + \frac{EI\pi^4}{mL^4} \left[\frac{1}{1 + \frac{2M}{mL}} \right] T =$$

$$\frac{2P}{mL + 2M} \sin 2\pi wt \tag{94}$$

where, from equation 75

$$\left[\frac{1}{1 + \frac{2M}{mL}}\right] = \frac{f_L^2}{f^2} \tag{95a}$$

and from the natural frequency equation for a simply supported beam

$$\frac{EI\pi^4}{mL^4} = p^2 = 4\pi^2 f^2. \tag{95b}$$

Substituting equations 95a and 95b into equation 94 gives

$$\frac{d^2T}{dt^2} + 4\pi n_b \left(\frac{f_L^2}{f^2}\right) \frac{dT}{dt} + 4\pi^2 f_L^2 T = \frac{2P}{mL + 2M} \sin 2\pi wt. \tag{95c}$$

The particular solution for T(t) in this differential equation will be of the general form

$$T_p = A \sin 2\pi wt + B \cos 2\pi wt \tag{96}$$

where T_p is the particular solution for T(t). Substitution of this general solution into equation 95c and equating the coefficients of the sine and cosine terms on both sides of the equation gives

$$\left[4\pi^2 f_L^2 - 4\pi^2 w^2\right] A - \left[8\pi^2 w n_b \frac{f_L^2}{f^2}\right] B = \frac{2P}{mL + 2M} \tag{97}$$

$$\left[8\pi^2 n_b w \frac{f_L^2}{f^2}\right] A + \left[4\pi^2 f_L^2 - 4\pi^2 f_L^2 - 4\pi^2 w^2\right] B = 0. \tag{98}$$

Solving these two equations for A and B gives

$$A = \frac{2P}{(mL + 2M)\, 4\pi^2 f_L^2} \frac{\left(1 - \frac{w^2}{f_L^2}\right)}{\left(1 - \frac{w^2}{f_L^2}\right)^2 + \left(\frac{4n_b^2 w^2}{f^4}\right)} \tag{99}$$

$$B = \frac{2P}{(mL + 2M)\, 4\pi^2 f_L^2} \frac{\left(\frac{2n_b w}{f^2}\right)}{\left(1 - \frac{w^2}{f_L^2}\right)^2 + \left(\frac{4n_b^2 w^2}{f^4}\right)}. \tag{100}$$

It is convenient to reduce this particular solution by using the trigonometric identity.

$$A \sin 2\pi wt + B \cos 2\pi wt = D \sin(2\pi wt - \alpha) \tag{101}$$

where

$$D = \sqrt{A^2 + B^2} \text{ and } \tan \alpha = \frac{B}{A}.$$

Thus the particular solution can be written, by using equations 79, 99, 100, and 101, as the following

$$y_p = \frac{2P}{(mL + 2M)\ 4\pi^2 f_L^2} \frac{\sin(2\pi wt - \alpha) \sin \frac{\pi x}{L}}{\sqrt{\left(1 + \frac{w^2}{f_L^2}\right)^2 + \left(\frac{2n_b w^2}{f^2}\right)^2}} \tag{102}$$

where y_p is the particular solution of equation 89. The first term on the right hand side of equation 102 can be expressed in the following form with the help of equations 95a and 95b

$$\frac{mL\ 2P}{(mL + 2M)\ 4\pi^2 f_L^2\ mL} = \frac{2P}{4\pi^2 mLf^2} \frac{W}{W} = \frac{2WL^3}{\pi 4EI} \frac{P}{W} \tag{103}$$

Writing equation 102 in terms of the static deflection in equation 103 resulting from a stationary load W, gives

$$y_p = \frac{2WL^3}{\pi^4 EI} \frac{P}{W} \frac{\sin(2\pi wt - \alpha) \sin \frac{\pi x}{L}}{\sqrt{\left(1 + \frac{w^2}{f_L^2}\right)^2 + \left(\frac{2n_b w^2}{f^2}\right)^2}}. \tag{104}$$

This equation represents the forced vibration or the particular solution of equation 89 with the forcing function defined by equation 90. The complete solution of the equation of motion, equation 89, is the sum of a complementary solution and the particular solution. The general form of the complementary solution is a free oscillation of the type

$$y_c = e^{-2\pi n_b \left[f_L^2/f^2 \right] t} \left[A \sin 2\pi f_{L_b} t + B \cos 2\pi f_{L_b} t \right] \sin \frac{\pi x}{L} \tag{105}$$

where f_{L_b} is the loaded damped frequency and is equal to

$$f_{L_b} = \sqrt{1 - \left(\frac{n_b f_L^2}{f^2}\right)}$$

Using the conditions that $y = 0$ when $t = 0$ and $dy/dt = 0$ when $t = 0$, the complementary solution can be evaluated. The complete solution, the complementary plus the particular, is given by

$$y_p + y_c = \frac{2WL^3}{\pi^4 EI}\,\frac{P}{W}\left[\frac{\sin(2\pi wt - \alpha) - e^{-q}(w/f_L)\,\sin 2\pi f_{L_b} t}{\sqrt{\left(1 - \frac{w^2}{f_L^2}\right)^2 + \left(\frac{2n_b w}{f^2}\right)^2}}\right]\sin\left(\frac{\pi x}{L}\right) \tag{106}$$

where $q = 2\pi n_b \left(\frac{f_L^2}{f^2}\right) t$. The first and second terms in the numerator of the brackets represent the particular and the complementary solutions respectively. The complementary solution varies as a function of the damping. Consequently it dies out as the load passes along the bridge, the ratio of successive amplitudes of oscillation being

$$e^{-2\pi n_b\,(f_L^2/f^3)}.$$

By the time the load has reached the center of the bridge, the frequency of the bridge vibration corresponds with the frequency of the particular solution. The complementary solution has then been significantly reduced so that its effect will be disregarded. Therefore the maximum amplitude of this vibration occurs near the center of the span, when the term $\left[\sin(2\pi wt - \alpha)\,\sin\frac{\pi x}{L}\right]$ is a maximum, and is defined by

$$\left[\frac{2WL^3}{\pi^4 EI}\right]\frac{P/W}{\sqrt{\left(1 - \frac{w^2}{f_L^2}\right)^2 + \left(\frac{2n_b w}{f^2}\right)^2}}. \tag{107}$$

Since this deflection occurs as a result of the oscillations of a stationary live load W, it is in effect the dynamic variation of the elastic curve about the static deflection position of this curve. Therefore, the impact factor, as previously defined, for the maximum amplitude of vibration is the ratio of this amplitude to the static deflection. By replacing the ratio P/W by the oscillating load effect v/2Lf, this impact factor can be written

$$\frac{v/2Lf}{\sqrt{\left(1 - \frac{w^2}{f_L^2}\right)^2 + \left(\frac{2n_b w}{f^2}\right)^2}} \tag{108}$$

All of the simplifications used to arrive at this result are based on the assumption that the dynamic deflection curve of a continuous bridge is sinusoidal. Therefore in applying this to a continuous structure, the length

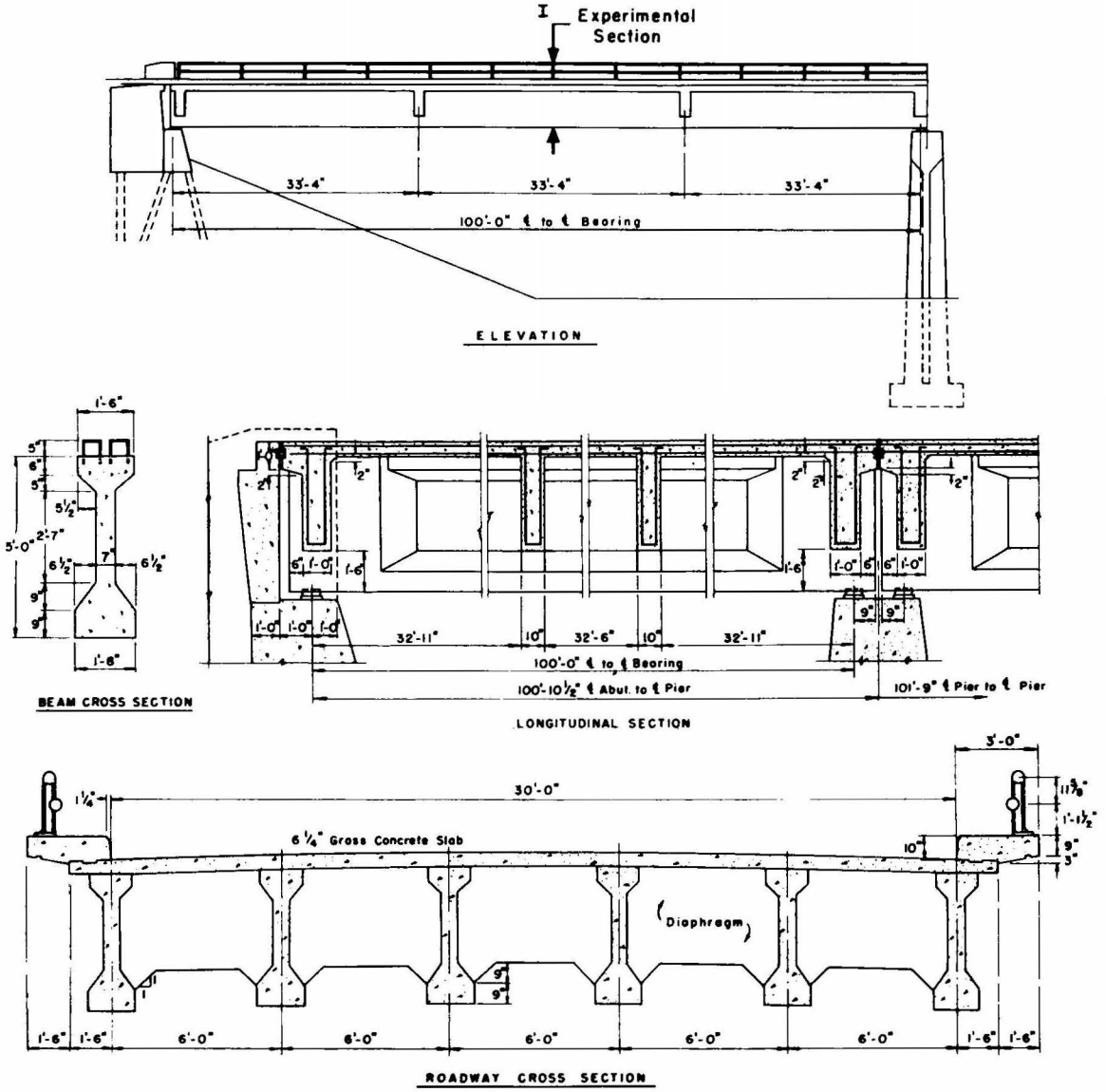

Fig. 7. Details of simple span prestressed concrete bridge.

L in the oscillating load term will be taken as the length of a simple span bridge with a natural frequency equal to the natural frequency of the continuous bridge. Thus, the equivalent length L_{eq} is

$$L_{eq} = \frac{\bar{L}_2}{(KL_2)} \pi. \qquad (109)$$

The impact factor (equation 108) closely resembles the amplification factor normally associated with forced vibrations. The ratio v/2Lf in the

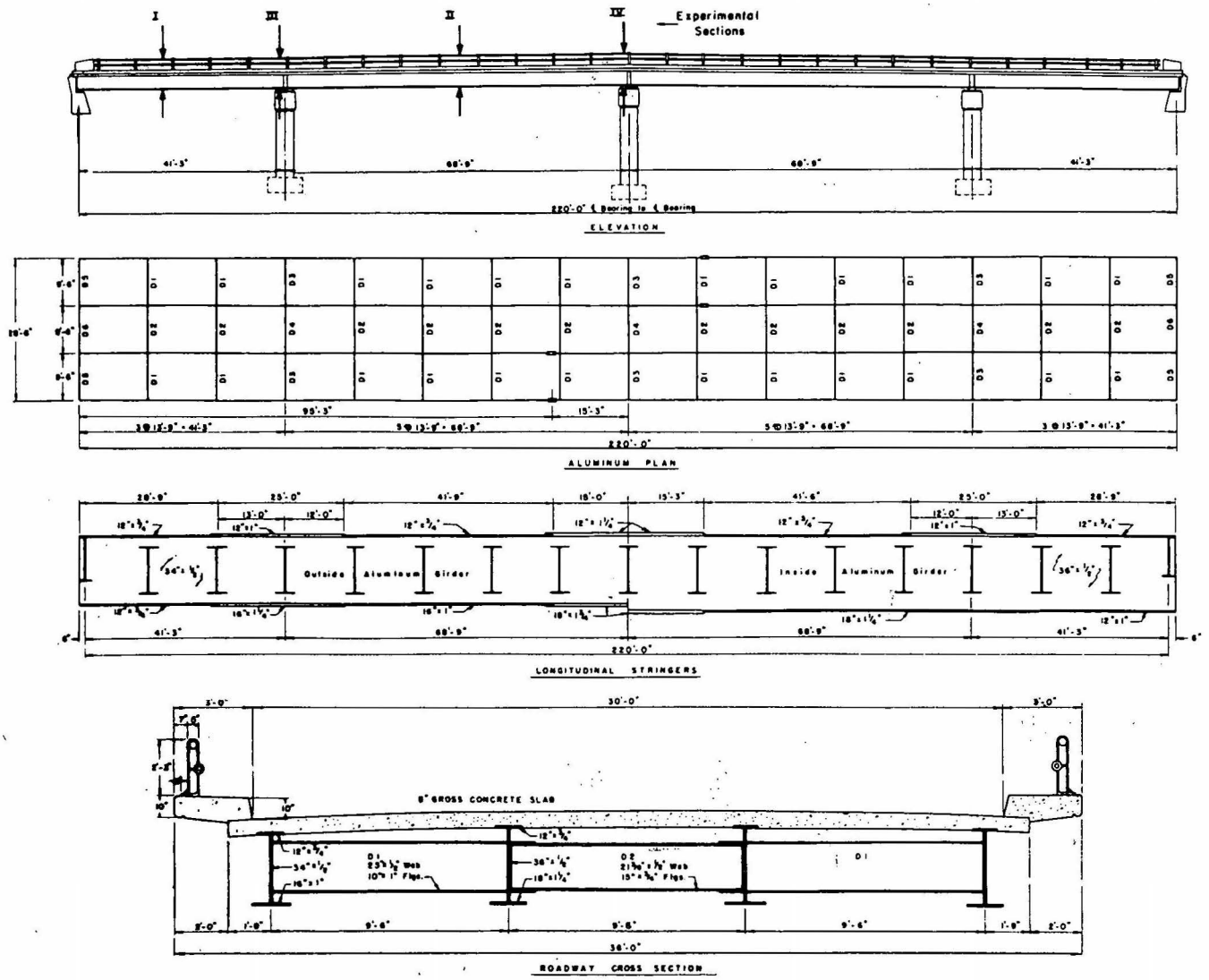

Fig. 8. Details of continuous aluminum stringer bridge.

numerator represents the amount of the load effective in the forcing function as the driving force, and is evaluated from the oscillations produced in a beam by a single moving load of constant magnitude. These oscilla-

tions, although they result from a load of constant magnitude, are similar to those of an oscillating driving force. The effect of these oscillations will be increased if a repetition of axles occurs with the moving load of constant magnitude and if these axles are in phase with the oscillating load. The phase difference between these two effects is not considered here since it is possible for the oscillating load effect and the repetitive axle effect to occur together at many different positions in a continuous structure.

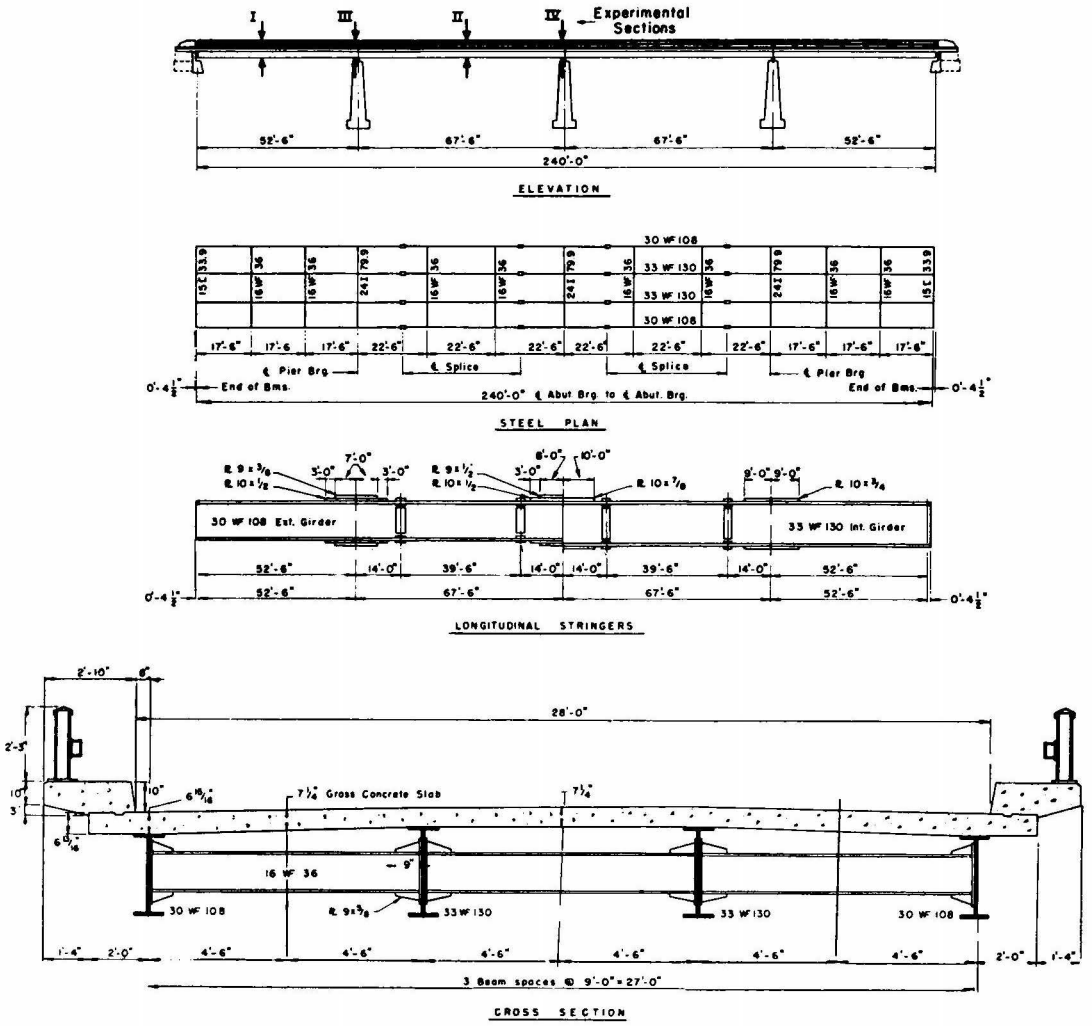

Fig. 9. Details of continuous steel WF stringer bridge.

Instead, these two effects are considered to be in phase, thus giving an upper boundary impact factor for the forced vibration of bridges by the optimum combination of the repetition of axles with the oscillating effect of a smoothly rolling load.

EXPERIMENTAL INVESTIGATION

The bridges tested in this research are part of the interstate highway system around Des Moines, Iowa. They have all been built within the last five years and are similar to the type of bridge being built in Iowa's primary and interstate road system. The approaches to these structures are paved and there is a smooth transition to the bridge roadway. One factor

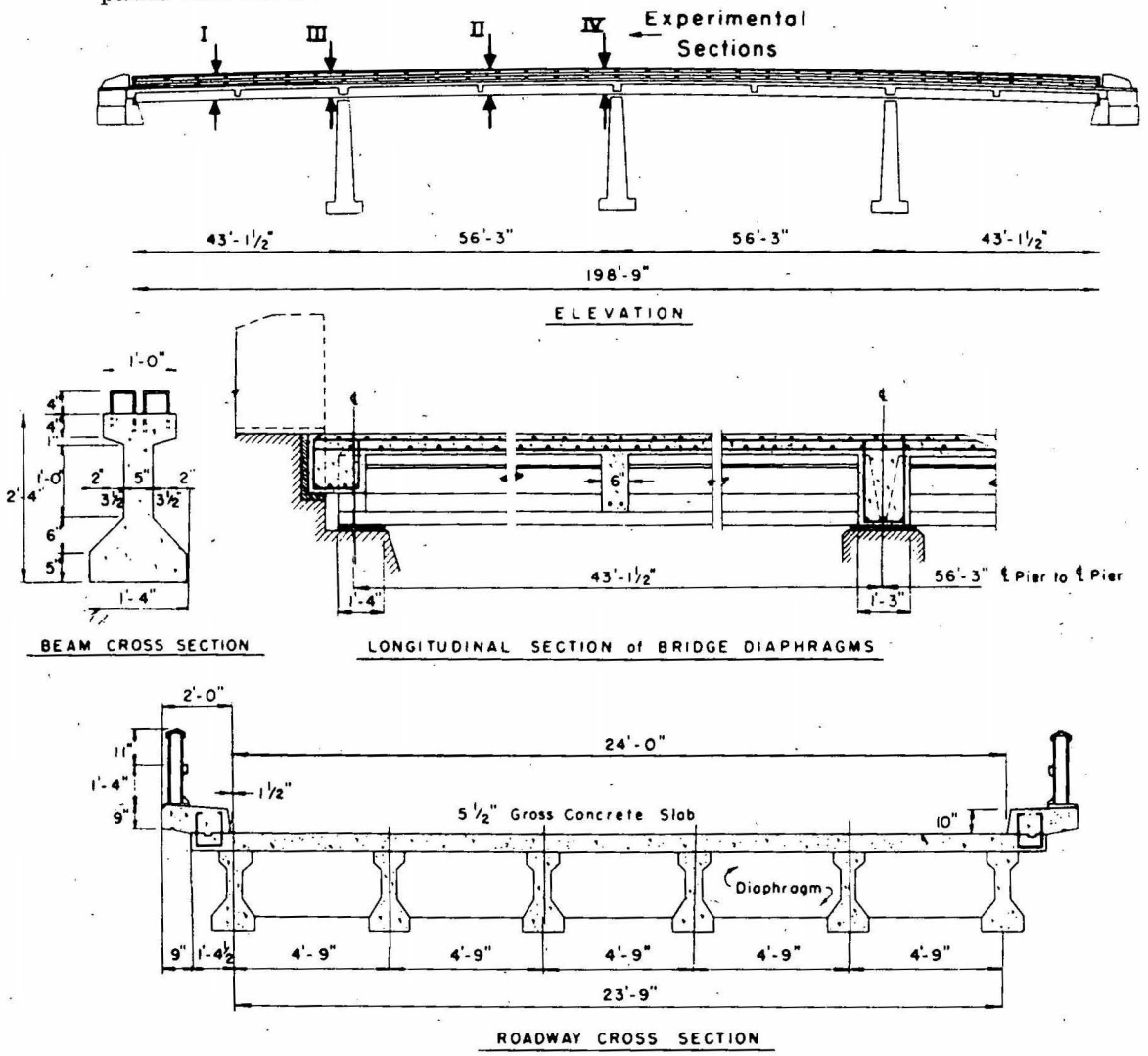

Fig. 10. Details of partially continuous prestressed concrete bridge.

used in selecting the bridges was the uniformity of their actual roadway profile. All of the bridges tested are constructed of longitudinal stringers designed to act integrally with a reinforced concrete roadway slab. How-

ever, a variety in this general type of structure was desirable to determine the limitations of the theoretical forced vibration approach presented herein. The variety was obtained by selecting three continuous bridges in which different materials were used to fabricate the longitudinal stringers. The mass per unit length is approximately the same in these bridges. A simple span bridge with a mass per unit length approximately double that of the other structures was also tested.

Simple span prestressed concrete bridge

The simple span bridge investigated has six postensioned prestressed concrete beams and a span of 100 ft. The stringers are designed and constructed to act compositely with the reinforced concrete roadway slab. The roadway is 30 ft wide with a 3 ft safety curb on both sides (figure 7). This structure is one span of a seven span bridge carrying westbound traffic on Interstate 80 over the Des Moines River north of Des Moines, Iowa. Each span of this bridge is isolated from adjacent spans by a one inch expansion joint.

Continuous aluminum stringer bridge

This structure is a 220 ft continuous four span bridge with four aluminum stringers which act compositely with a reinforced concrete roadway. This bridge has a 30 ft roadway with a 3 ft safety curb on both sides (figure 8). It carries traffic on Clive Road over Interstate 35 northwest of Des Moines, Iowa.

Continuous steel stringer bridge

This 240 ft continuous four span structure is very similar to the previous bridge except for the longitudinal stringers. The four steel stringers act compositely with a reinforced concrete roadway which is 28 ft wide with a 3 ft. safety curb on both sides (figure 9). This structure carries the traffic on Ashworth Road over Interstate 35 west of Des Moines, Iowa.

Partially continuous prestressed concrete bridge

This four span bridge is 198.75 ft long with a 24 ft roadway. The reinforced concrete roadway slab is continuous over the interior supports and has a 2 ft safety curb on both sides. In each of the four spans there are six pretensioned prestressed concrete beams. The ends of the simple span beams are encased by a cast-in-place diaphragm at the piers. These pier diaphragms plus the continuous roadway slab, which acts compositely with the stringers, result in a relatively continuous bridge structure (figure 10). This structure carries traffic over Interstate 35 at the Cumming Interchange southwest of Des Moines, Iowa.

The Test Vehicles

The vehicle effect has been simplified as much as possible in the theoretical analysis. The only parameters which are considered to be af-

fected by the vehicles are the forcing function and the loaded frequency of the bridge. The forcing function is a function of the axle spacing and the velocity of the vehicle, and the loaded frequency of the bridge is a function of the ratio of the mass of the vehicle to the mass of the bridge span. The other variables of the loading vehicles, and there are many, were disregarded.

Vehicle A. Vehicle A is an International L-190 van type truck (figure 11). This truck used to check the Iowa State Highway Commission scales has a wheel base of 14 ft 8 in and a tread of 6 ft. It weighs 40,650 lbs with 31,860 lbs on the rear tandem axle. The forced vibration resulting from this vehicle at any velocity, has two possible frequencies;

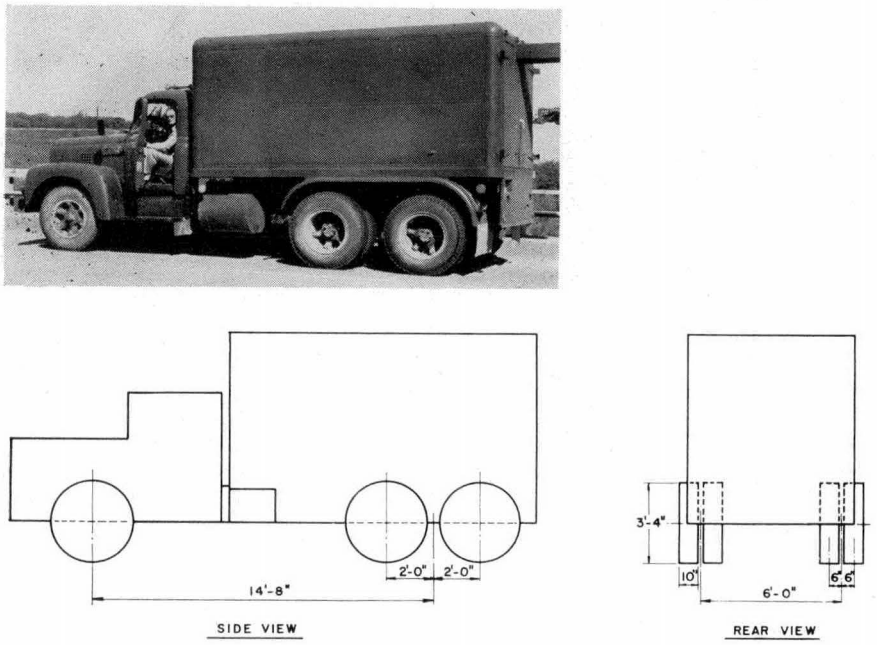

Fig. 11. Vehicle "A".

that is, this vehicle could have the forced vibration frequency determined by the passage of the individual axles in the tandem rear axle, in which the forcing frequency is v/4, or it could have a frequency determined by the passage of the front and rear axles, in which the forcing frequency is v/14.67. In the latter the axle spacing has been taken as the distance to the center of the rear tandems.

Vehicle B. Vehicle B is a tandem axle, International VF-190 truck tractor pulling a 36 ft Monnon flat bed trailer (figure 12). The tractor has a wheel base of 13 ft 1 in and a tread of 6 ft. The trailer wheel base is 23 ft, and the tread of the trailer wheels is 6 ft. The total weight of

this vehicle is 73,500 lbs, with 32,900 lbs on the trailer tandem axle and 31,700 lbs on the tractor tandem rear axle. This vehicle has three effective axle spacings, and therefore the forced vibration resulting from this vehicle for any given velocity has three possible frequencies. These three frequencies are v/4 resulting from the individual axle spacings of the tractor and trailer tandem axles, v/13.08 resulting from the tractor wheelbase axle spacing, and v/23 resulting from the trailer wheelbase axle spacing. For the tractor and trailer wheelbase, the axle spacing has been taken as the distance to the center of the tandems.

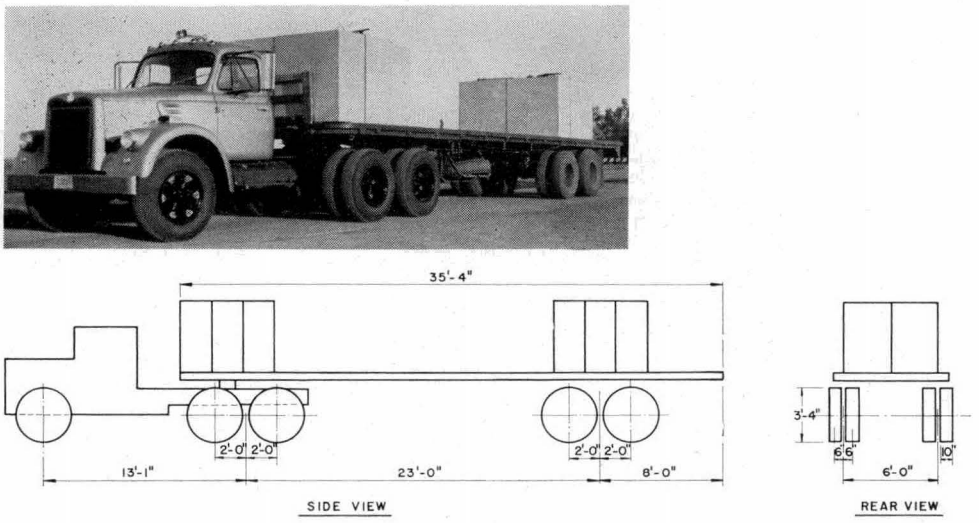

Fig. 12. Vehicle "B".

Instrumentation

To determine the dynamic effect of the vehicles, the static and dynamic bridge moments were computed from the strain measured at the extreme bottom fiber of each stringer. To measure the strains, standard SR-4 strain gages were used. The types of SR-4 gages used were A-1, A-5, and A-9. The resistance to the ground of the SR-4 gages used on the steel and aluminum girders was as follows: The A-1 gages 100,000 to 1,000,000 ohms. The A-5 gages 500,000 to 1,000,000 ohms. The A-9 gages have approximately a six inch gage length and were used to record the strains in the concrete girders.

The strain readings were recorded by a Brush universal amplifier (BL-520) and a Brush direct-writing recorder (BL-274). This equipment produces a continuous record of strain for which the time base can be varied by the speed of the recording paper. The speeds available vary

from 1 to 250 mm per sec. For a check of the time base as determined by the speed of the paper, a one second timer was used to actuate an event marker on the edge of the record. The Brush Universal amplifiers have a number of attenuator settings which vary from 1 microinch per inch of strain per attenuator-line to 1,000 microinch per inch of strain per attenuator-line, and therefore allow a wide choice of amplification of the strain. The power for this Brush recording equipment was obtained from a 10 KW Onan motor generator.

Location of strain gages

The strains were measured in all the stringers at the center line of the single span bridge and in the outer and inner spans and at the interior supports for the continuous bridges. This allowed the impact to be evaluated at all the sections of maximum bending moment for the entire length of the bridge structures. Because the continuous bridges are symmetrical about their center interior support it was necessary to instrument only one half of these bridges with strain gages.

Experimental sections. The experimental sections instrumented for the evaluation of the bridge moments are described below and shown on the elevation view of each respective bridge plan.

I. Section I is located at a point four-tenths of the outer span from the end support for all the four span continuous bridges. Section I for the simple span prestressed concrete bridge is at the middle of the span.

II. Section II is located at the middle of the interior span for the continuous steel stringer and aluminum stringer bridges. In the partially continuous four span prestressed concrete structure, section II was offset 1 ft 6 in toward the center interior support to eliminate the effect of a transverse diaphragm at the middle of the interior span.

III. Section III is located at the first interior support of the continuous bridges. To eliminate or reduce any effect which the reaction diaphragms might have, section III was offset from the center line of the reaction toward the exterior span, one foot six inches, and one foot eight inches, for the aluminum stringer, the steel stringer, and the prestressed concrete stringer bridge.

IV. Section IV is located at the center interior support of the continuous bridges. This section is offset from the center line of the reaction a distance equal to the offset of section III for each respective continuous structure.

All of the bridges were instrumented at each of the above sections with an SR-4 strain gage at the center of the bottom flange, or the extreme lower fiber of each stringer.

Experimental neutral axes. To obtain the moments required to evaluate the impact, the section moduli or relative section moduli of the string-

ers was required at the sections where the strains were measured. The effective section of the steel and the aluminum stringers vary considerably depending upon their cross section, due to cover plates or variable flanges, and the proximity of the curbing to the outer stringers. These changes in cross section result in large changes in the moments of inertia and section moduli from one section to another. The actual section moduli and moments of inertia of the longitudinal stringers were determined experimentally by obtaining the position of the neutral axis of the longitudinal stringers. Since the bridges are symmetrical about their lateral and longitudinal center lines, it was necessary to instrument only one quadrant of each bridge for the determination of the position of the neutral axes of all the experimental sections used to evaluate impact. To obtain the neutral axis five SR-4 strain gages were positioned on each stringer. One gage was located at the center of gravity of the longitudinal stringer, and the other four gages at the extreme fibers and the quarter points of the stringer. The locations of the neutral axes were then used to determine the amount of concrete slab which acts compositely with the stringers. The entire roadway slab thickness was used in these calculations. The moment of inertia was then determined using the necessary amount of slab. A modular ratio of 10 was used for the steel stringer bridge and a ratio of 3.33 was used for the aluminum stringer bridge in these calculations. However, once the position of the neutral axis is known the moment of inertia is independent of the modular ratio used.

In both of the prestressed concrete stringer bridges, the lateral spacing of the stringers is much smaller and the cross sections of the stringers do not vary along the beams. Moreover, the magnitude of the strains in the web and upper flanges of the prestressed concrete stringers were so small as to make the determination of a neutral axis very uncertain. Therefore, the section moduli of the longitudinal prestressed concrete stringers were assumed to be equal at each section investigated. It was found that in the steel and aluminum stringers, in which the experimental neutral axes were determined, that the actual variation in the section moduli made very little difference in the impact since the impact is a difference in moments or a relative difference in the recorded strains. Thus the assumption made in the prestress concrete bridges will not appreciably affect the results regardless of the exact section moduli.

Experimental Procedure

Performance of the tests. The impact resulting from the action of the loading vehicles has been derived analytically. To experimentally determine the dynamic effect, the impact, static tests were first performed by the loading vehicle creeping across the bridge with the motor idling. The maximum moment in the bridge cross section and the longitudinal position of the vehicle was computed. This was used as a base for the evaluation of the results of the dynamic tests. The dynamic tests were

then conducted at vehicle speeds beginning at approximately 10 mph and increasing by increments up to the maximum attainable speed. The maximum dynamic moment was obtained in the cross section for the vehicle in approximately the same longitudinal position as the maximum static moment. The dynamic and static tests were performed along four different lanes on the bridge roadway, two lanes for each direction of travel with one lane corresponding to the highway lane and the other lane at the longitudinal center line of the bridge. For each assigned lane, the left front tire of the vehicle was guided along a painted stripe indicating the lane on the bridge roadway. During the runs a variation to one side or the other of the painted stripe was never more than one and one-half inches.

Pneumatic tubes were placed across the bridge roadway at the center line of one exterior support and at the center line of the center interior support for the continuous bridges and at the center line of both exterior supports for the simple span bridge. The signal produced when the vehicle tire passed over this tube activated an event marker on the strain record. Knowing the chart speed and the distance between tubes, the average vehicle velocity was computed. These event markers on the strain record also enabled the longitudinal position of the vehicle to be determined at any time.

The testing of the continuous aluminum and steel stringer bridges was divided into two series for both test vehicles due to the limitation of the number of channels of Brush recording equipment. Sections I and III were tested in one series and sections II and IV in the second series. Both vehicles A and B were used in the dynamic testing of these bridges. The increased number of stringers in both the prestressed concrete bridges necessitated one series of tests for the test vehicle for each experimental section. Only vehicle A was used in the dynamic testing of these bridges. At each test section the strain was measured at the extreme lower fiber of the stringers. In each series of tests the vehicle made four static runs, one in each lane, and sixteen or twenty dynamic runs, four or five in each lane, depending on the maximum speed obtainable for the particular structure. A continuous strain time record was obtained for each run. Each strain record, therefore, contains a continuous recording of the outer fiber strains for the stringers at the test section, an event marker trace for the longitudinal location of the vehicle and vehicle speed, and a time base with a one second interval.

Data reduction. The test record shown in figure 13 is a typical dynamic strain record showing the variation of the outer fiber strain as a vehicle moves across the bridge. The static strain time curve has been superimposed on the dynamic strain time curve and is indicated by a dotted line. This record was obtained from a stringer at section I of the simple span prestressed concrete stringer bridge with vehicle A traversing the bridge at 38.4 feet per second.

The maximum static bridge moment is obtained by summing the moments in all the stringers computed from the maximum static strains. Similarly, the total maximum dynamic bridge moment is determined by summing the dynamic moments in all the stringers computed from the maximum dynamic strains. The dynamic effect, or the impact, of the vehicle was then evaluated from the moments as the ratio of the difference of the total dynamic and static bridge moments to the total static bridge moment.

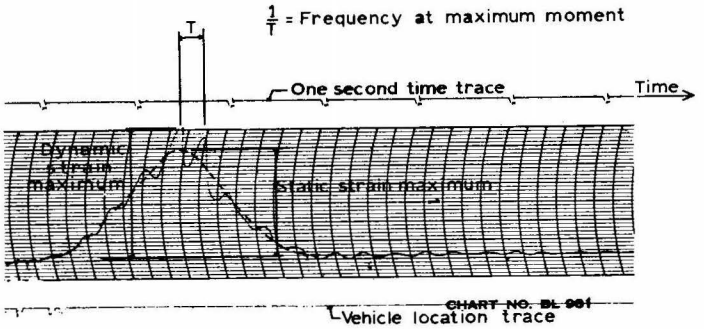

Fig. 13. Typical strain record.

The passage of the front axle and each individual axle of the tandems over the pneumatic tubes is clearly shown by the vehicle location trace. In effect, the vehicle is moving from left to right, and this trace indicates the time each individual axle crosses over the center line of the exterior supports.

The upper event marker, used as the time base, indicates time in one second intervals. This time base was used for determining the vehicle speed and the frequency of bridge vibration. The frequency of vibration of the bridge at maximum moment was determined by using the maximum peak-to-peak period of vibration indicated by the T in figure 13.

The amplitude of the residual vibration which continues after the vehicle has gone off the bridge was very small in this run. This was the usual case for the concrete stringer bridges; however, the amplitude of residual vibration for the steel and aluminum stringer bridges was usually much larger. The unloaded natural frequency of the bridge and the bridge damping was evaluated from this residual vibration.

RESULTS AND DISCUSSION

Natural Frequencies

First mode of vibration. The general theoretical method employed to determine the natural frequencies of continuous bridges assumes that the stiffness, the product of E and I, is constant throughout the length of the bridge. This solution is applicable for most steel stringer and prestressed concrete stringer bridges since their cross section usually remains constant except for the usual cover plates near the interior supports of the steel bridges. As discussed previously, the effect of increased stiffness at the piers, due to cover plates, should not appreciably affect the first mode of vibration. However, the alumnium bridge has a different value of EI in each span in addition to the increased stiffness at the piers. Thus a solution was obtained for this bridge which takes into account the large change in stiffness of the various spans but is applicable only for the first mode and higher odd modes of vibration.

Table I. Natural frequencies.

Bridge	Aluminum stringer bridge	Steel stringer bridge	Continuous concrete stringer bridge	Simple span concrete stringer bridge
L_2(ft)	68.75	67.50	56.25	100.0
$\frac{L_1}{L_2}$	0.60	0.777	0.766	
E_2I_2(lb-in^2)	185.1×10^{10}	213.4×10^{10}	197.8×10^{10}	1.609×10^{10}
$\frac{E_1I_1}{E_2I_2}$	0.615	1.0	1.0	
$m_2\frac{(\text{lb-sec}^2)}{(\text{in}^2)}$	0.924	0.889	0.889	1.721
$\frac{m_1}{m_2}$	0.989	1.0	1.0	
KL_2(Radians)	3.40	3.399	3.408	3.1416
$f_{theo.}$ (cps)	3.825	4.34	6.06	3.34
$f_{exper.}$ (cps)	3.97	4.57	7.80	4.26
$\frac{f_{theo.}}{f_{exper.}}$	0.964	0.951	0.78	0.784

The solutions of the frequency equations yield values of KL from which the natural frequencies are determined. Values of KL can be obtained from figures 1, 2, or 3, since these figures graphically represent the first mode solution of the various frequency equations. The natural frequency is then found by using equation 40,

$$f = \frac{(KL_2)^2}{2\pi L^2_2} \sqrt{\frac{E_2 I_2}{m_2}}$$

Values of KL_2 of 3.400, 3.339, and 3.408 were determined analytically for the aluminum, steel, and continuous prestressed concrete bridge respectively. The natural frequencies resulting from these values of KL are compared with the experimentally obtained natural frequencies in table 1. Also shown in this table are the parameters of the various bridges which are required for the determination of the resonant frequencies. The moment of inertia used in the stiffness parameter E_2I_2 is the moment of inertia of the entire cross section at section II of the various continuous bridges and includes the sidewalk curb. For the simple span bridge, the solution of the frequency equation yields a value for KL of $n\pi$ which is given in most tests on vibrations[21]. The first mode of natural frequency obtained for this bridge is compared with the experimental value in table I. A modular ratio, the modulus of elasticity of the stringer over the modulus of elasticity of the reinforced concrete slab, of 3.44, 10, and 1.25 was used in the aluminum, steel and both concrete bridges respectively. Thus the modulus of elasticity of the reinforced concrete roadway slab and the pretressed concrete stringers were taken as the value used in design for each case; this probably accounts for most of the error in the theoretical frequency determination of the prestressed concrete stringer bridges. It was observed during the experimental testing that the natural frequency of the bridges reduces more than theory indicates it should when a vehicle first enters the bridge span. However, once the vehicle is on the bridge the reduction in natural frequency, as the vehicle position changes, is similar to the theoretically calculated value; but it is very difficult to measure accurately.

Higher modes of vibration. The first mode of vibration was usually found to be prevalent in controlling the response of the bridges to the forcing function of the axles. This was true in most cases and at experimental sections III and IV where the first mode, or higher odd modes, have the least effect. However, an outstanding exception occurred in the case of the aluminum stringer bridge. In this structure the experimental impact at section IV, the section at the center interior support, was found to be a function of a higher mode of vibration. The resonance condition in this case is a function of the second mode. This is the first root of the even mode frequency equation for a four span symmetrical bridge (equation 39), and corresponds approximately to the vibration of the beam with

both ends fixed. Therefore, it is reasonable to assume that this vibration, when it occurs, will result in the largest dynamic increase in moment at the supports. The theoretical second mode solution was found by using equation 39, which was derived by assuming a uniform cross section. This equation was used because the increased accuracy of a special solution including the effect of the change in stiffness of each span would be insignificant when compared to the large change in stiffness near the piers due to the increase in cross section of the aluminum stringers at that point. The value of KL_2 for the second mode is 4.345, which yields a vibratory frequency of 6.25 cycles per second. This theoretical mode frequency agrees closely with the measured frequencies occurring while the vehicle is on the inner spans vibrating the bridge at its second mode. However, this frequency could not be compared with an experimental unloaded natural frequency because this mode of vibration occurred only when the vehicle was on the inner span.

Effect of the vehicle. The loaded natural frequency is applied in the determination of the natural frequency of the brige which occurs when the vehicle is on the span. This value of loaded natural frequency will control the resonance condition of the frequency of the vehicle forcing function with the natural frequency of the bridge. This resonance condition has the greatest effect on the amount of impact when the vehicle is near the position of maximum moment.

The reduction in natural frequency due to the mass of the vehicle has been theoretically determined; and although it could not be correlated with the experimental reduction, due to the difficulty of measuring it, it is desirable that the effect of the vehicle mass be taken into account. This effect can be considered either by the total effect of the individual axles or by the effect of the entire mass at its center of gravity. If the effect of each axle is determined individually, the over-all effect of the vehicle is different than if the mass of the entire vehicle is placed on the bridge at one point. The actual vehicle, although applied to the bridge by means of several axles, is usually made up of a rather concentrated mass. For this reason vehicle A was used as a concentrated mass. The truck and trailer, vehicle B, was made up of large concrete blocks representing the load and located directly over the tandem axles of the truck and trailer. Therefore for this loading, the individual effect of the truck tractor and the trailer was found when the center of gravity of the truck tractor and the center of gravity of the trailer axles were at the center of the span.

The different lengths of the spans in the continuous bridges result in a different loaded natural frequency for the load in each span. Therefore in the correlation of the experimental and theoretical impact, an impact curve is obtained for the loaded frequency as each span is loaded. Moreover, since the truck tractor and trailer of vehicle B was used separately, the reduction in frequency is different for each part of the vehicle. All of

the various values of loaded frequency will have an individual impact curve determined by equation 108. To reduce the number of these closely spaced curves and to simplify the presentation of the impact data, only two curves are shown for the reduction in natural frequency. These curves are for vehicle A and the truck tractor of vehicle B in the outer and inner spans. These two loads have the same effect on the reduction in frequency since their masses are within 0.1% of each other. These various theoretical loaded natural frequencies obtained for the vehicles in the outer and inner spans are 98.0% and 94.9%, 97.1% and 95.2%, and 96.6% and 94.6% of the unloaded natural frequencies of the continuous aluminum, steel, and concrete stringer bridges respectively. The loaded natural frquency of the simple span bridge is 95.3% of the unloaded natural frequency for vehicle A at the center of the span.

Forced Vibration

Forcing function. In the determination of impact, the frequency of the forcing function of the vehicle has been taken as the cyclical repetition of the axles. This cyclical repetition is determined by the frequency of passage of the axles across the bridge. This action of the axles might be interpreted as the forcing of a nodal point across the structure by each

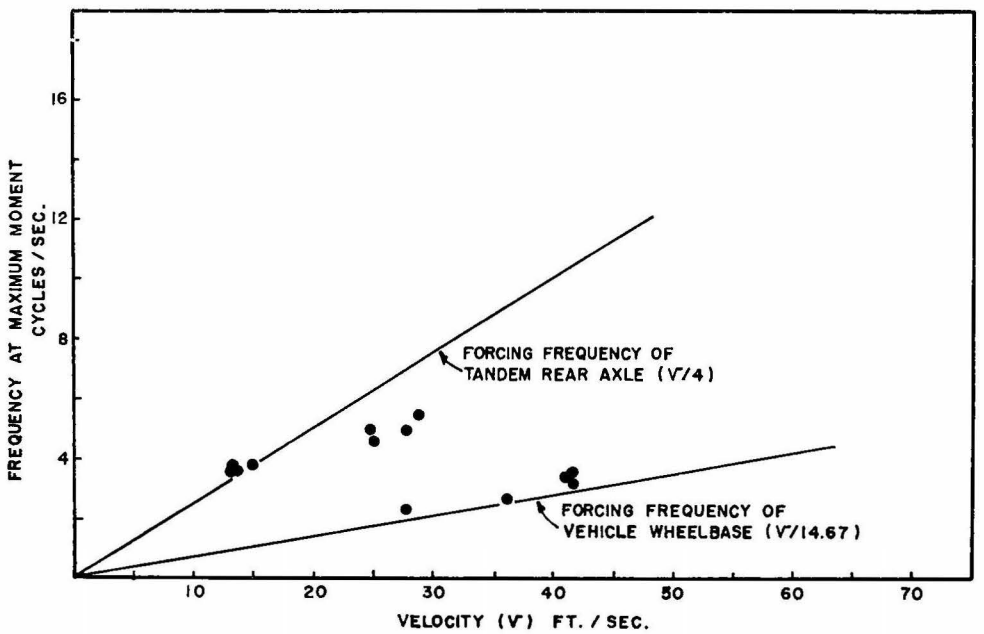

Fig. 14. Frequency of forced vibration of simple span concrete bridge for Vehicle "A".

axle. Therefore for the fundamental mode of forced vibration with no higher harmonics, the spacing of axles will be one wave length of the

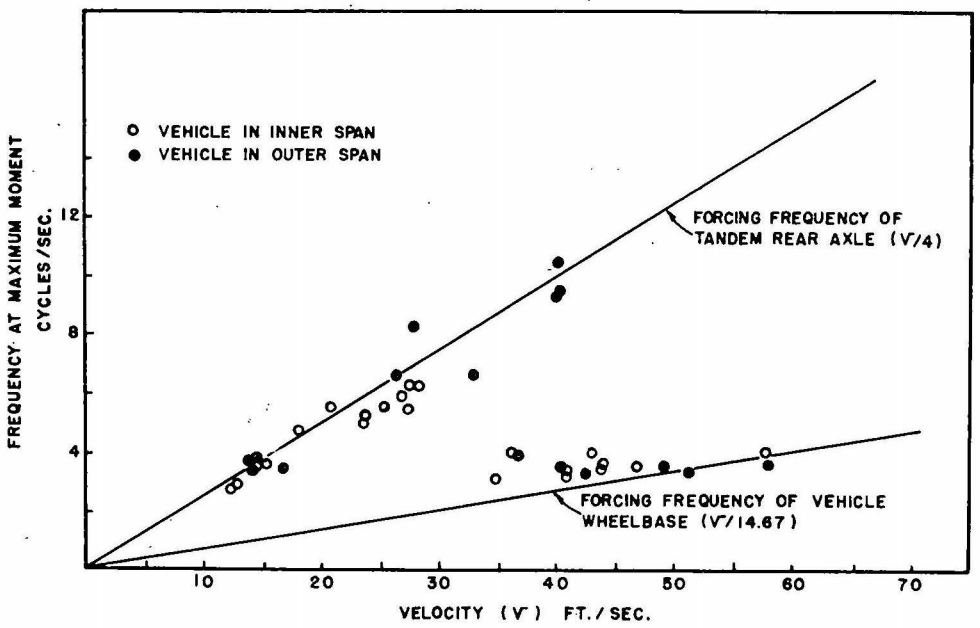

Fig. 15. Frequency of forced vibration of aluminum stringer bridge for Vehicle "A".

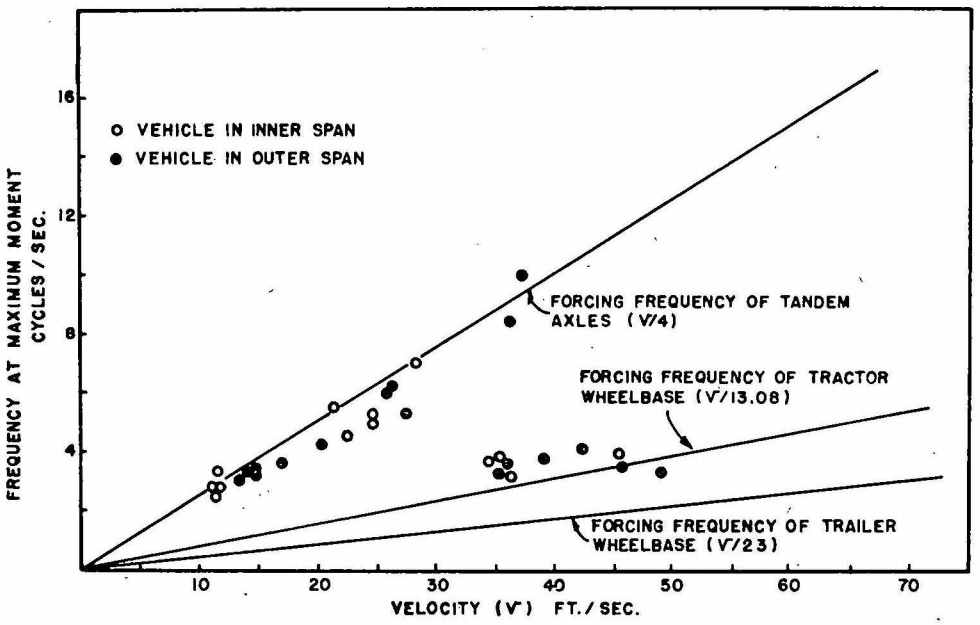

Fig. 16. Frequency of forced vibration of aluminum stringer bridge for Vehicle "B".

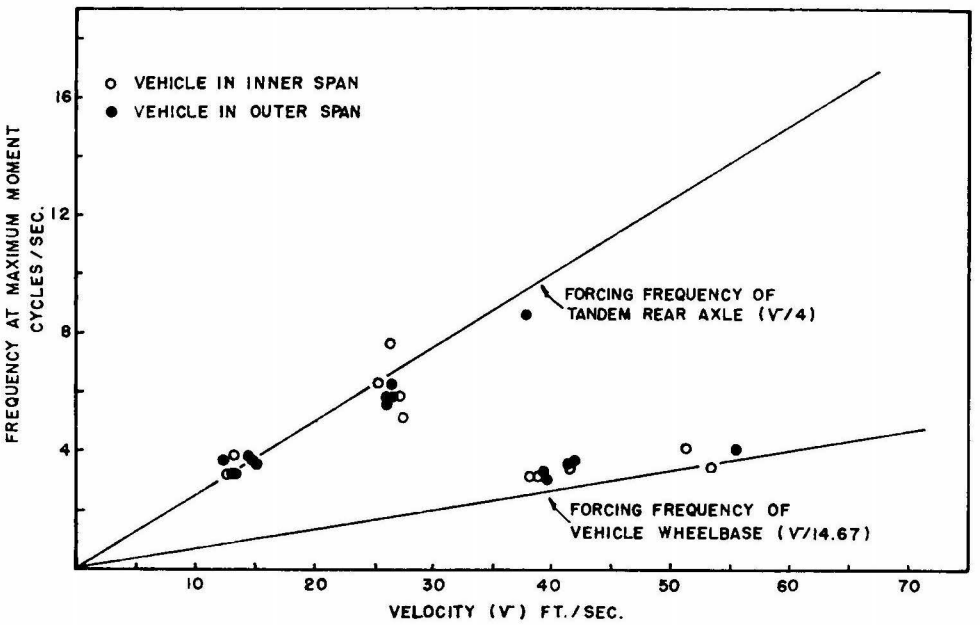

Fig. 17. Frequency of forced vibration of steel stringer bridge for Vehicle "A".

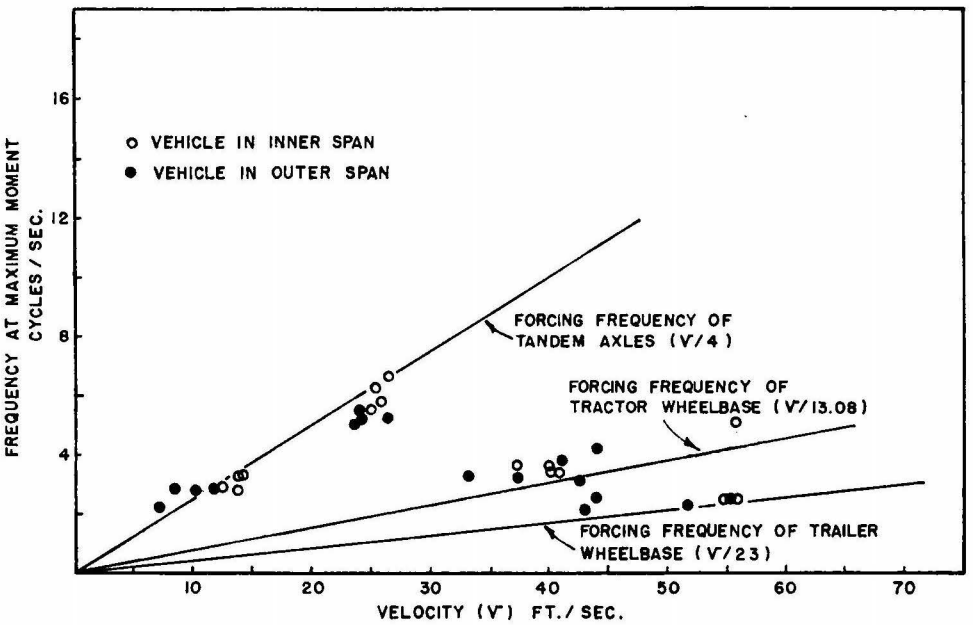

Fig. 18. Frequency of forced vibration of steel stringer bridge for Vehicle "B".

bridge vibration. The solution obtained for the differential equation of motion of a beam subjected to this forcing function consists of two parts, the complementary solution and the particular solution. The complementary solution represents the free vibration of the beam and the particular solution represents the steady state forced vibration occurring after the complementary solution has been reduced to an insignificantly small part of the total vibration. This steady state forced vibration, the particular solution, has the same vibratory frequency as the forcing function. Therefore, in the cases in which only the particular solution is applicable, that is, when the complementary solution has been reduced significantly, the frequency of the vibratory motion of the structure should correspond to the frequency of the forcing function. To determine the applicability of this concept, it must be shown that the forcing frequency of the axles is predominant in the forced vibration of the bridge, or that the response of the bridge is similar to that of a steady state forced vibration. The frequency of vibration of the structure was determined at the time the vehicle was producing the maximum moment. This value of frequency was obtained by using the one or two cycles of vibration at the maximum amplitudes of vibration. It was found in this experimental work that the natural frequency of the structure was prevalent as the vehicle entered the bridge, and further, that this natural frequency more nearly corresponds to the computed value than to the experimental value of natural frequency obtained when no vehicle was on the bridge. As the vehicle approached the position of maximum moment the frequency became approximately equal to the frequency of the forcing function (figures 14 to 18). Since there were two different forcing frequencies available for vehicle A and three different forcing frequencies available for vehicle B, there were a number of different frequencies which could be used as the frequency of the forcing function. However, only one axle spacing was predominant in determining the frequency of the forcing function. This is readily shown in figures 14 to 18 in which the frequency of the bridge at maximum moment is shown as a function of the velocity of the vehicle. Variations in this result from the tendency of the bridge vibration to remain near the resonant frequency of the structure at higher speeds where the forcing frequency is impressed by the axle spacing of the vehicle wheelbase.

An exception to the well-defined forcing frequency of the velocity divided by the axle spacing occurred in the continuous prestressed concrete bridge (figure 19). This structure was constructed by placing a continuous reinforced concrete roadway over four spans of simply supported prestressed concrete beams. Unlike the other bridges tested, this bridge does not have a point bearing to allow free rotation at the supports and it is not fully continuous. The interior supports have a fifteen inch reinforced concrete diaphragm resting on an 11/32 inch preformed fabric bearing pad. These diaphragms encase the ends of the beams at each interior support and combine with the roadway slab to make the structure

partially continuous. The exterior supports have approximately sixteen inches of the end of the beam resting on similar 11/32 inch bearing pads. The effect of the large flat bearing surfaces at the supports heavily damps the vibration of the continuous bridge. These bearings also cause a cer-

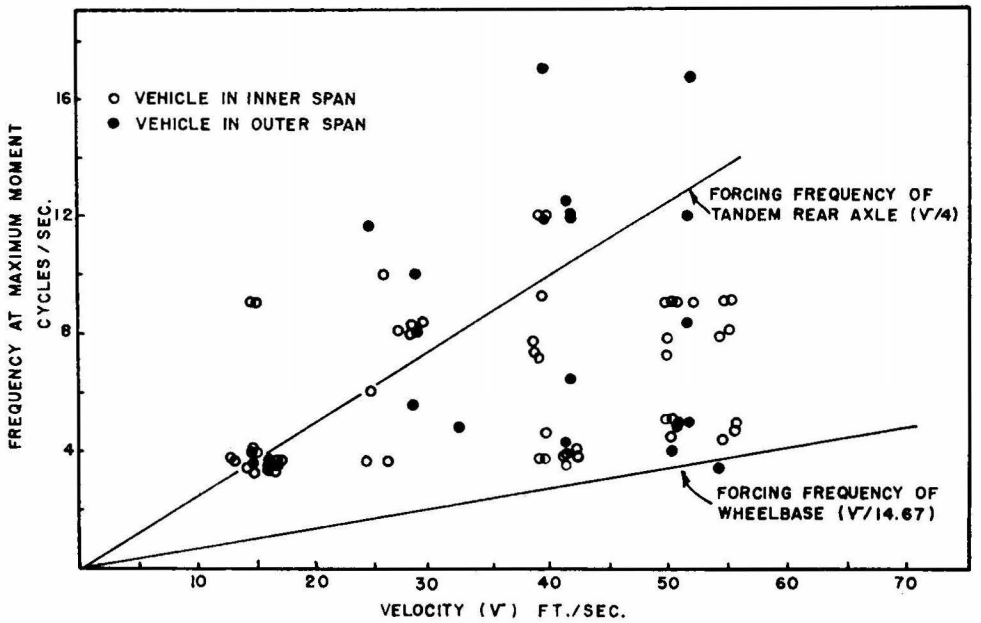

Fig. 19. Frequency of forced vibration of continuous concrete stringer bridge for Vehicle "A".

tain amount of fixity at each support, thus further complicating the vibratory system. Moreover, the pier diaphragms acting with the continuous reinforced concrete roadway slab allow only the negative moments to be transmitted across the piers or interior supports. Positive bending at the piers is eliminated due to the tension in the bottom fibers of the pier diaphragms. These diaphragms are not reinforced to resist tension in that direction. Therefore it is very difficult to establish a well defined vibratory system in such an incongruous structure. This is exemplified in figure 19 by the random vibration of the structure at the maximum moment which results from the passage of vehicle A. For this reason, the application of the forced vibration theory presented herein for the determination of the response of this structure to the forcing function of the repetition of axles has very little significance.

Impact. The impact as determined herein is a function of the amplitude of forced vibration. The derivation of the theoretical impact was made by assuming that the forcing frequency of the axles was predominant in producing the impact. The denominator of the theoretical impact factor is a function of the ratio of the forcing frequency to the loaded natural frequency of the structure and the ratio of the damping factor to the

unloaded natural frequency of the structure. The numerator of this impact factor is a function of the ratio of velocity to the length of the span. Therefore since the forcing frequency is the ratio of the velocity of the vehicle to the axle spacing, the magnitude of the theoretical impact will depend upon the velocity, axle spacing, length of span, loaded natural frequency, unloaded natural frequency, and the damping factor.

The damping factor was obtained experimentally from the decreasing amplitude of the residual vibrations. To experimentally determine this, the amplitude of displacement Y of the strain time curve is measured at time t_0 and at a later time t_N which is N cycles later. The ratio of these amplitudes Y_0/Y_N is a constant, for viscous damping and 1/N times the natural logarithm of this ratio is called the average logarithmic decrement. This quantity therefore does not depend on the way the damping was defined in the original equation of motion and thus is often used as the measure of the damping capacity of a structure. The average logarithmic decrement is then given as

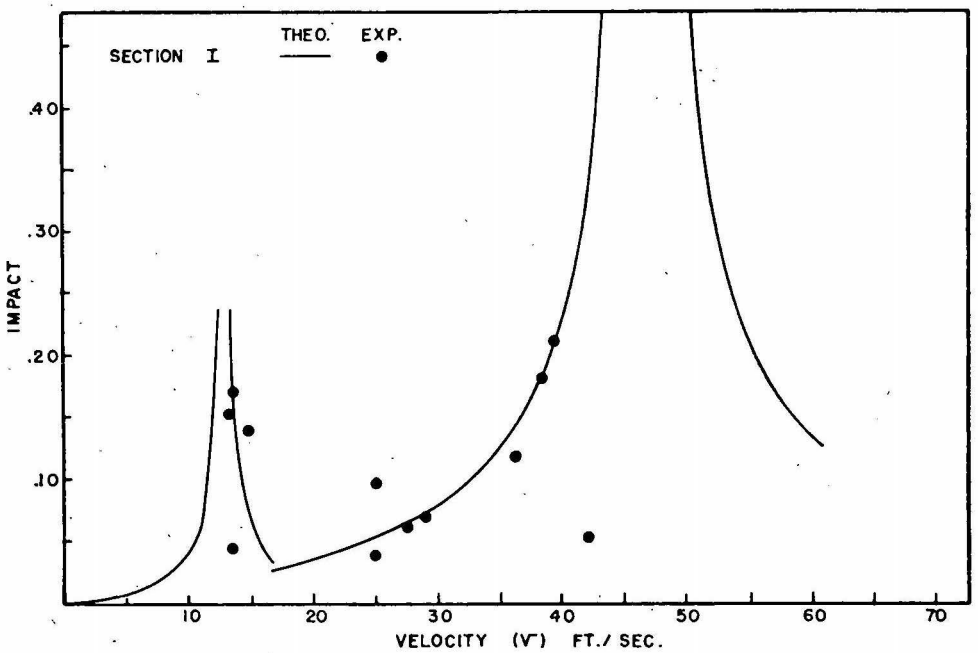

Fig. 20. Impact for simple span concrete stringer bridge at Section I for Vehicle "A".

$$\frac{1}{N} \log_e \frac{Y_0}{Y_N}$$

The damping capacity of each bridge will be given in terms of the average logarithmic decrement.

Simple span prestressed concrete bridge. The correlation of the experimental and theoretical impact for the postensioned prestressed concrete bridge is shown in figure 20. The experimental impact values determined at the center line of the simple span (section I) are shown with the theoretical impact curves obtained by equation 108. A loaded natural frequency which is 95.3% of the theoretical natural frequency of 3.34 cycles per second was used in determining the theoretical impact curves. The average logarithmic decrement for this bridge is 0.0916. The resulting amount of damping did not affect the theoretical curves except at resonance. Therefore for the portion of the impact curves shown in this figure, the effect of the damping is insignificant. Resonance occurs when the ratio of the forcing frequency or the frequency of the repetition of the axles to the loaded natural frequency of the structure is one. This condition occurs two times for vehicle A. The individual axles of the tandem rear axle unit acting individually cause a resonance at the smaller velocities, and the front axle combined with the tandem rear axle acting as one unit cause resonance at the larger velocities. The impact increases as the ratio of the forcing function to the loaded natural frequency approaches one. The experimental impact values agree with the theoretical impact curves which, as previously discussed, yield an upper limit of impact for the assumptions made in the derivation. The maximum vehicle velocity limited a complete investigation of the wheelbase resonance condition.

Continuous aluminum stringer bridge. The experimental and theoretical impact for this structure is shown in figures 21 to 24. The theoretical curves show a good agreement with the experimental impact values. As previously discussed an additional resonance occurred in this structure when the bridge was excited at its second mode of vibration by the individual axles of the tandem rear axle unit. This condition is most prominent at the center interior support. A correlation of the theory presented herein for the upper limit of the wheelbase resonance condition was not obtained due to the limited velocity of the vehicles. Similarly, the resonance condition of the trailer wheelbase could not be investigated. A loaded natural frequency of 98.0% and 94.9% of the theoretical natural frequency of 3.825 cycles per second was used for the outer and inner span resonance curves respectively. The average logarithmic decrement for this bridge is 0.050. The resulting amount of damping did not affect the theoretical curves except at resonance. The maximum values of impact written as a percentage vary from 20.6-31.9% and 19.1-20.8% for vehicles A and B at the positive and negative sections respectively. Moreover it should be noted that the resonance condition of the individual axles of the tandem rear axle unit cause an experimental impact almost as large as the resonance condition of the vehicle wheelbase at higher velocities. Therefore the

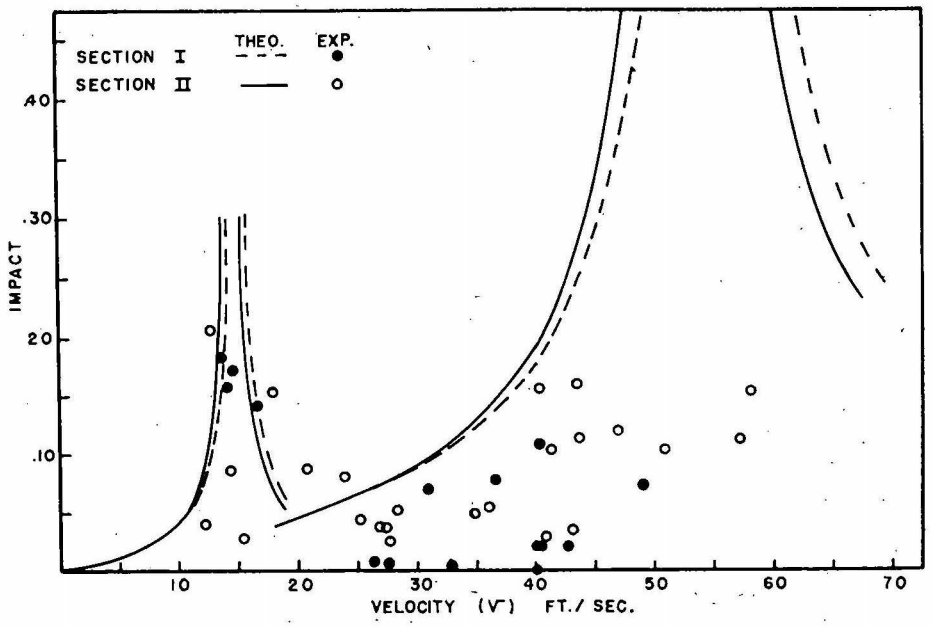

Fig. 21. Impact for aluminum strin ger bridge at Sections I and II for Vehicle "A".

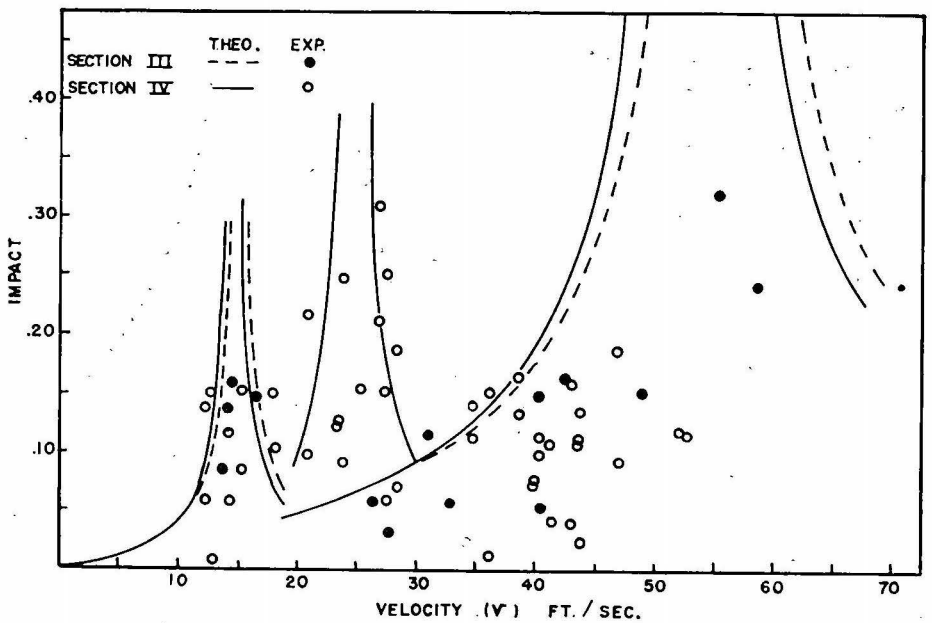

Fig. 22. Impact for aluminum stringer bridge at Sections III and IV for Vehicle "A".

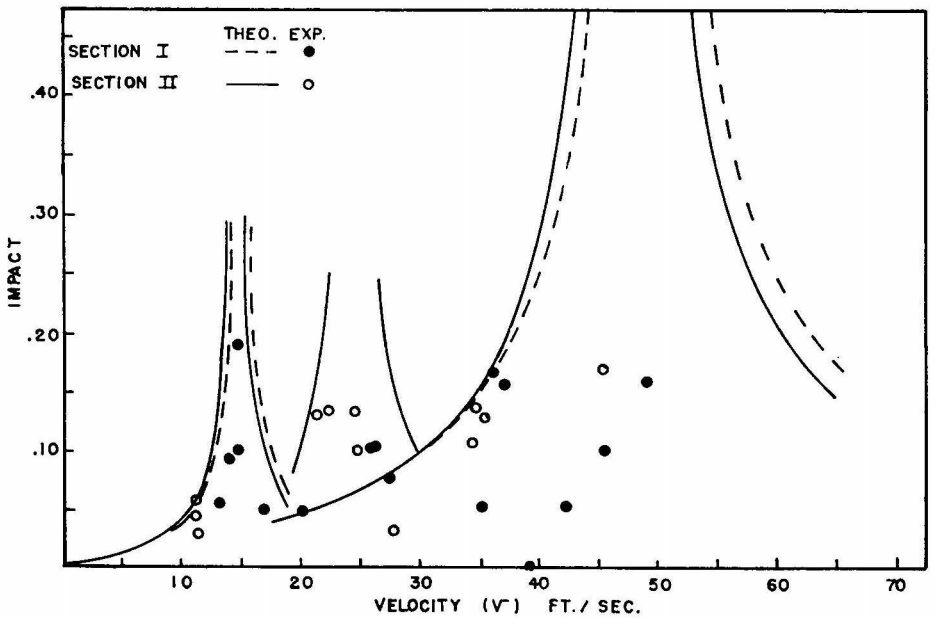

Fig. 23. Impact for aluminum stringer bridge at Sections I and II for Vehicle "B".

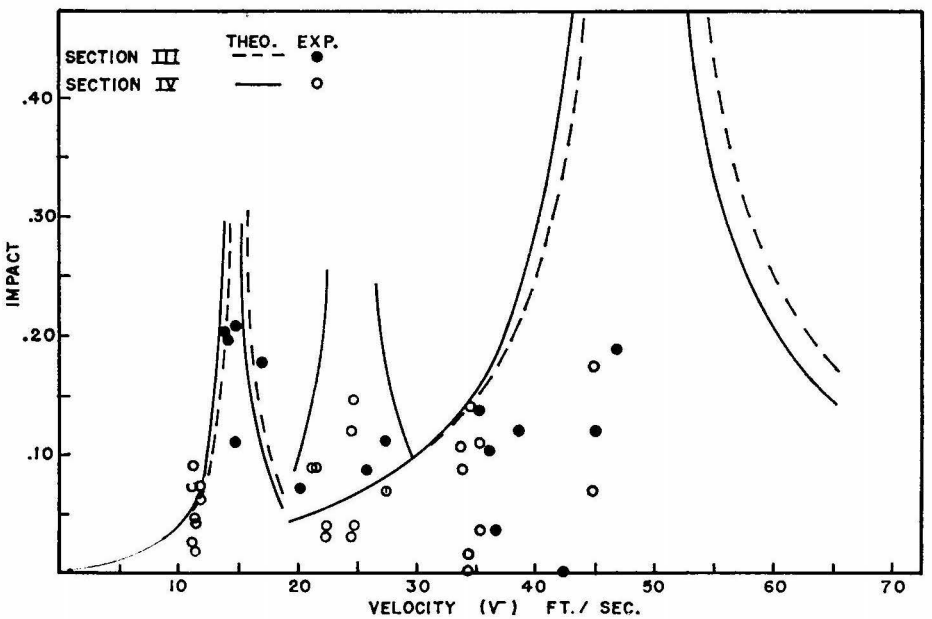

Fig. 24. Impact for aluminum stringer bridge at Sections III and IV for Vehicle "B".

resonance effect of the repetition of axles is important at the slower speeds.

Continuous steel stringer bridge. The correlation of the experimental and theoretical impact for this bridge is shown in figures 25 to 28. More experimental impact values lie outside the theoretical impact envelope in this bridge than in the previous bridges. The greatest discrepancy occurs as the resonance condition is approached from the left side of the figure. That is, the large number of experimental points outside the theoretical envelope at velocities lower than the resonance velocities might result from the loaded natural frequency of the bridge being smaller than the value used to obtain the impact curves. A smaller loaded natural frequency would move the theoretical curves to the left in these figures. However, the theoretical curves shown still qualitatively describe the variations in the experimental impact. There is no indication in this

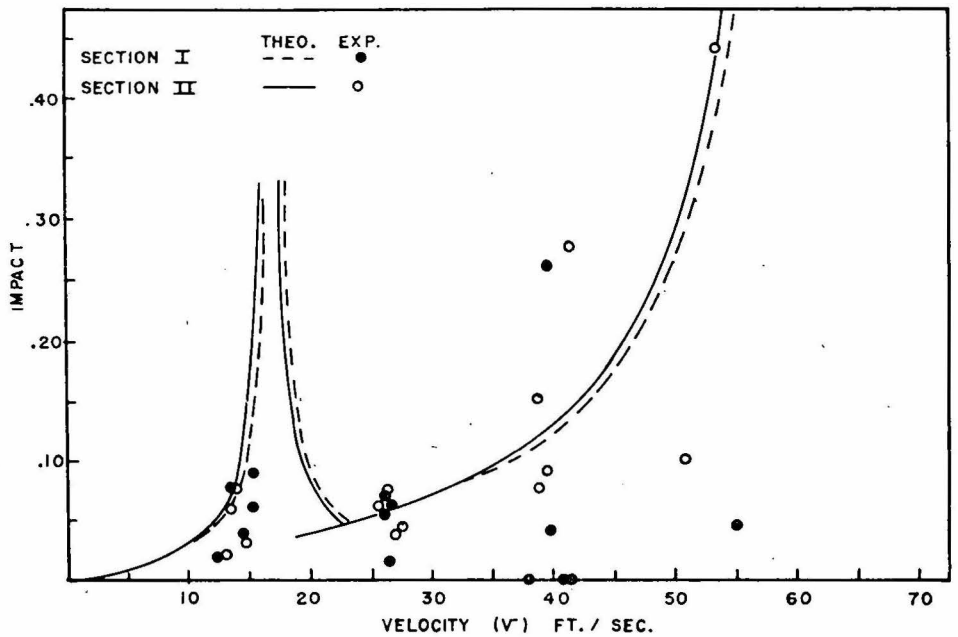

Fig. 25. Impact for steel stringer bridge at Sections I and II for Vehicle "A".

structure of any higher modes of vibration. Moreover, not enough experimental data was obtained for a good evaluation of the resonance condition of the individual axles of the tandem axle unit with the first mode of vibration. Therefore, the experimental impact values for the tandem axles were smaller than those obtained by the resonance condition for the vehicle wheelbase. Also, a large enough velocity was not obtained for the trailer wheelbase to cause a resonance condition. The maximum values of impact,

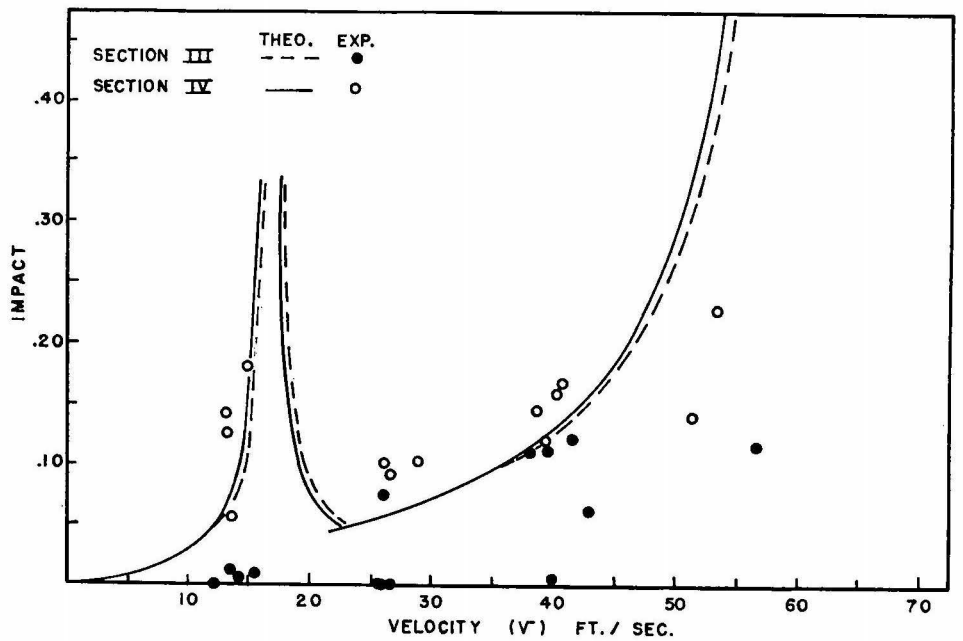

Fig. 26. Impact for steel stringer bridge at Sections III and IV for Vehicle "A".

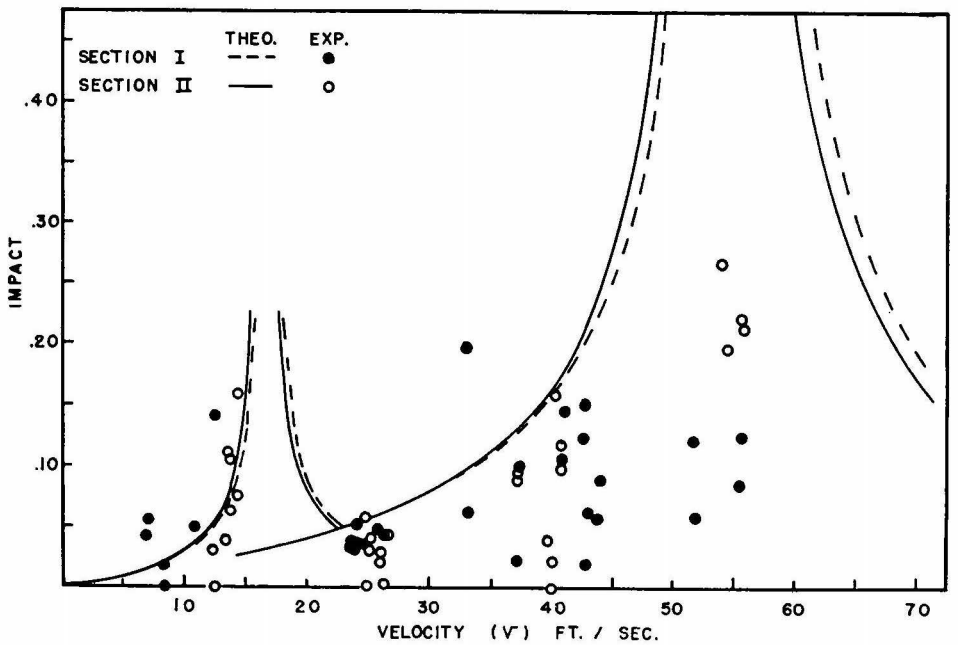

Fig. 27. Impact for steel stringer bridge at Sections I and II for Vehicle "B".

written as a percentage, vary from 44.1-26.5% and 22.8-39.2% for vehicles A and B at the positive and negative sections respectively. A loaded natural frequency of 97.1% and 95.2% of the theoretical unloaded natural frequen-

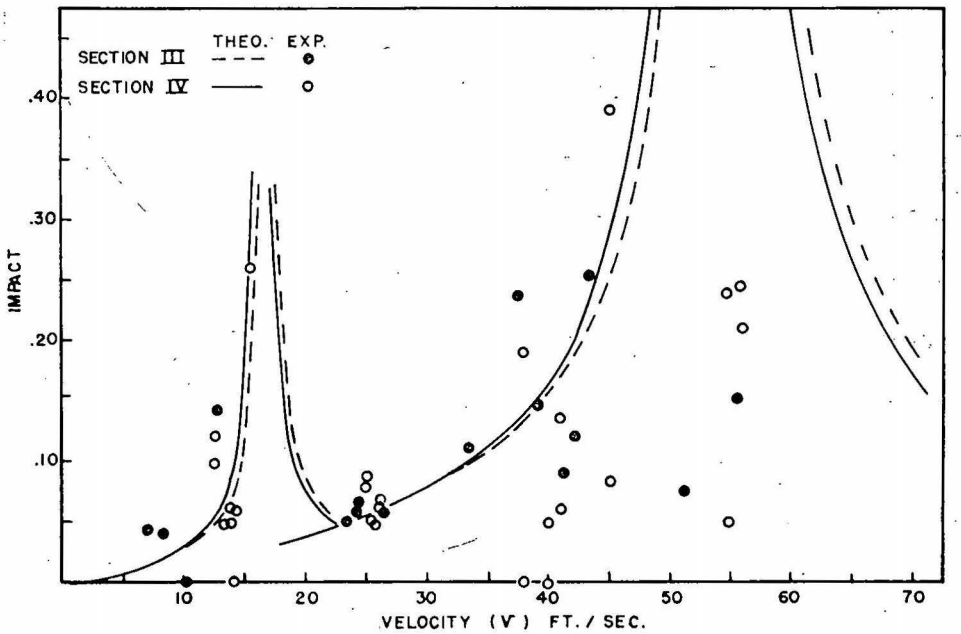

Fig. 28. Impact for steel stringer bridge at Sections III and IV for Vehicle "B".

cy of 4.34 cycles per second was used for the outer and inner span impact curves respectively. The average logarithmic decrement of this bridge is 0.062. This amount of damping did not affect the theoretical curves except at resonance.

Partially continuous concrete stringer bridge. The correlation of the experimental and theoretical impact for this bridge is shown in figures 29 and 30. A loaded natural frequency of 94.6% of the theoretical unloaded natural frequency of 6.06 cycles per second was used to obtain this curve. The curve for the vehicle on the outer span is not shown since it is just to the right of this curve similar to those in the previous figures. This curve includes the effect of damping, which was considerably larger for this structure than for the previous structures. The average logarithmic decrement of the residual vibration of this structure is 0.406. This amount of damping results in a reasonable upper limit for the impact curves of 0.298 for the resonance condition caused by the individual axles of the tandem axle unit. Since there is not enough experimental impact data at the velocity corresponding to this resonance condition, this upper limit could not be verified. The experimental impact values show some agree-

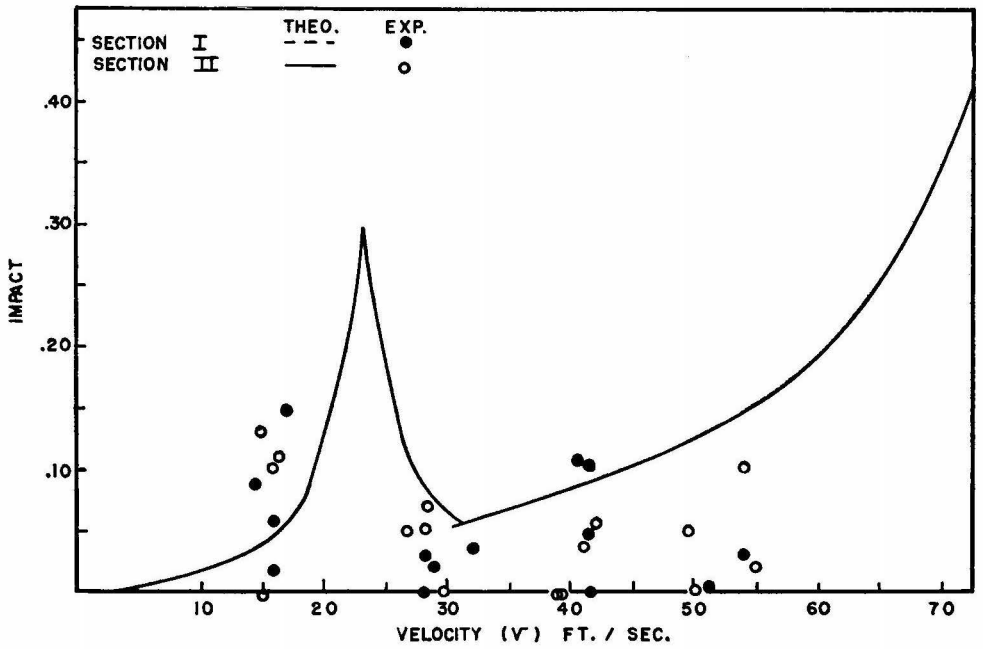

Fig. 29. Impact for continuous concrete stringer bridge at Sections I and II for Vehicle "A".

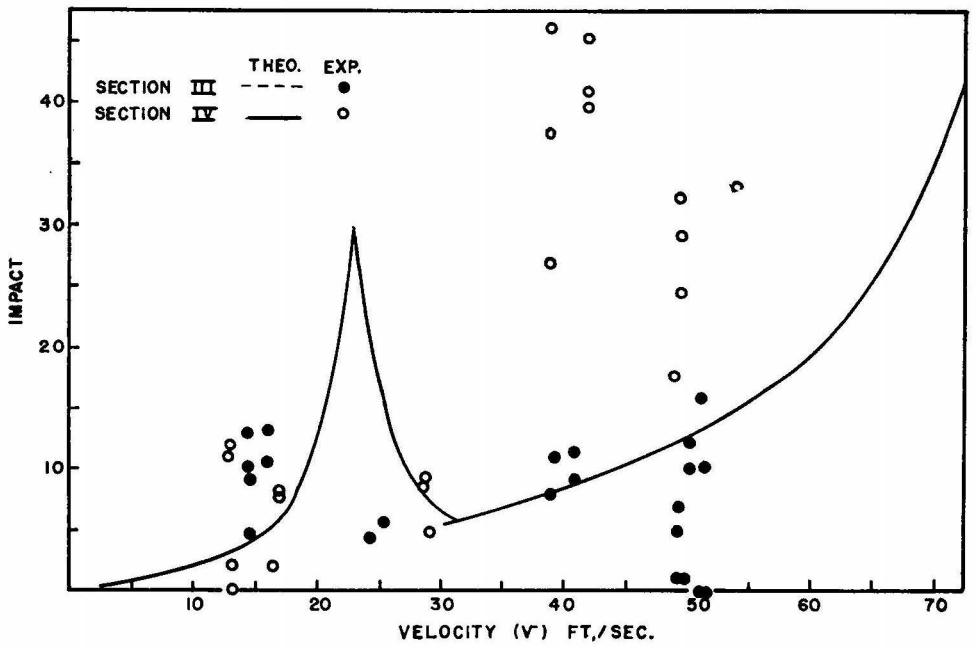

Fig. 30. Impact for continuous concrete stringer bridge at Sections III and IV for Vehicle "A".

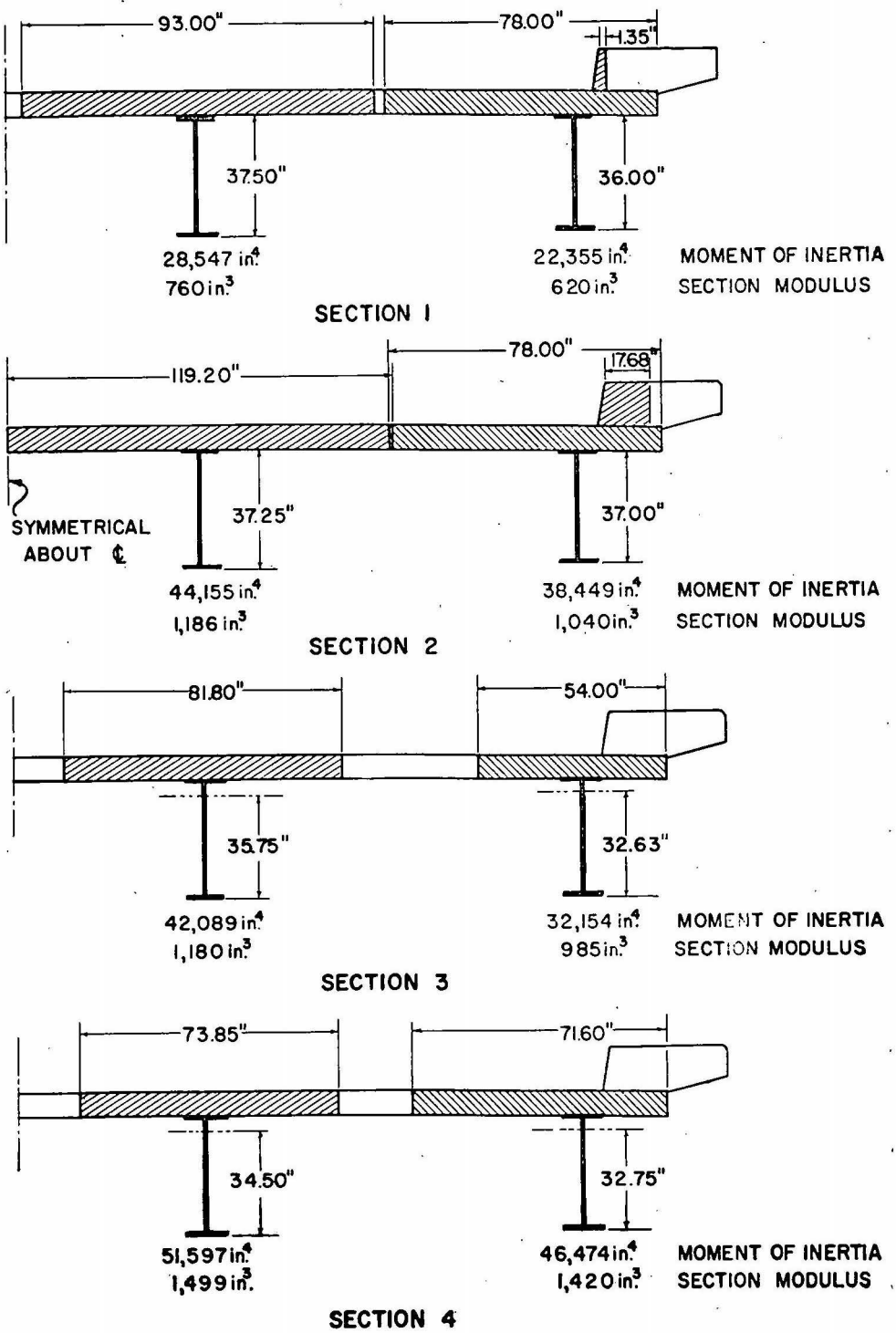

Fig. 34. A cross section of the aluminum stringer bridge at sections I, II, III, and IV showing the composite moments of inertia, section moduli, and the effective slab.

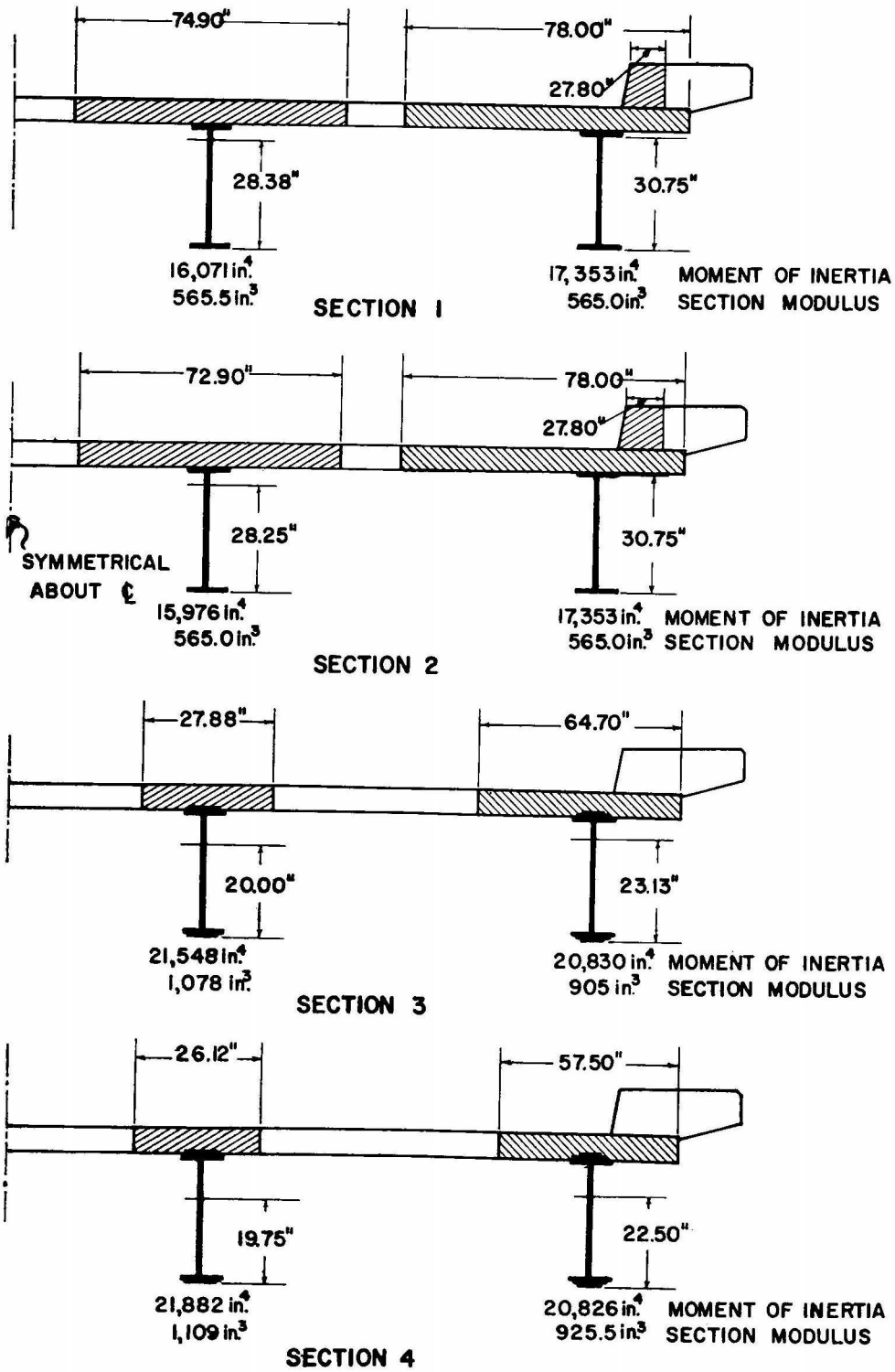

Fig. 35. A cross section of the steel stringer bridge at sections I, II, III, and IV showing the composite moments of inertia, section moduli, and the effective slab.

TEST RESULTS

Composite section

The neutral axes of the stringer cross sections were determined at the four experimental sections shown in figures 8, 9 for the aluminum and the steel stringer bridges. Once the neutral axis was obtained, the amount of slab necessary to balance the various experimentally located neutral axes was determined. The moments of inertia were then computed. A modular ratio of 10 was used for the steel stringer bridge and a ratio of 3.33 was used for the aluminum stringer bridge. It should be noted, however, that when the position of the neutral axis is known the moment of inertia is independent of the modular ratio used.

Since the bridges are symmetrical about their lateral and longitudinal center lines, only one quadrant of each bridge needed to be instrumented to determine the position of the neutral axes of all the experimental sections. A cross section of the aluminum and steel stringer bridges at sections I, II, III, and IV are shown in figures 34 and 35 respectively. These figures show the composite moments of inertia, section moduli, and the slab effective in the composite section.

The neutral axes results are not intended for a complete analysis of the variations in cross section along the entire length of the bridges. They do show, however, that the actual composite cross section varies greatly at different sections along the bridges as indicated in previous research.[27]

Load distribution

Static live load. The distribution of load in a slab stringer bridge is

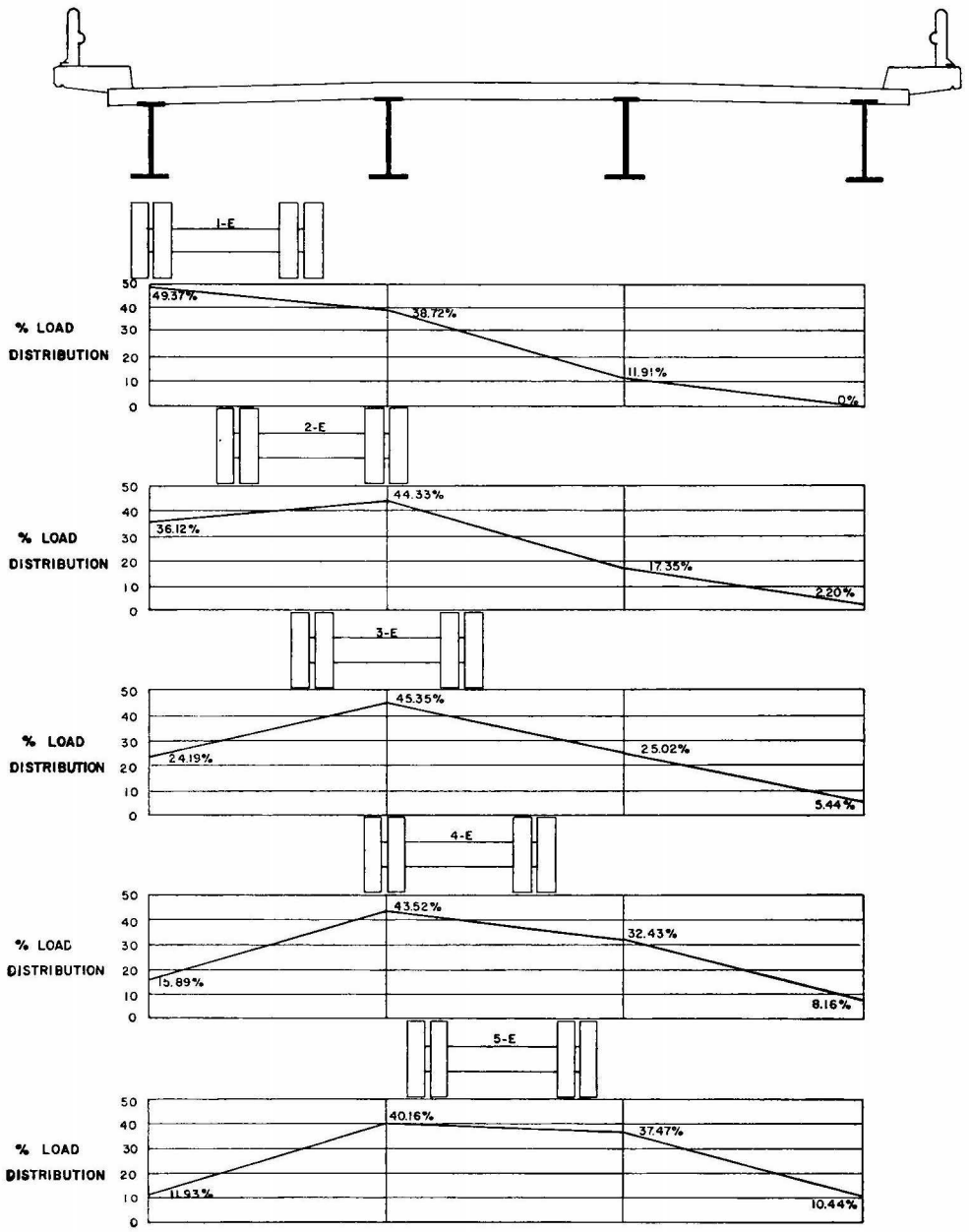

Fig. 36. Static load distribution for aluminum stringer bridge at section I.

not readily analyzed by an exact method, but some theoretical methods which offer a convenient means of determining the amount of the live load distributed to each longitudinal stringer have been proposed[25, 26, 28]. However this part of the report includes only the presentation of data with no attempt to correlate the data to any theoretical results.

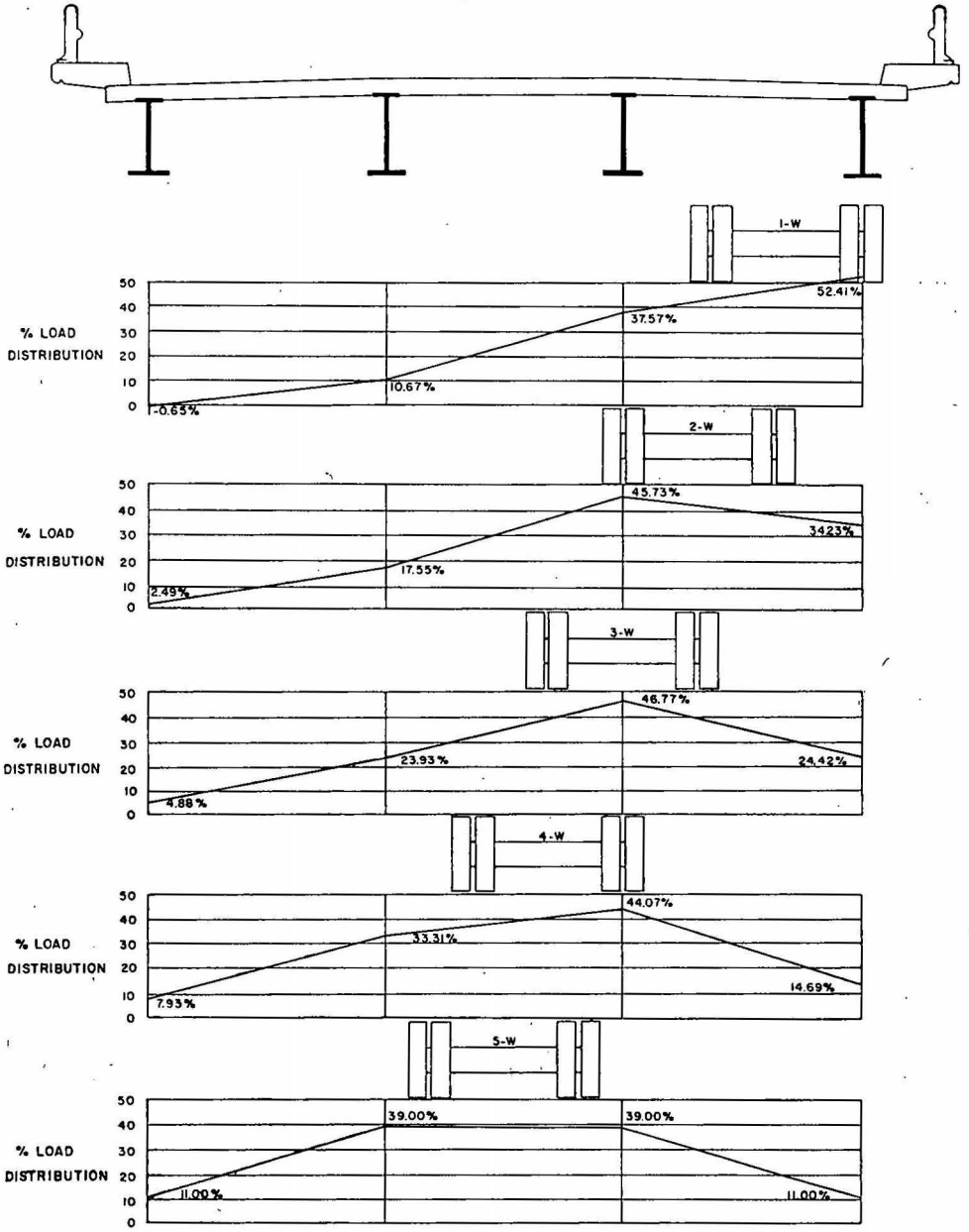

Fig. 36, continued.

The two vehicles used in this experimental study are very similar to the type of vehicle loading used in the design of primary and interstate bridges. Moreover, since these vehicles are similar to each other, except

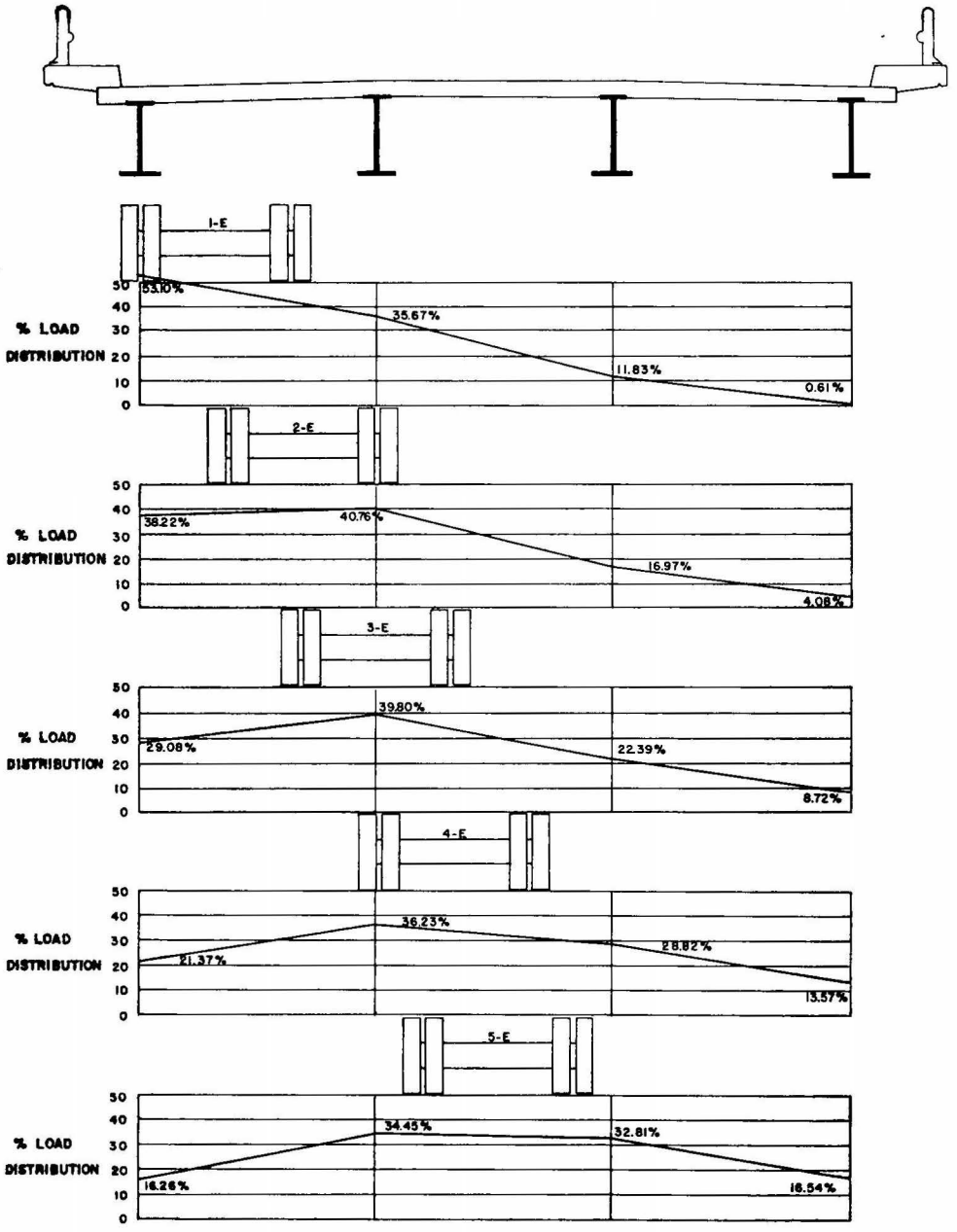

Fig. 37. Static load distribution for aluminum stringer bridge at section II.

for the trailer axles, the experimental load distribution is presented only for vehicle A. The experimental load distribution is determined by using the individual moment in each stringer as a percent of the total moment in the bridge cross section. This procedure gives the percentage of the

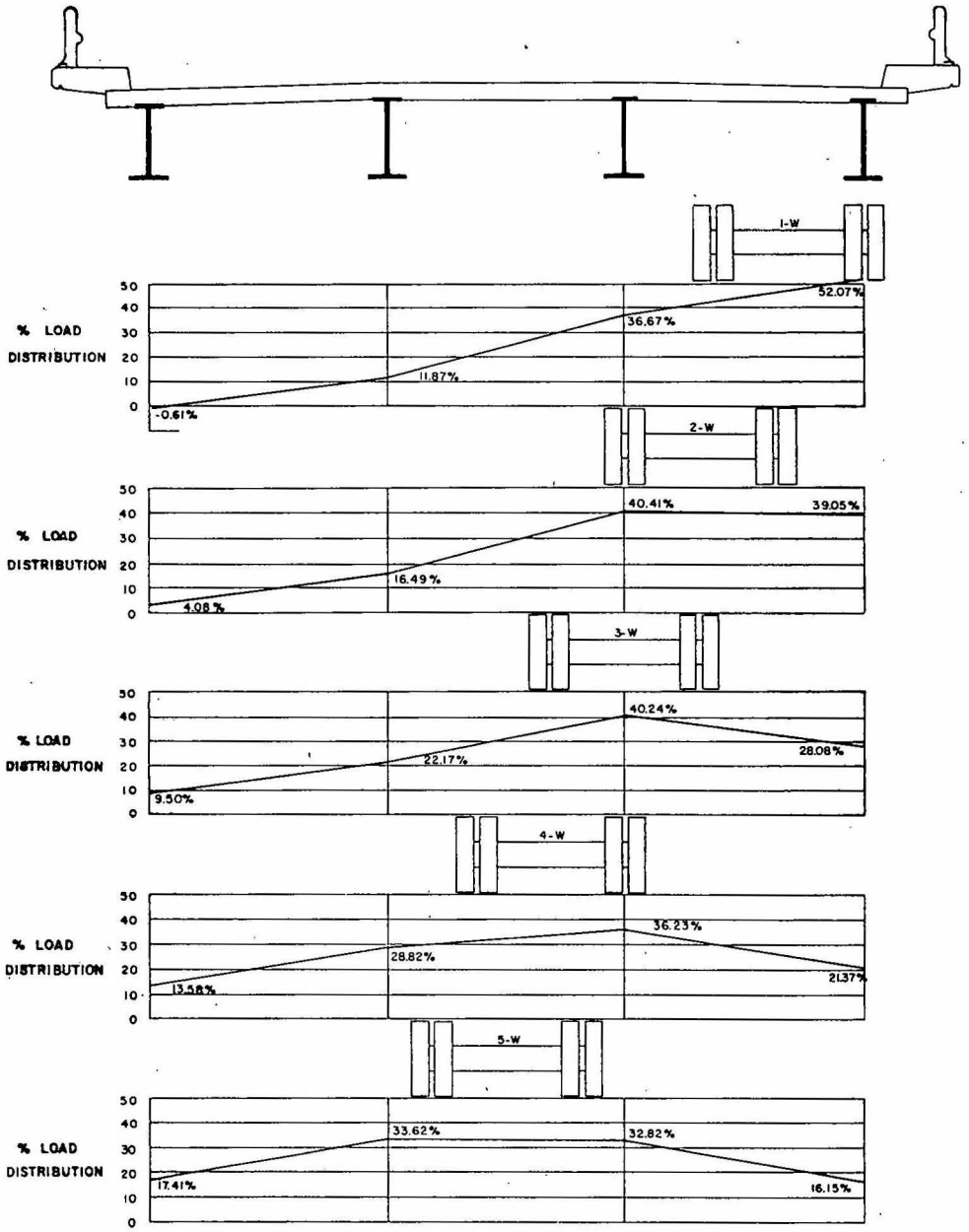

Fig. 37, continued.

total live load distributed into each stringer if the moment diagrams for all the stringers are identical in shape. This assumption is used in the design of this type of bridge structure. The live load moments in the

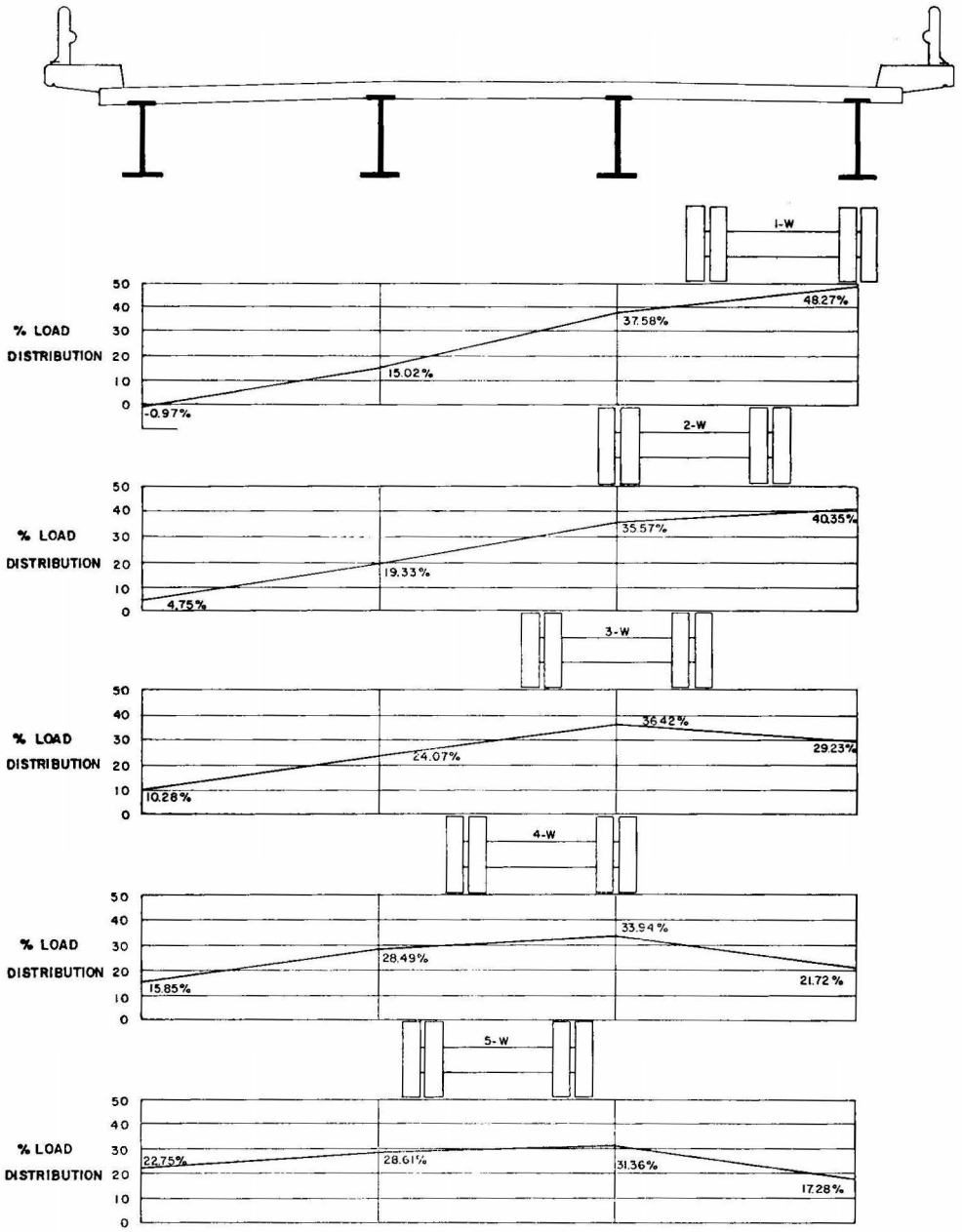

Fig. 38. Static load distribution for aluminum stringer bridge at section III.

stringers were obtained from the measured live load strains, from the modulus of elasticity for the stringers, and from the section moduli for the composite cross sections. The percentage load distribution for the alum-

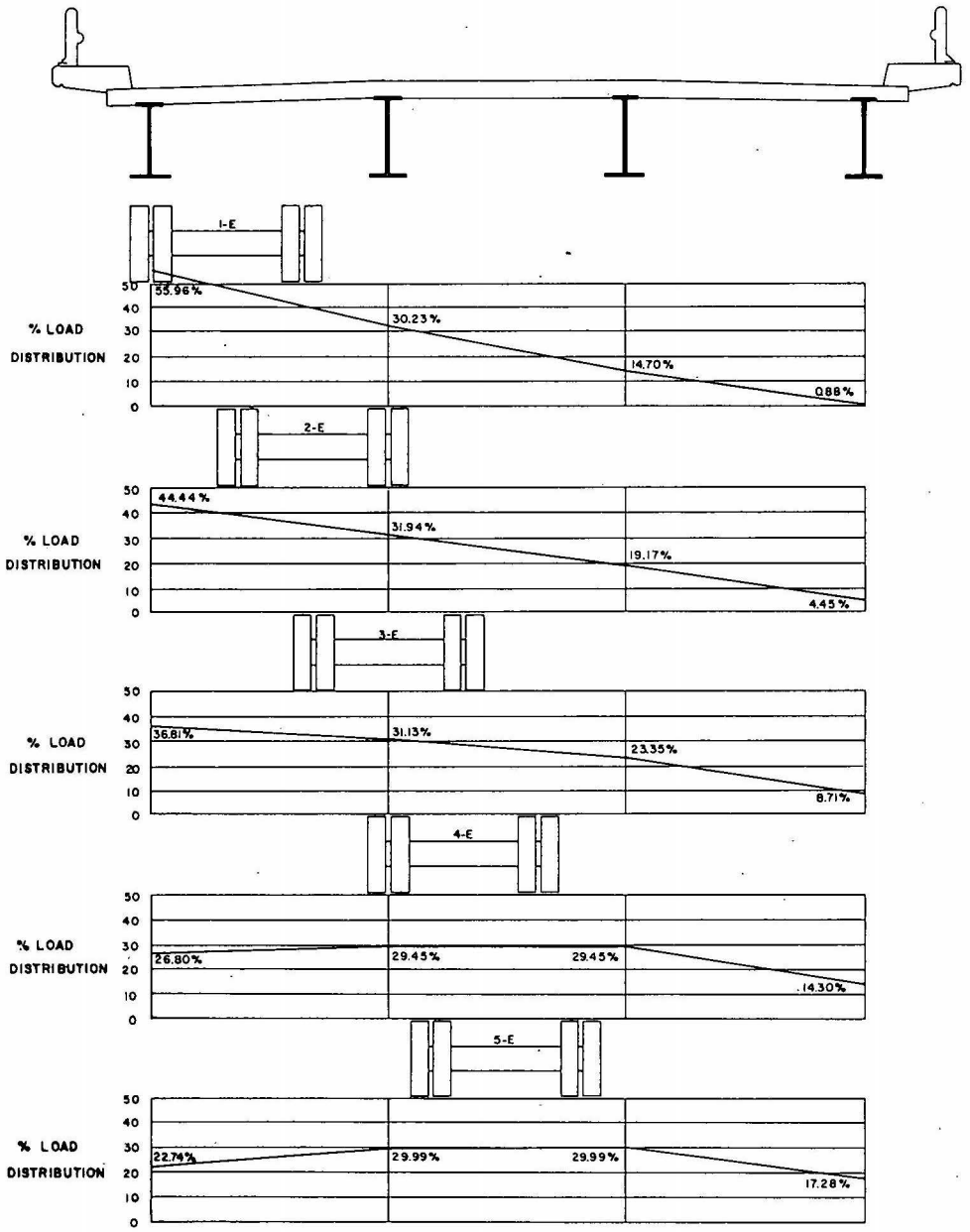

Fig. 38, continued.

inum, steel, and concrete stringer bridges are shown in figures 36 through 45.

The effective composite sections for the prestressed concrete bridge

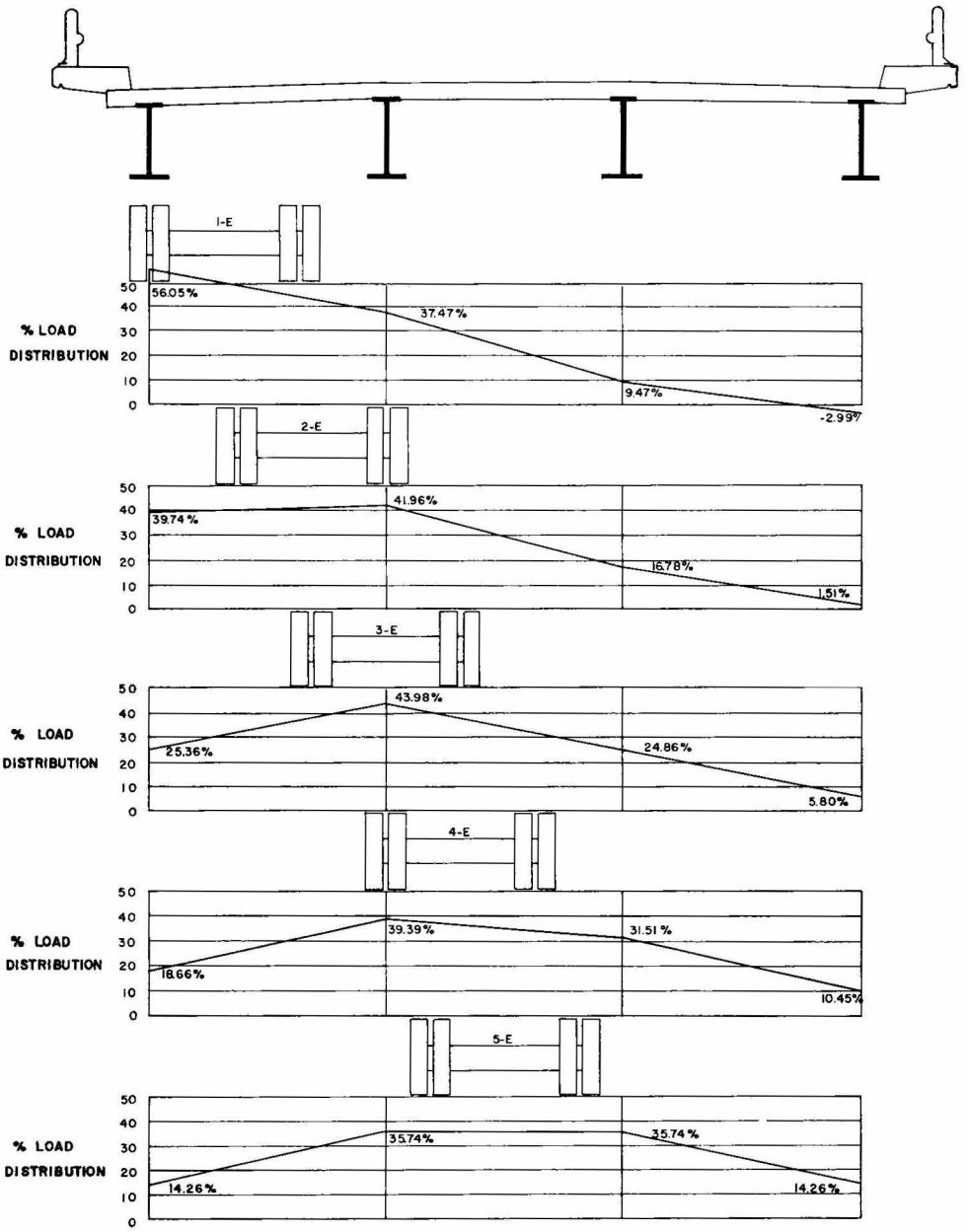

Fig. 39. Static load distribution for aluminum stringer bridge at section IV.

stringers were not evaluated, and therefore the percentage load distribution for this bridge is based on the assumption that the section moduli of the various stringers at each cross section are equal. In the prestressed concrete stringer bridge, only the two positive moment sections I and II were

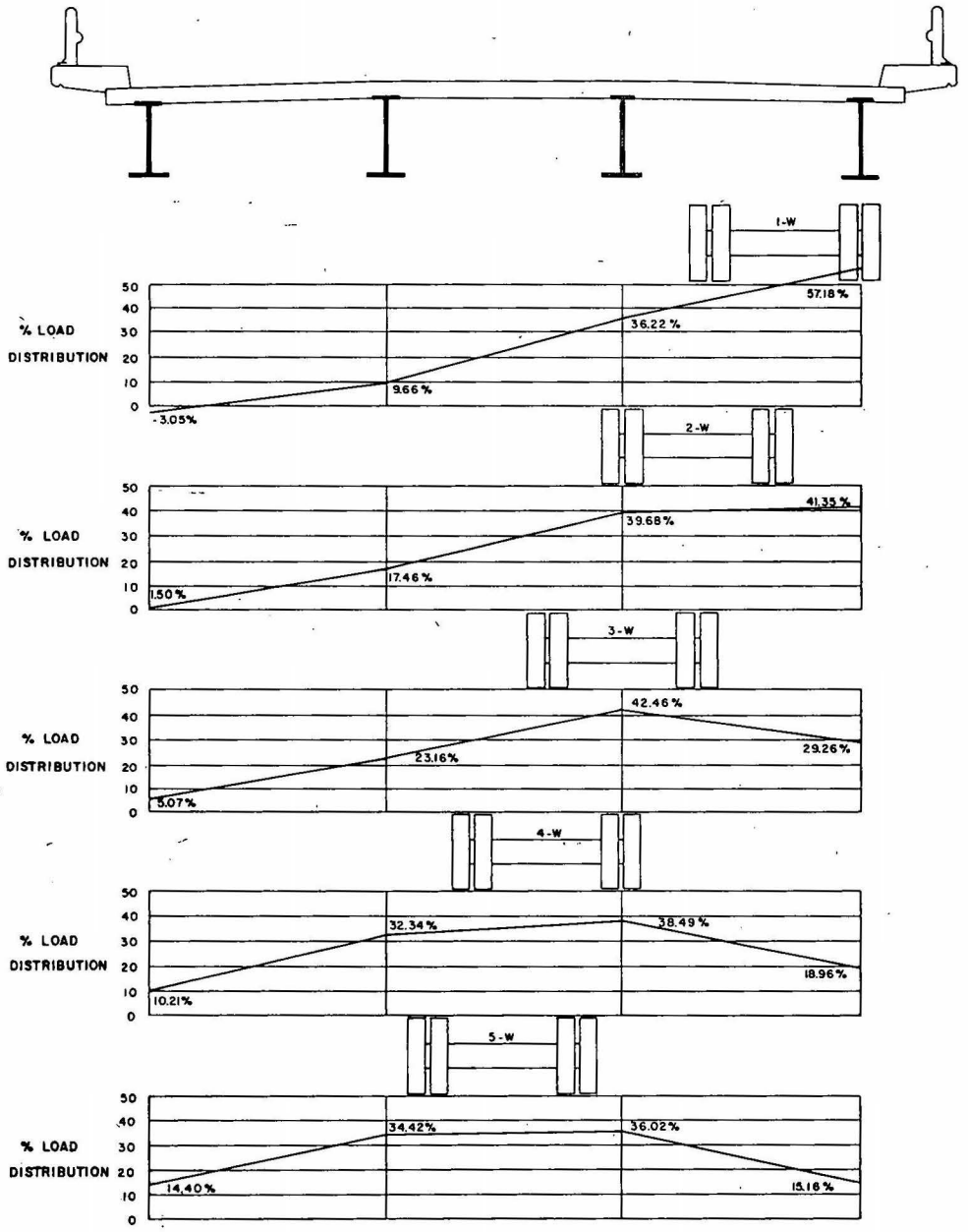

Fig. 39, continued.

analyzed for load distribution. However, for the aluminum and steel stringer bridges the load distribution is shown for both the positive and negative moment sections (sections I, II, III, and IV).

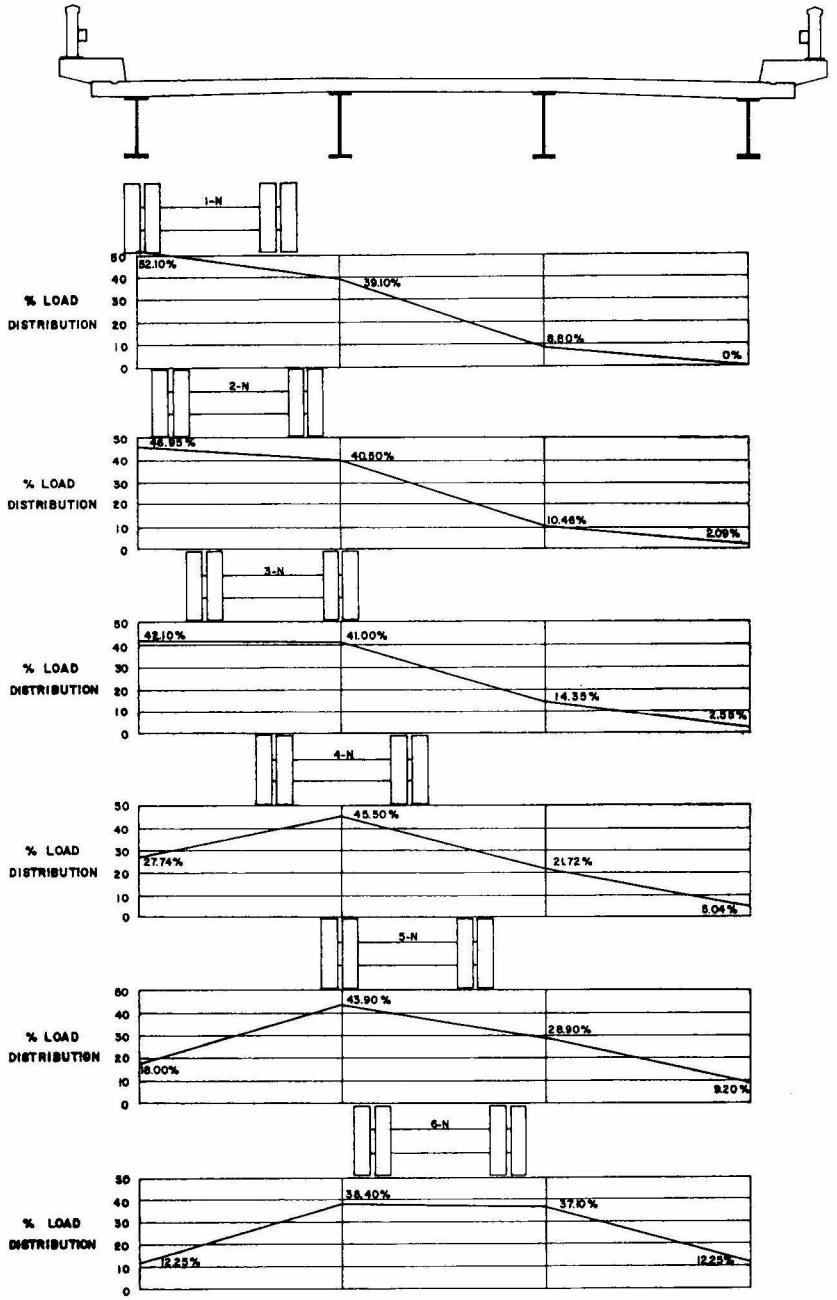

Fig. 40. Static load distribution for steel stringer bridge at section I.

Dynamic load. The dynamic response of the bridges tested was obtained by moving load tests. These moving load tests were performed on four test lanes, two for each direction of travel for vehicle speeds begin-

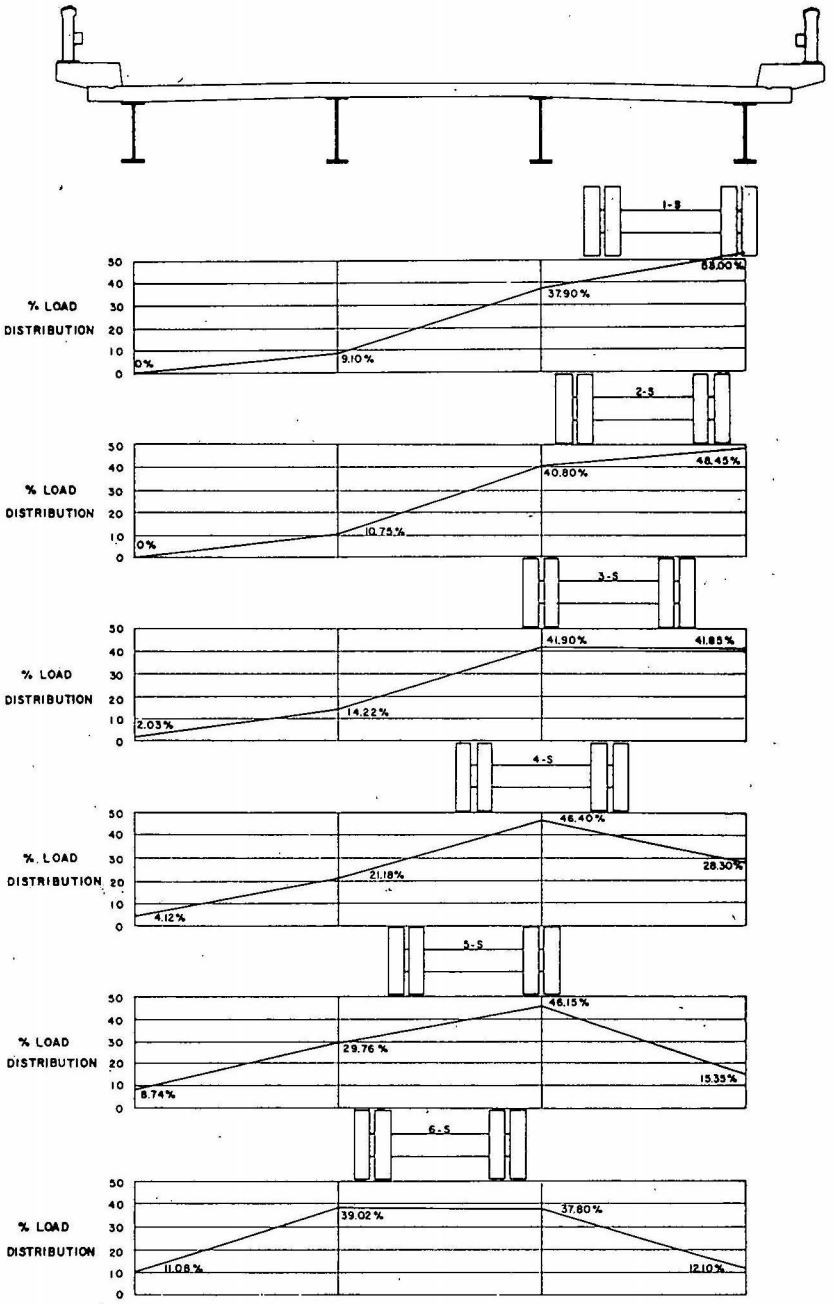

Fig. 40, continued.

ning at approximately 10 mph and increasing by increments up to the maximum attainable speed. The data from the continuous strain time

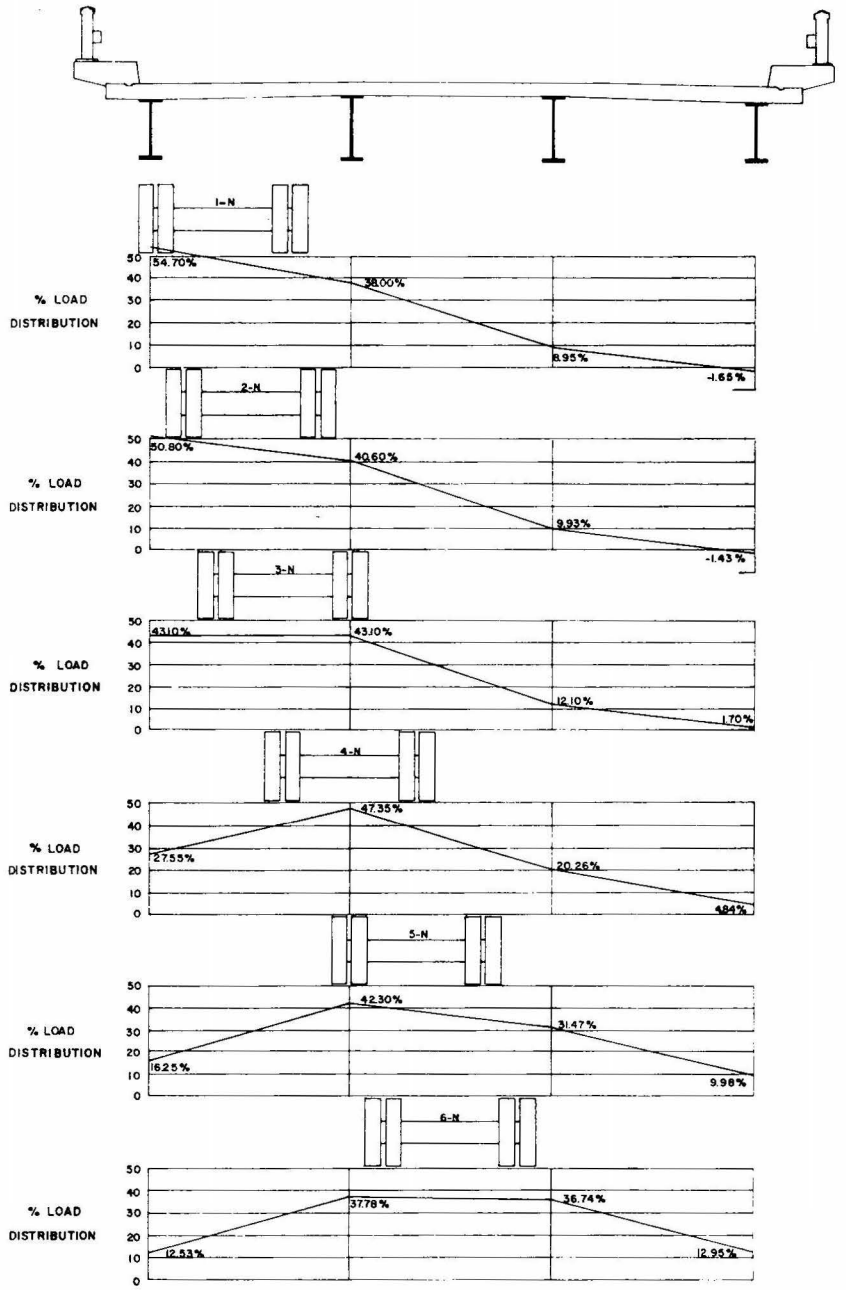

Fig. 41. Static load distribution for steel stringer bridge at section II.

records obtained was reduced as before to obtain the maximum moment in each longitudinal stringer for the vehicle in approximately the same longitudinal position as the maximum static moment.

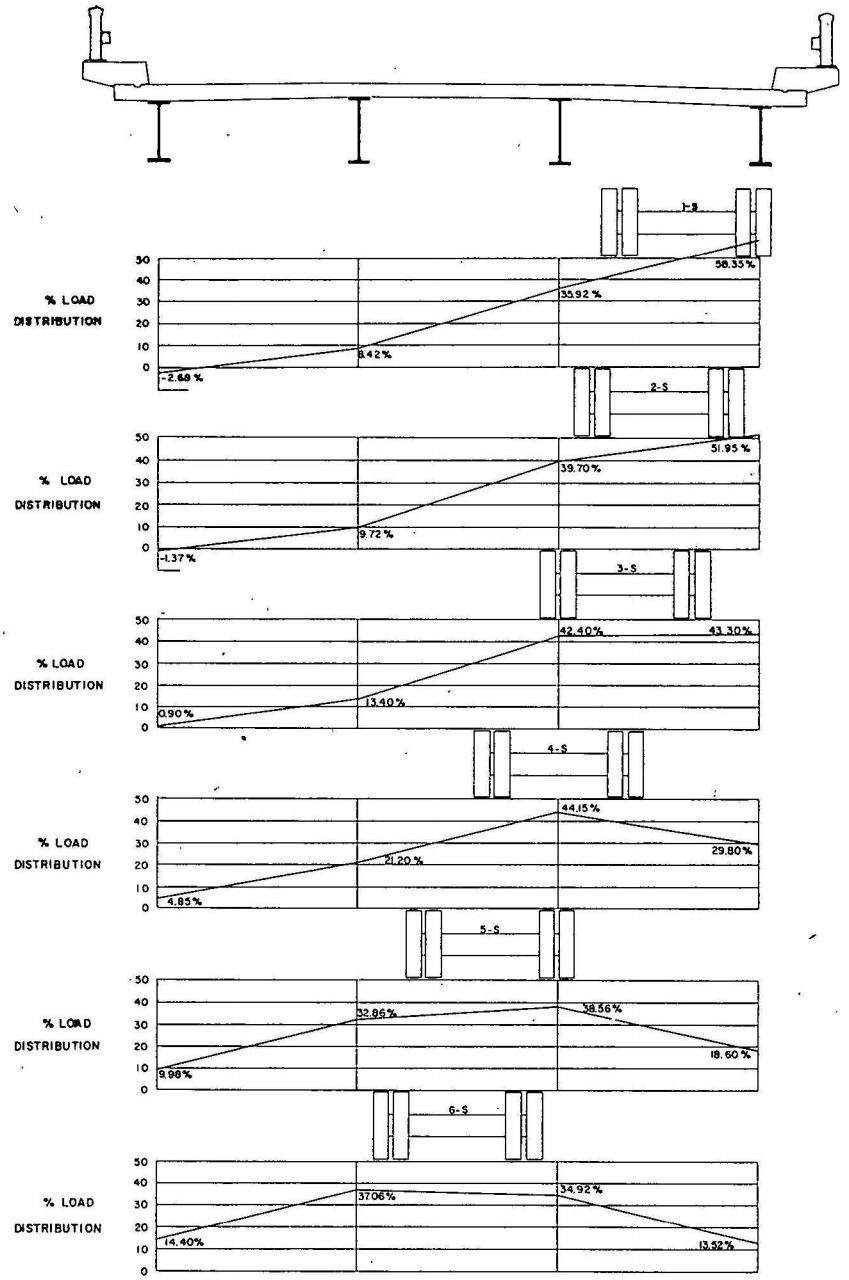

Fig. 41, continued.

From these data the dynamic load distribution was obtained for the vehicle traveling in the experimental lanes at different speeds. The distri-

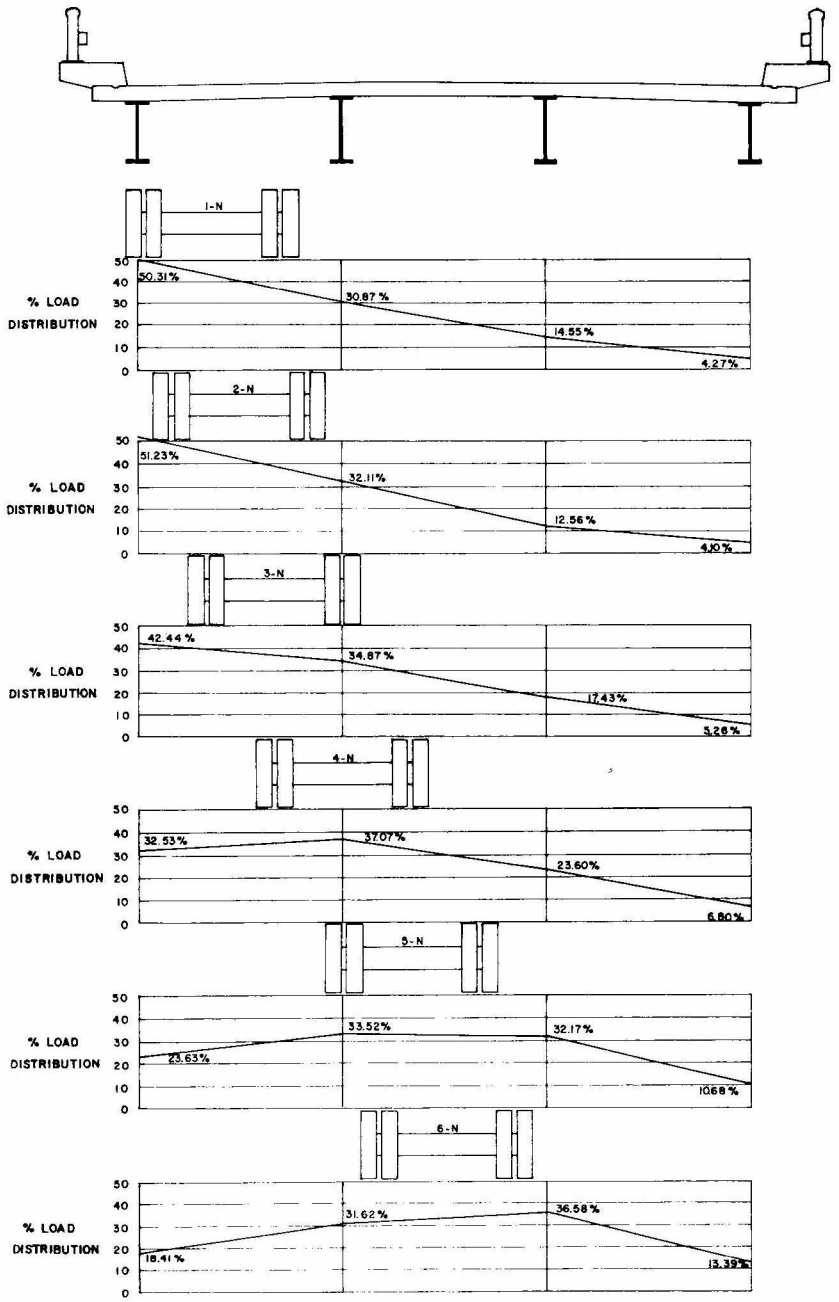

Fig. 42. Static load distribution for steel stringer bridge at section III.

bution of load to the longitudinal stringers, as obtained from the moments, for the vehicle traveling on the experimental lanes at various speeds is shown in figures 46 through 53 for the aluminum and steel stringer bridges

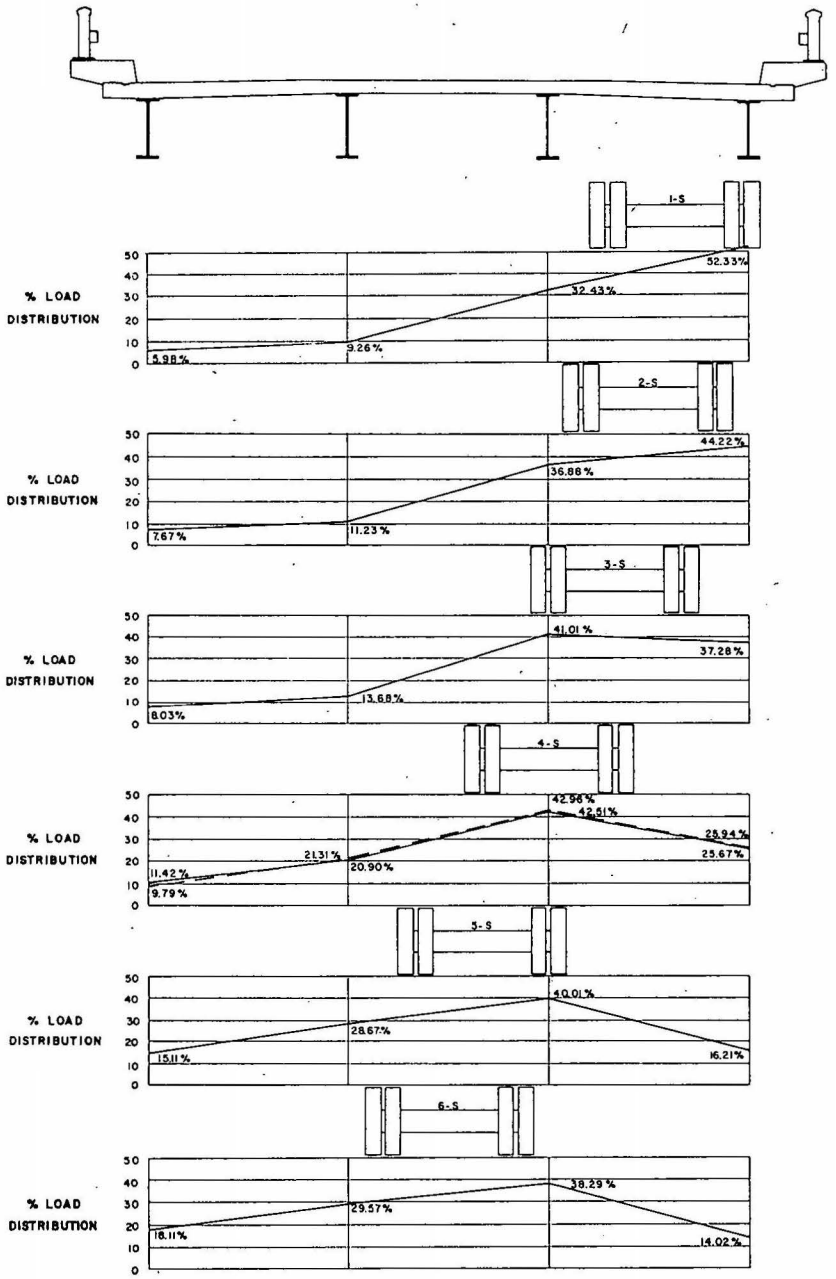

Fig. 42, continued.

at the positive and negative experimental sections, sections I, II, III, and IV. The bridge cross section and the vehicle position is shown at the top

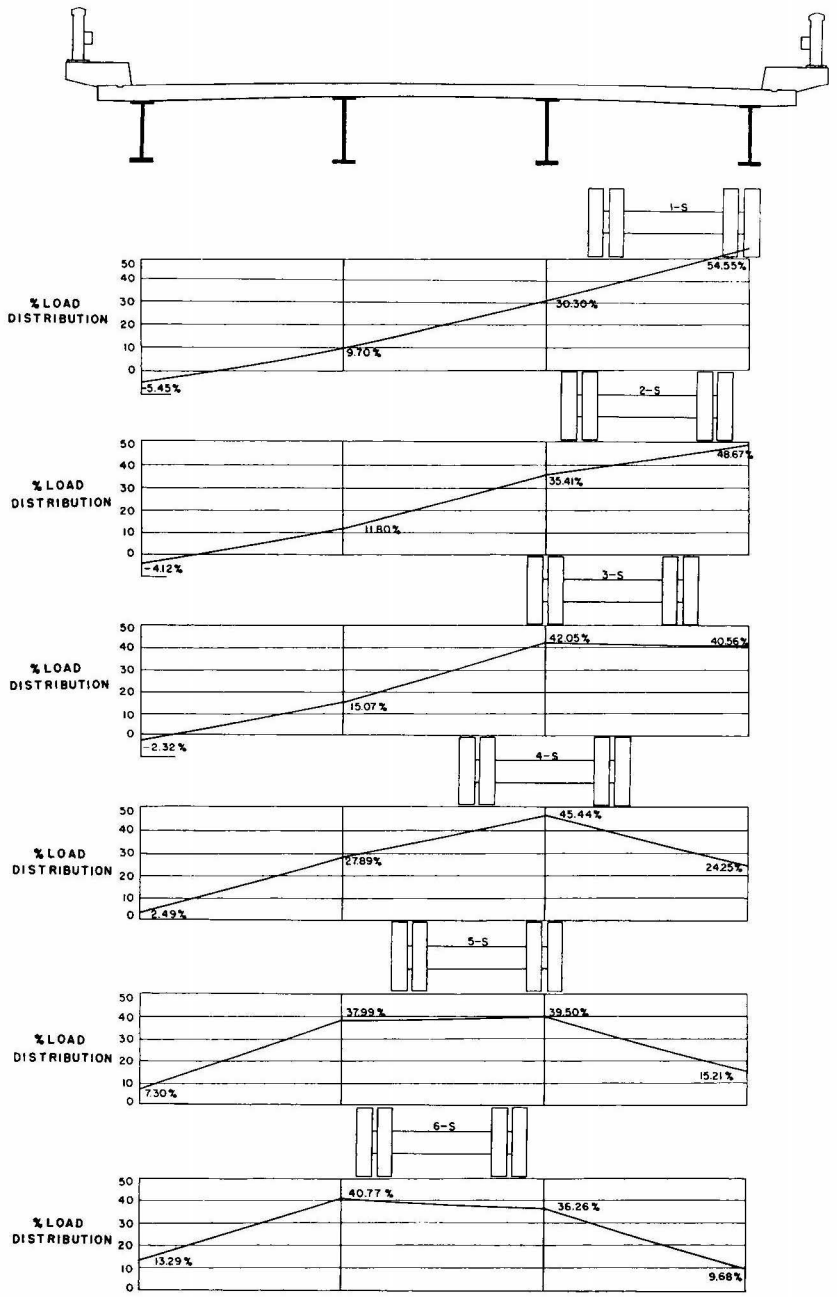

Fig. 43. Static load distribution for steel stringer bridge at section IV.

of the graph. Each point of the graph indicates the load distribution for a different speed. The solid line indicates this dynamic load distribution, and the dotted line represents the value obtained from the static tests at

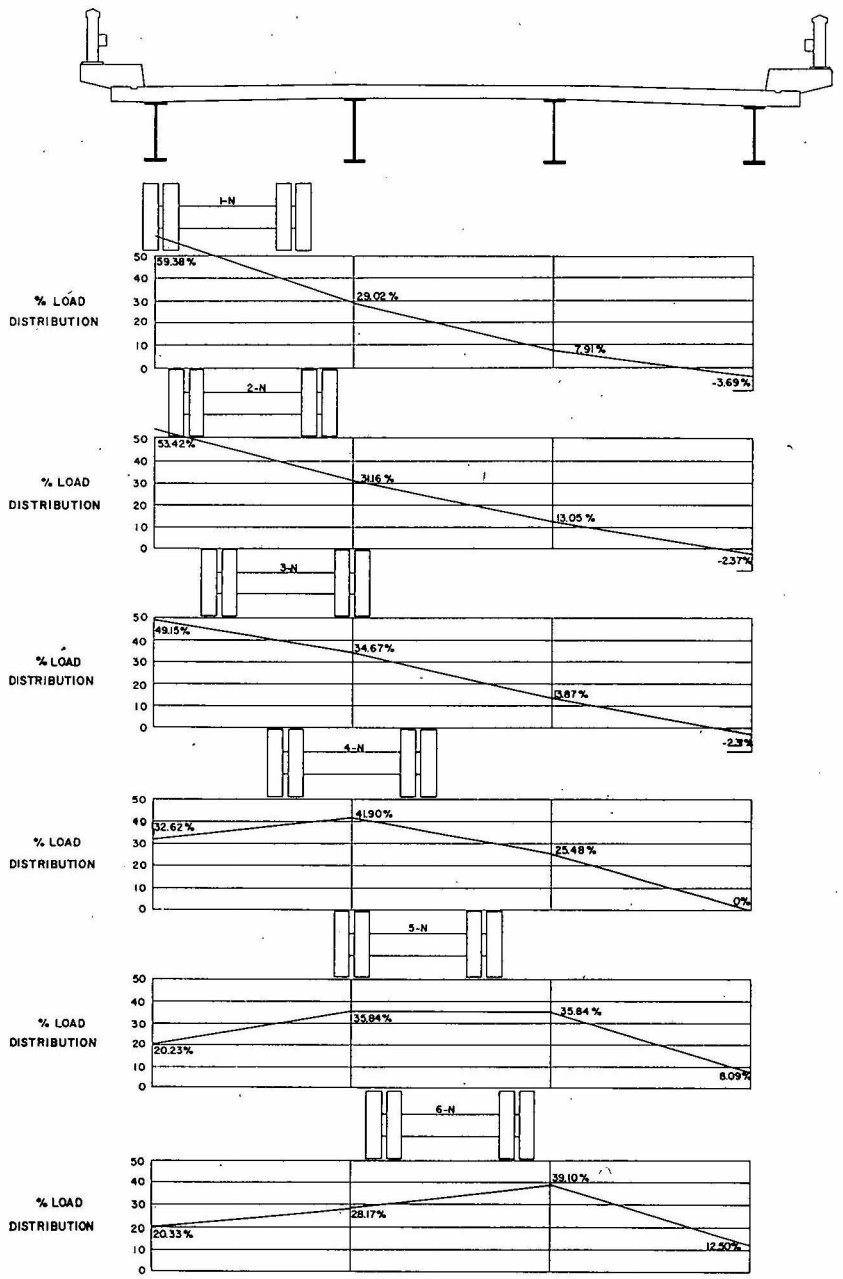

Fig. 43, continued.

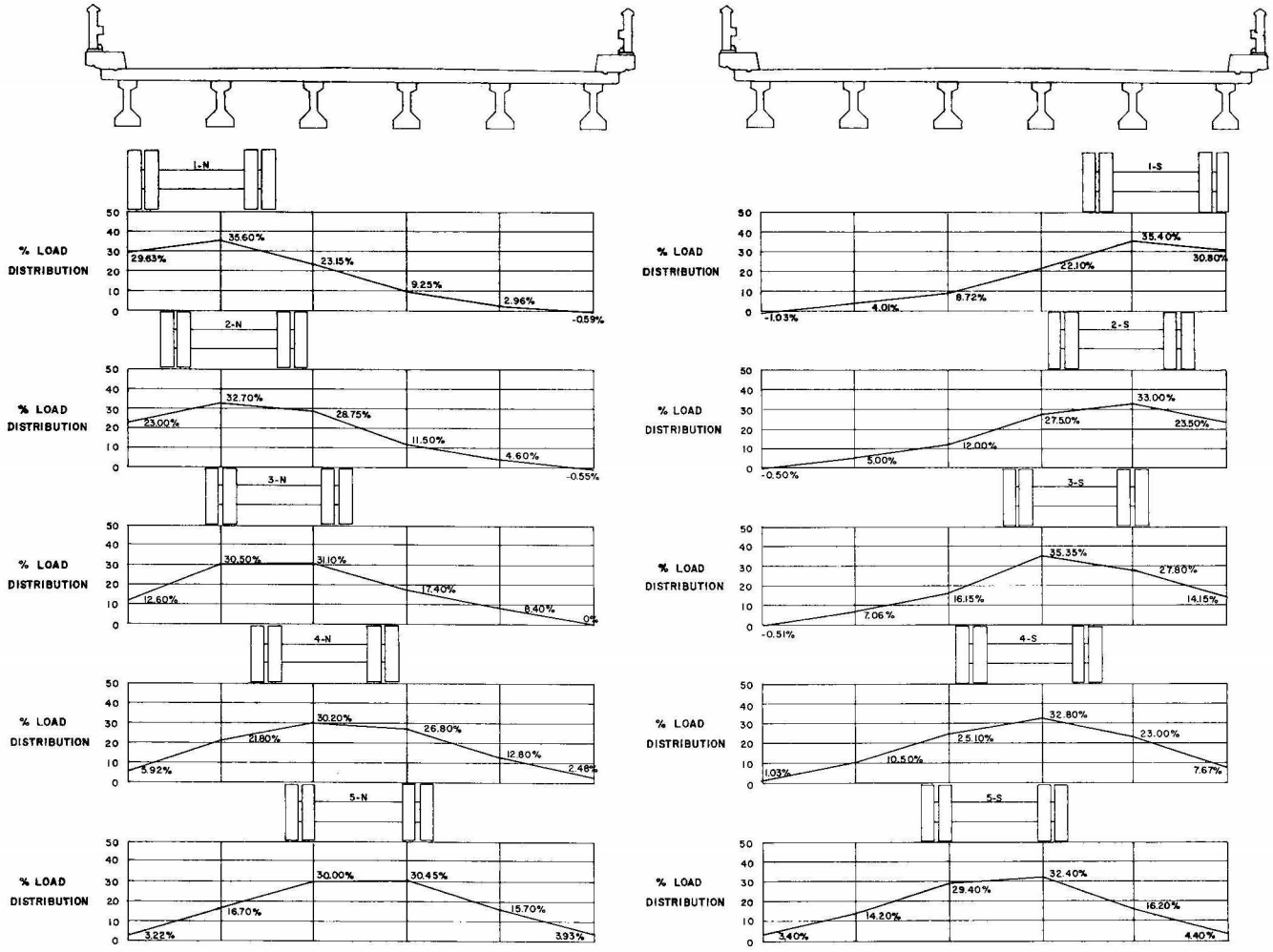

Fig. 44. Static load distribution for the pretensioned prestressed concrete bridge at section I.

the same section. The static load distributions are the same as the values shown previously. Since these results are typical of the comparison obtained for the other bridges tested, and since this correlation has been previously

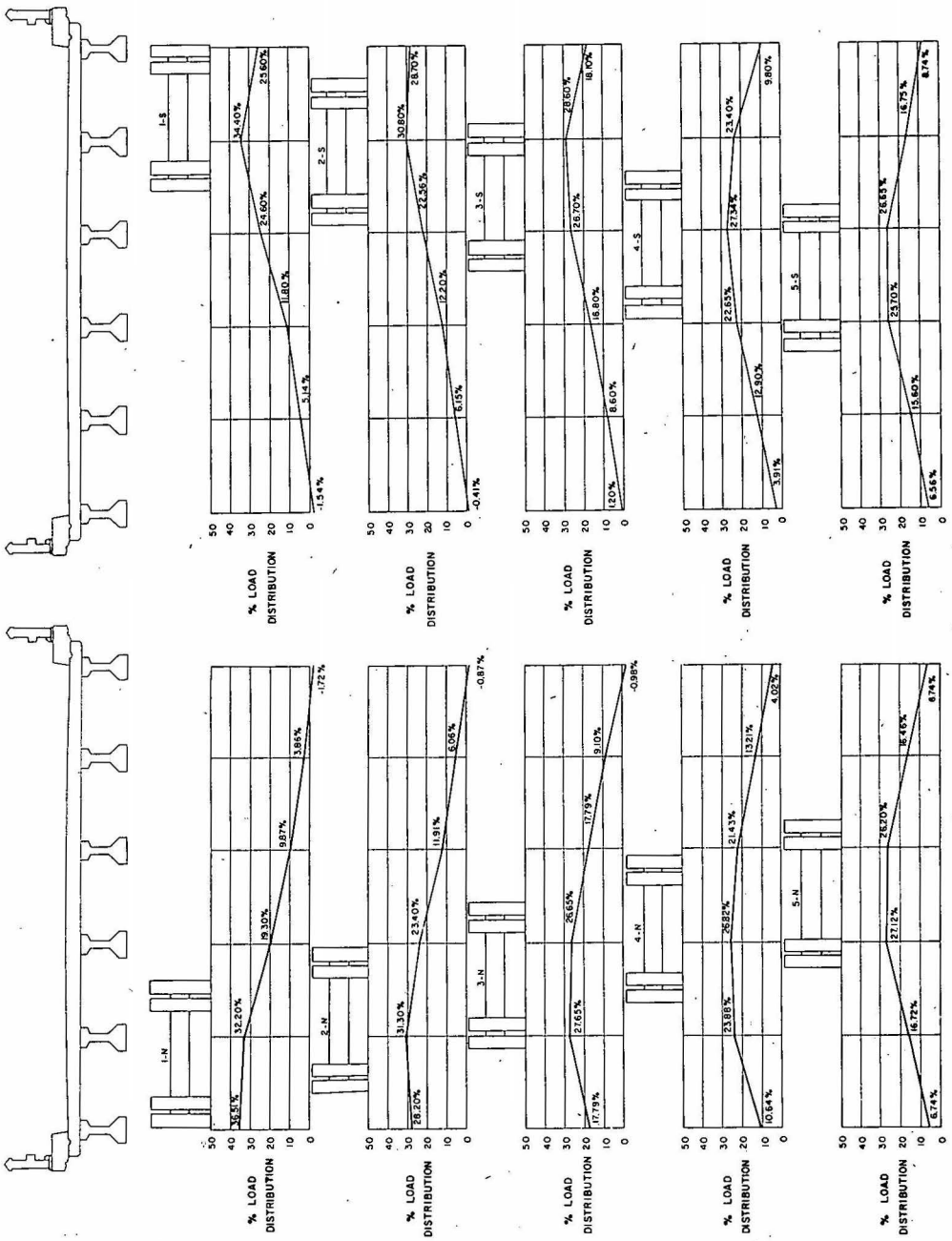

Fig. 45. Static load distribution for the pretensioned prestressed concrete bridge at section II.

presented[27], the comparison of dynamic and static load distribution is shown only for the aluminum and steel stringer bridges at all the experimental sections.

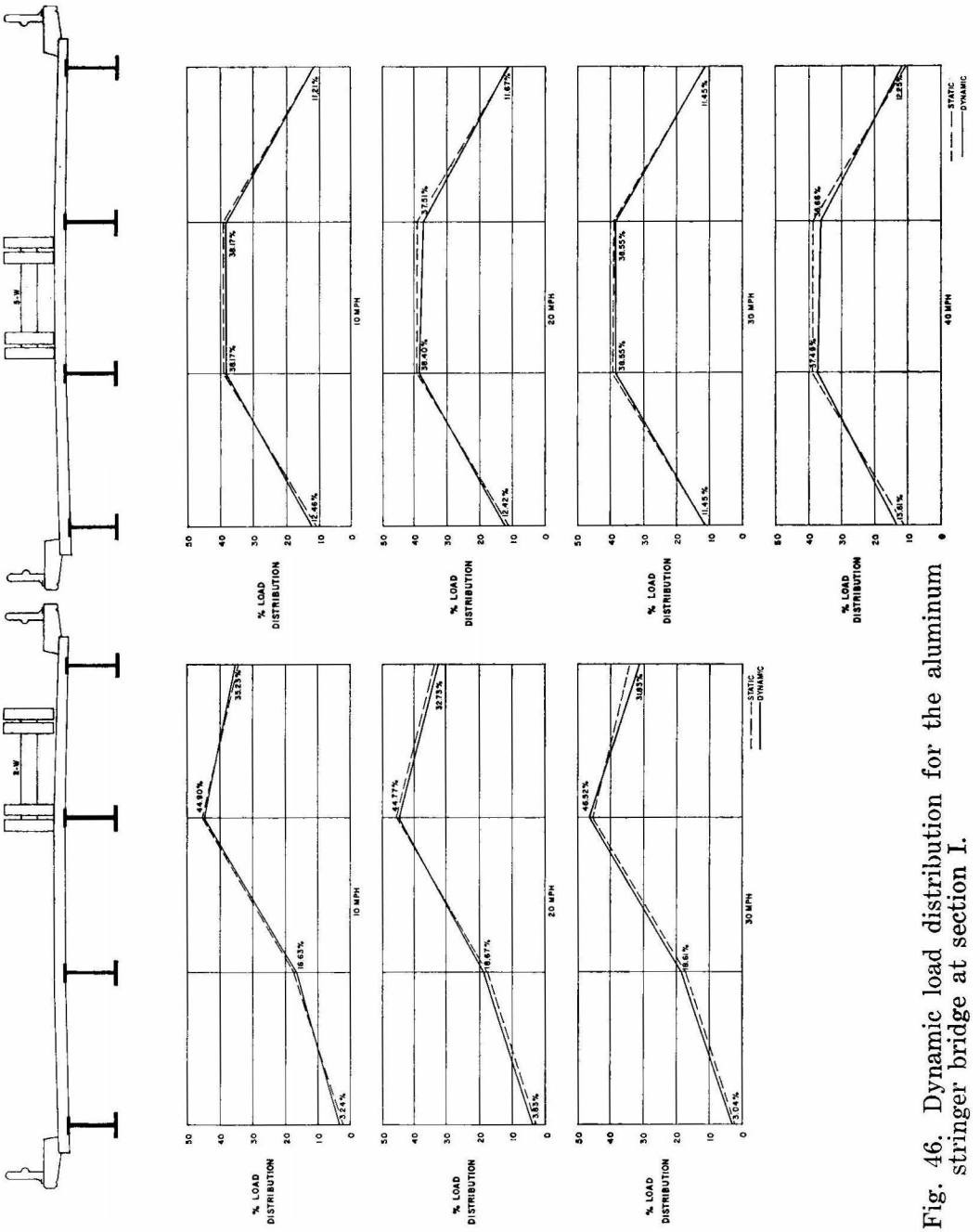

Fig. 46. Dynamic load distribution for the aluminum stringer bridge at section I.

Influence lines for the stringers

The use of the static load distribution curves is facilitated by the construction of influence lines for the percentage load in each stringer.

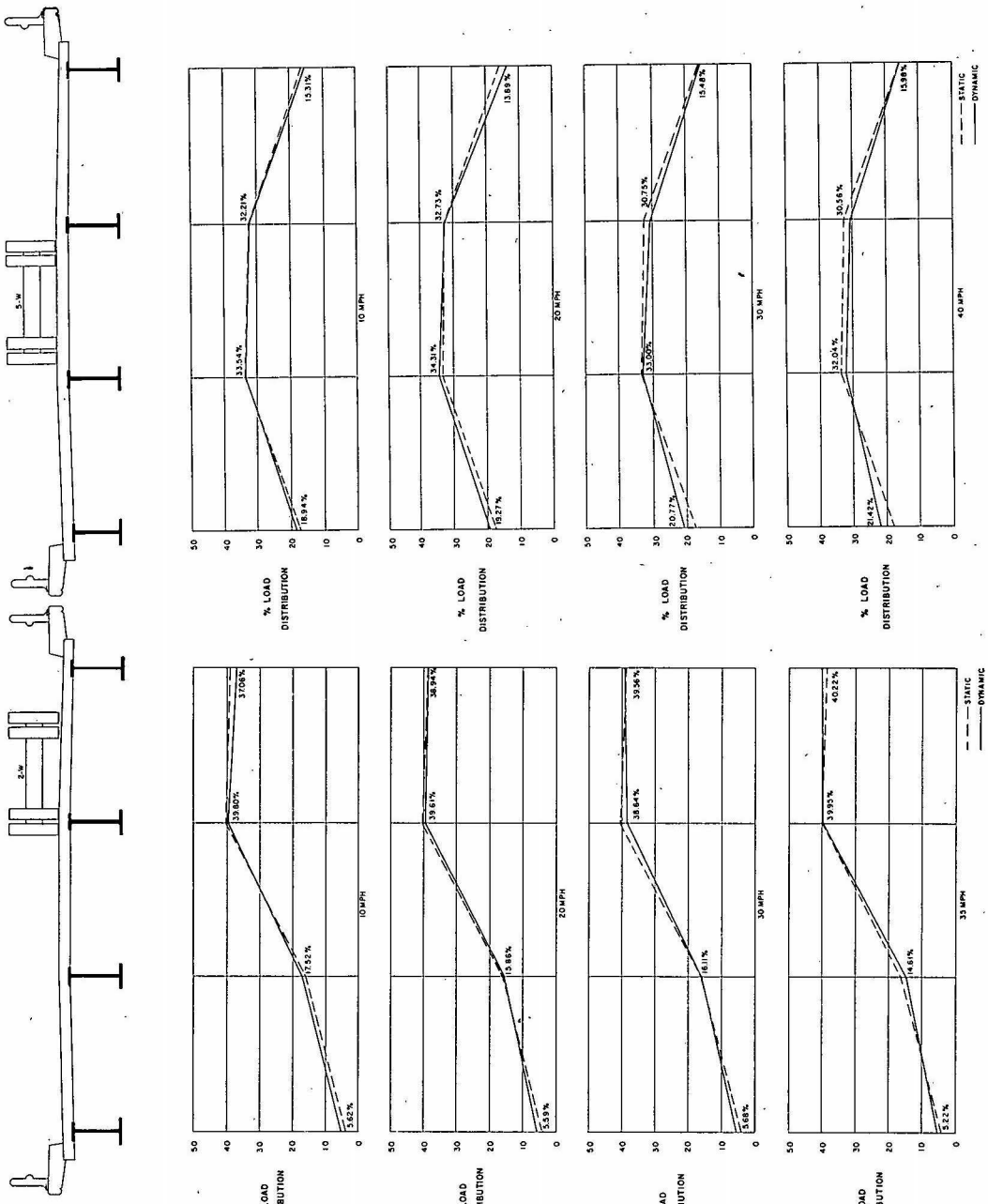

Fig. 47. Dynamic load distribution for the aluminum stringer bridge at section II.

To obtain these influence lines the static load distribution values were averaged for the symmetrical stringers which correspond with the loading of symmetrical lanes. For example, the value from one outside stringer with the load in lane 2-S is averaged with the value from the other outside

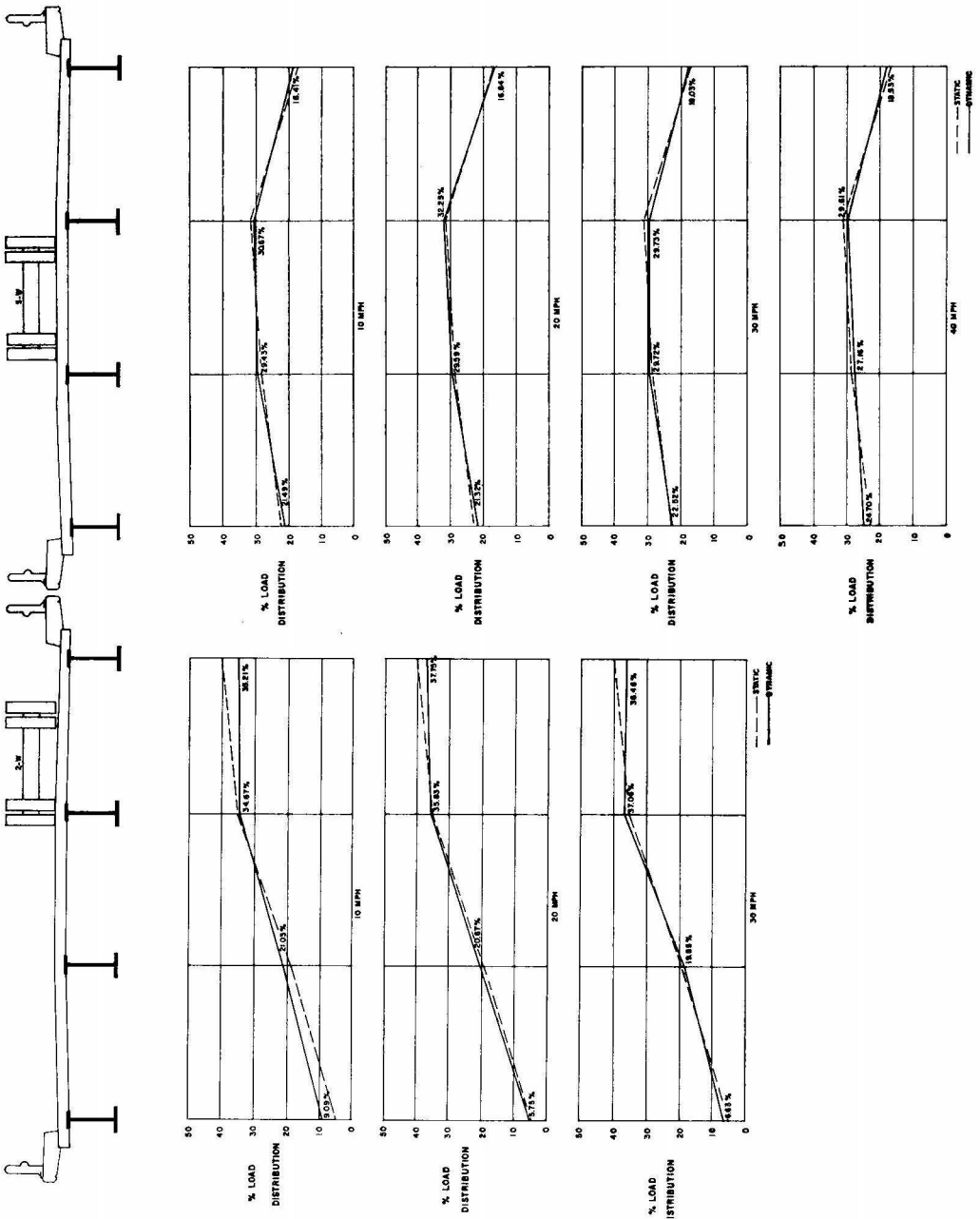

Fig. 48. Dynamic load distribution for the aluminum stringer bridge at section III.

stringer with the load in lane 2-N. These average values were then plotted to correspond with the center line of the vehicle. The resulting influence lines (figures 54 and 55) indicate the percentage of a unit vehicle distri-

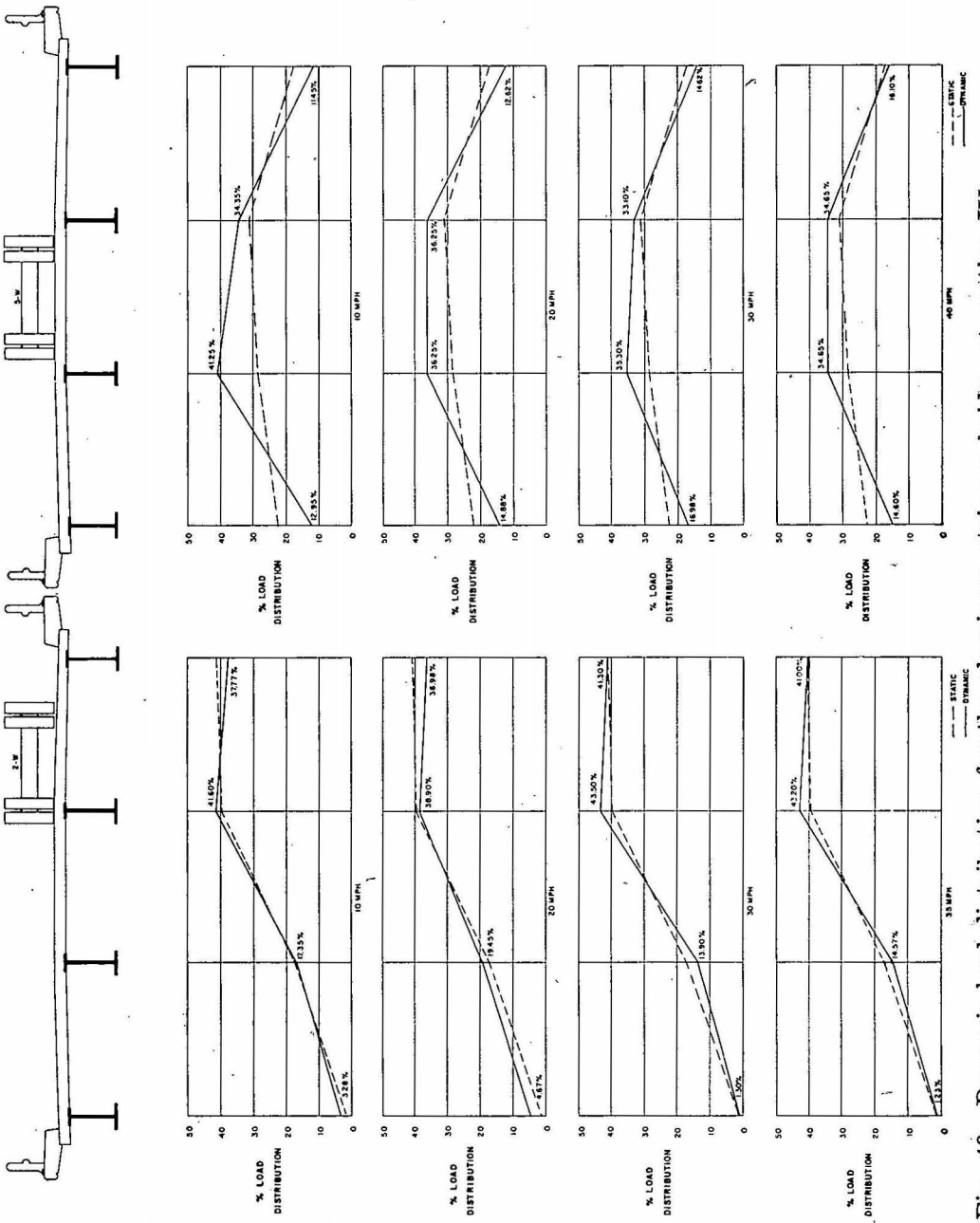

Fig. 49. Dynamic load distribution for the aluminum stringer bridge at section IV.

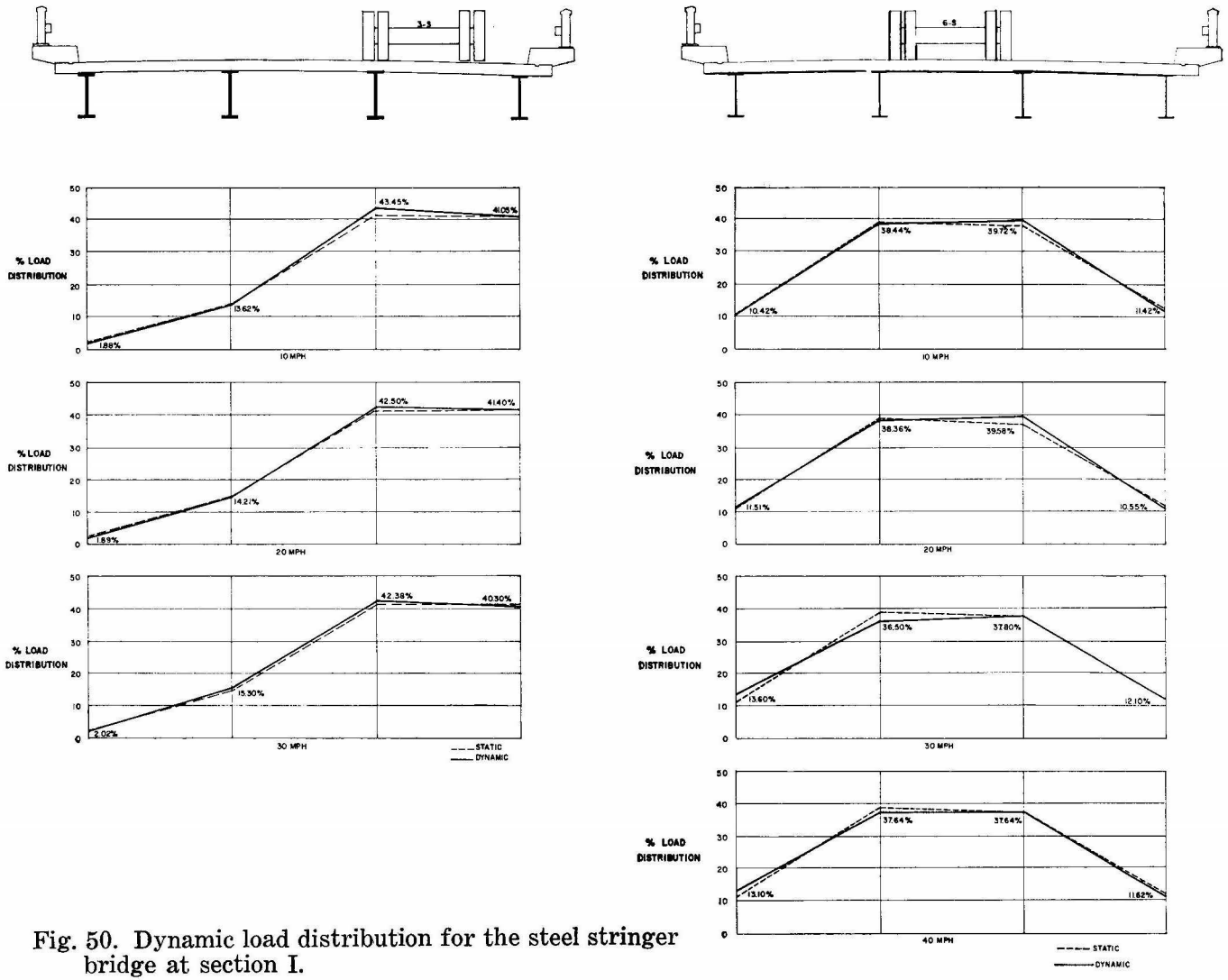

Fig. 50. Dynamic load distribution for the steel stringer bridge at section I.

buted to each respective stringer by the ordinate corresponding to the center line of the vehicle. The influence lines presented are only for the positive moment sections (section I and II).

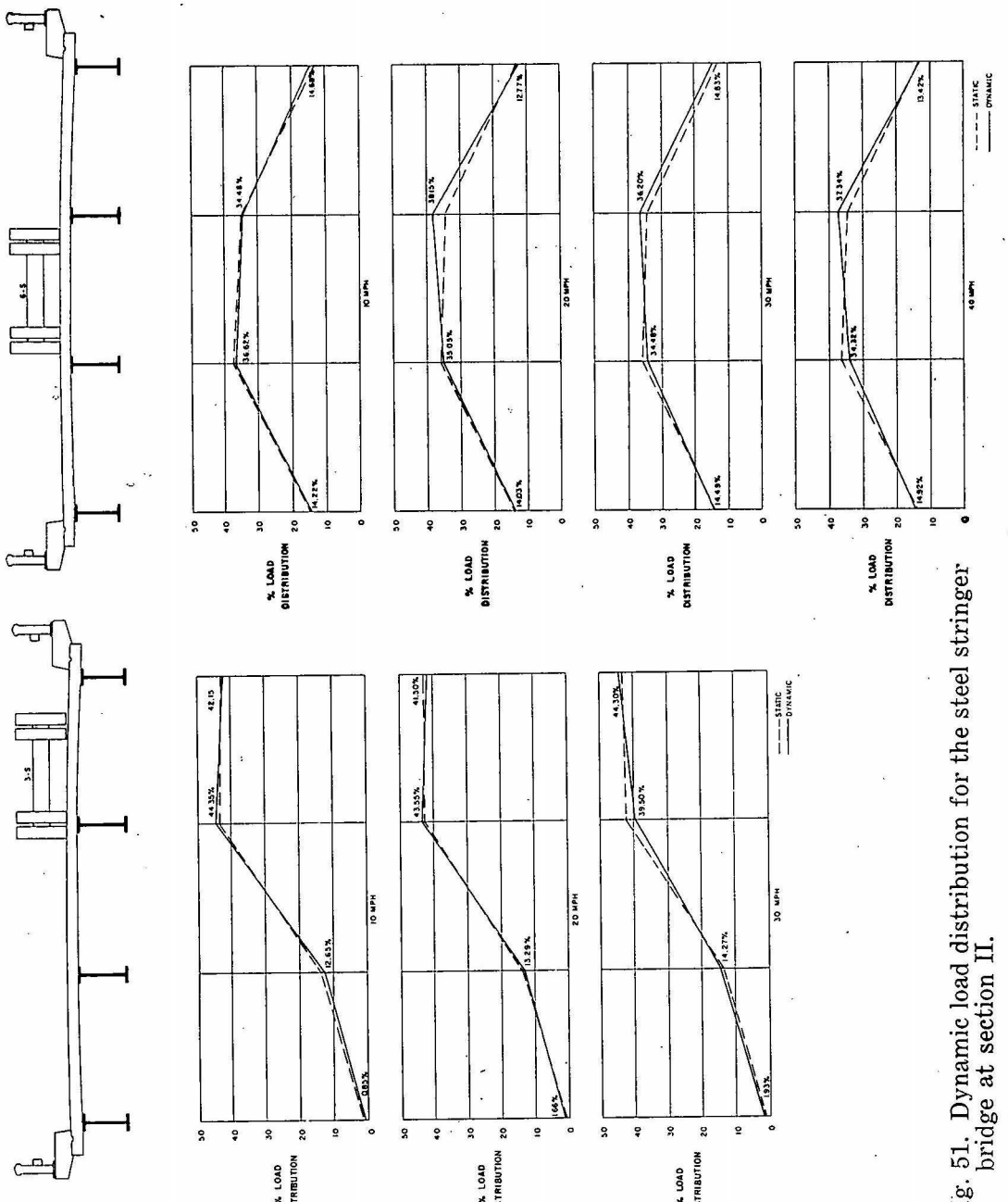

Fig. 51. Dynamic load distribution for the steel stringer bridge at section II.

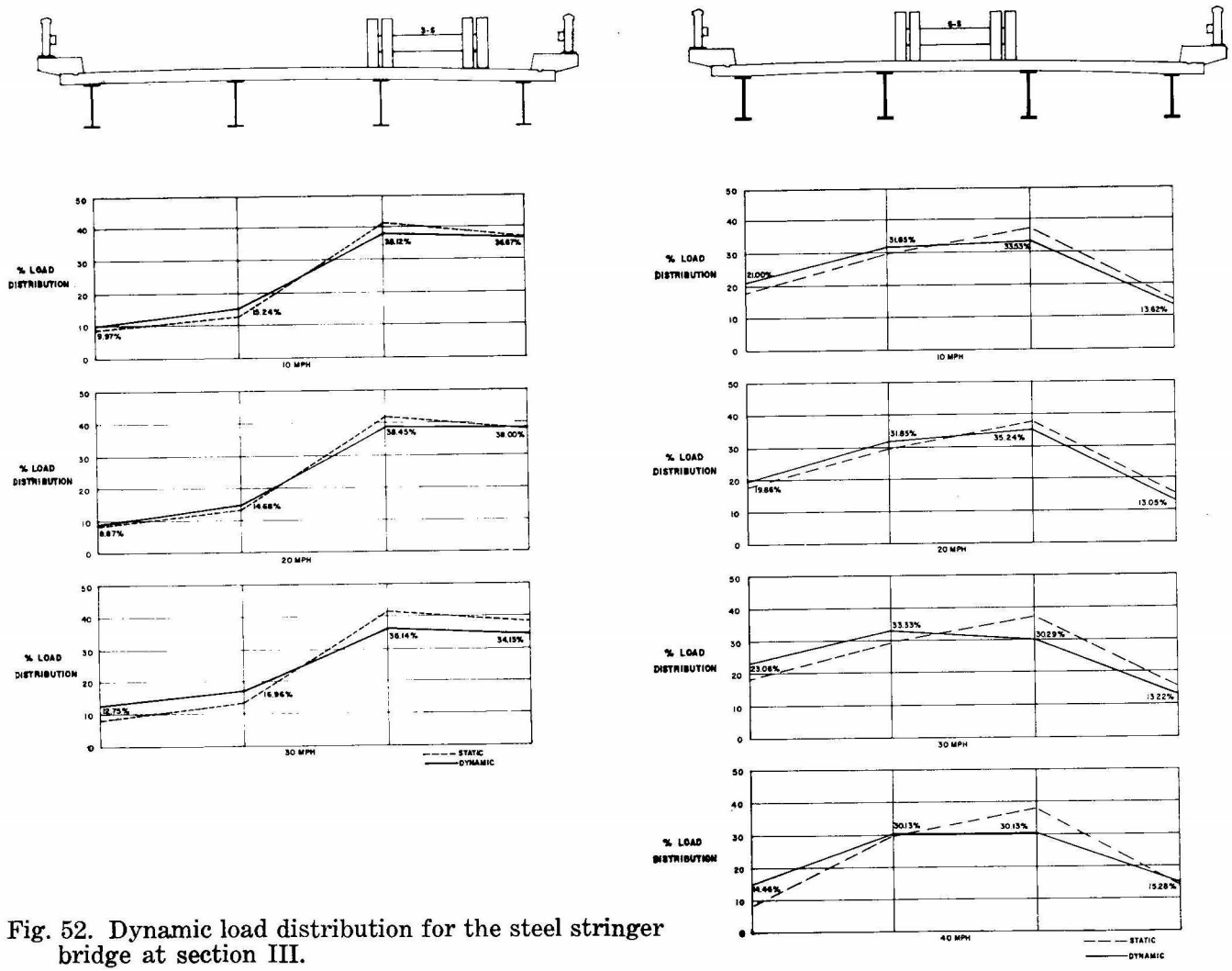

Fig. 52. Dynamic load distribution for the steel stringer bridge at section III.

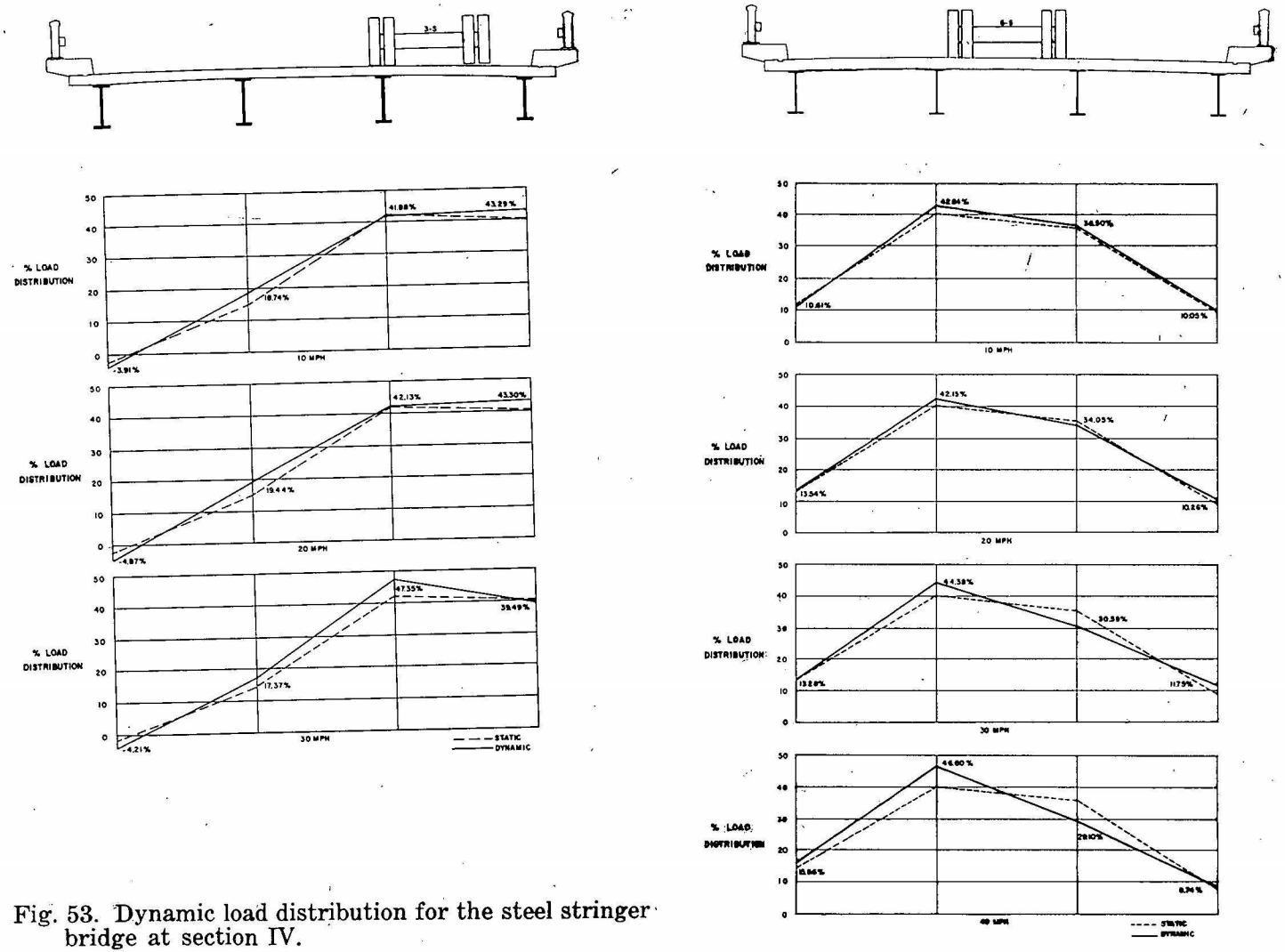

Fig. 53. Dynamic load distribution for the steel stringer bridge at section IV.

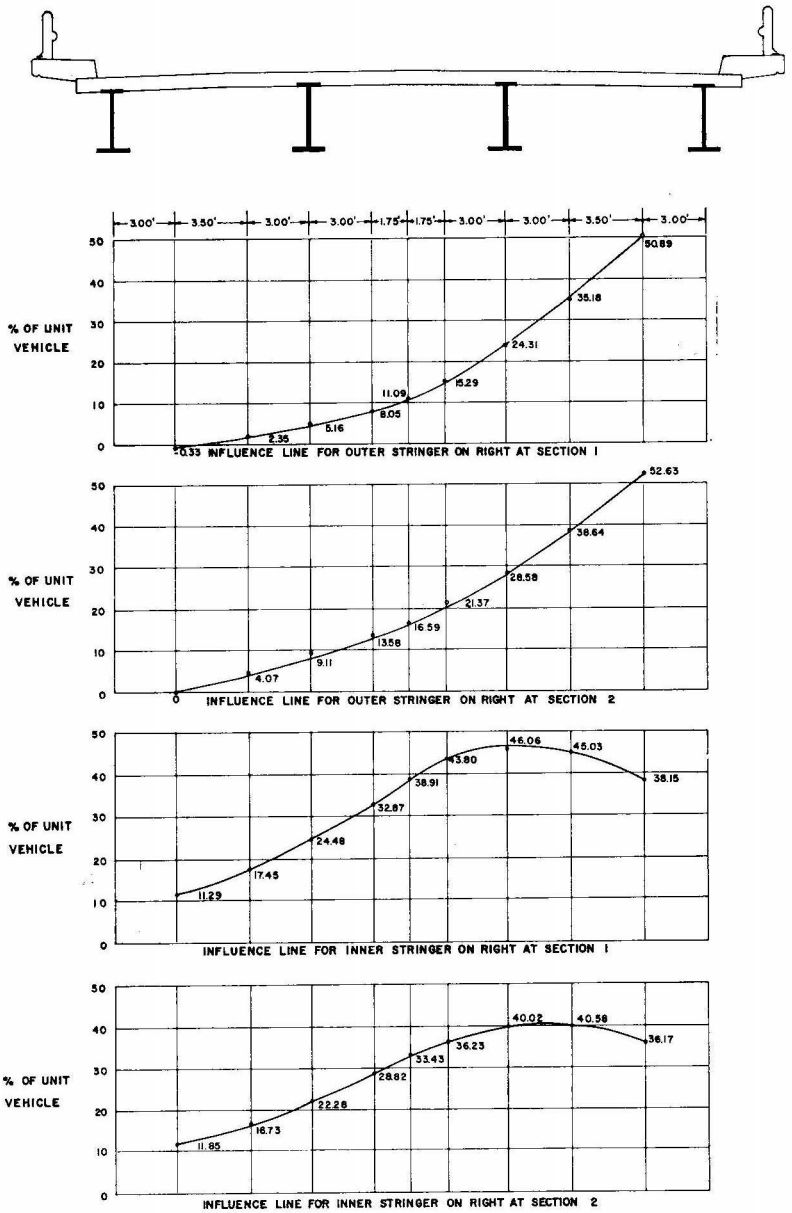

Fig. 54. Influence lines for aluminum stringer bridge.

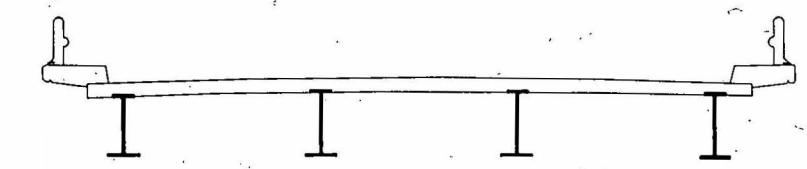

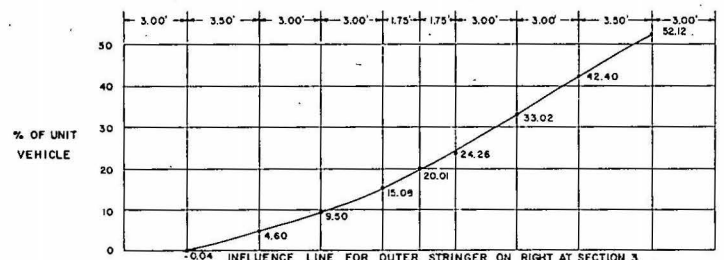

INFLUENCE LINE FOR OUTER STRINGER ON RIGHT AT SECTION 3

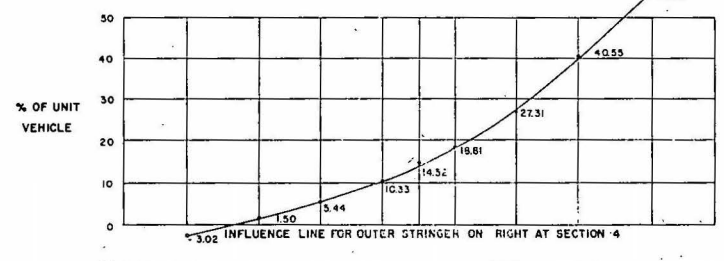

INFLUENCE LINE FOR OUTER STRINGER ON RIGHT AT SECTION 4

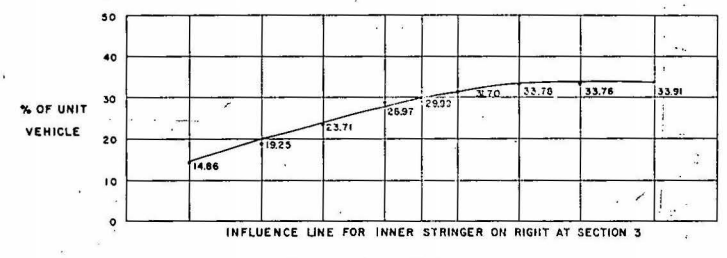

INFLUENCE LINE FOR INNER STRINGER ON RIGHT AT SECTION 3

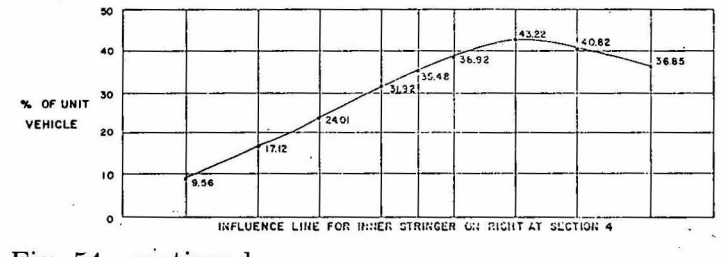

INFLUENCE LINE FOR INNER STRINGER ON RIGHT AT SECTION 4

Fig. 54, continued.

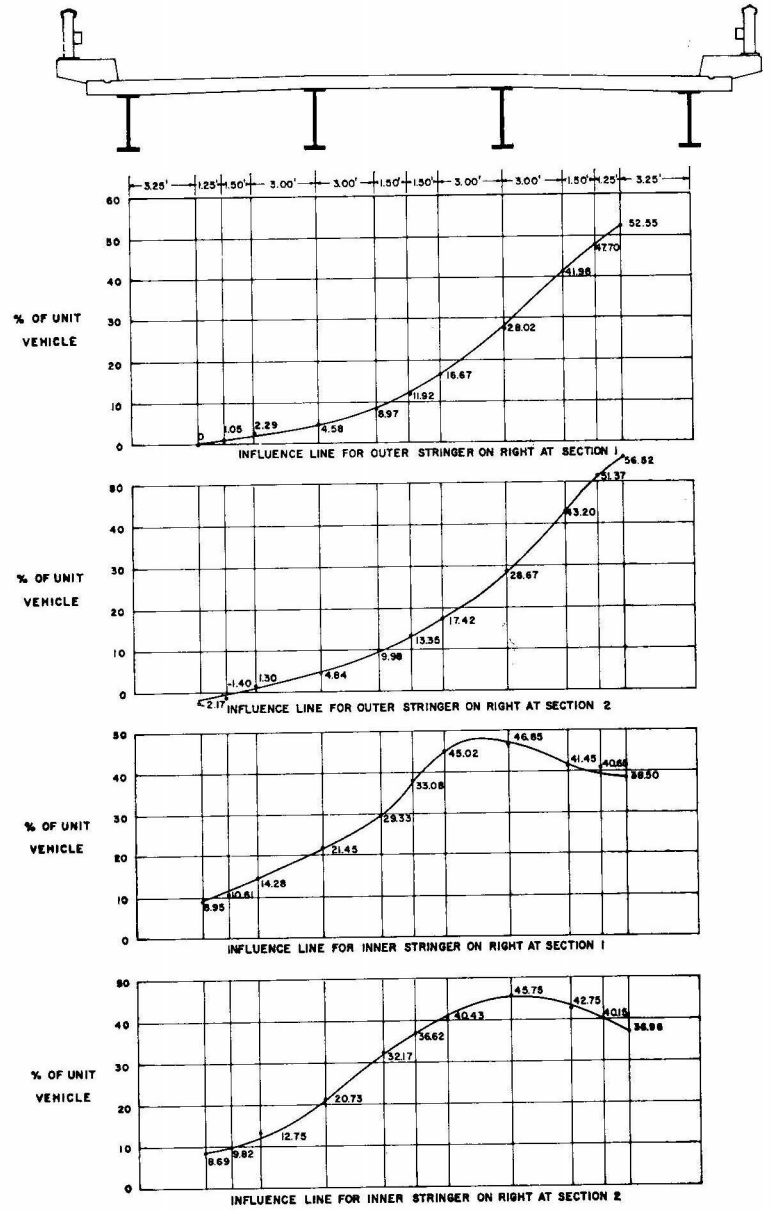

Fig. 55. Influence lines for steel stringer bridge.

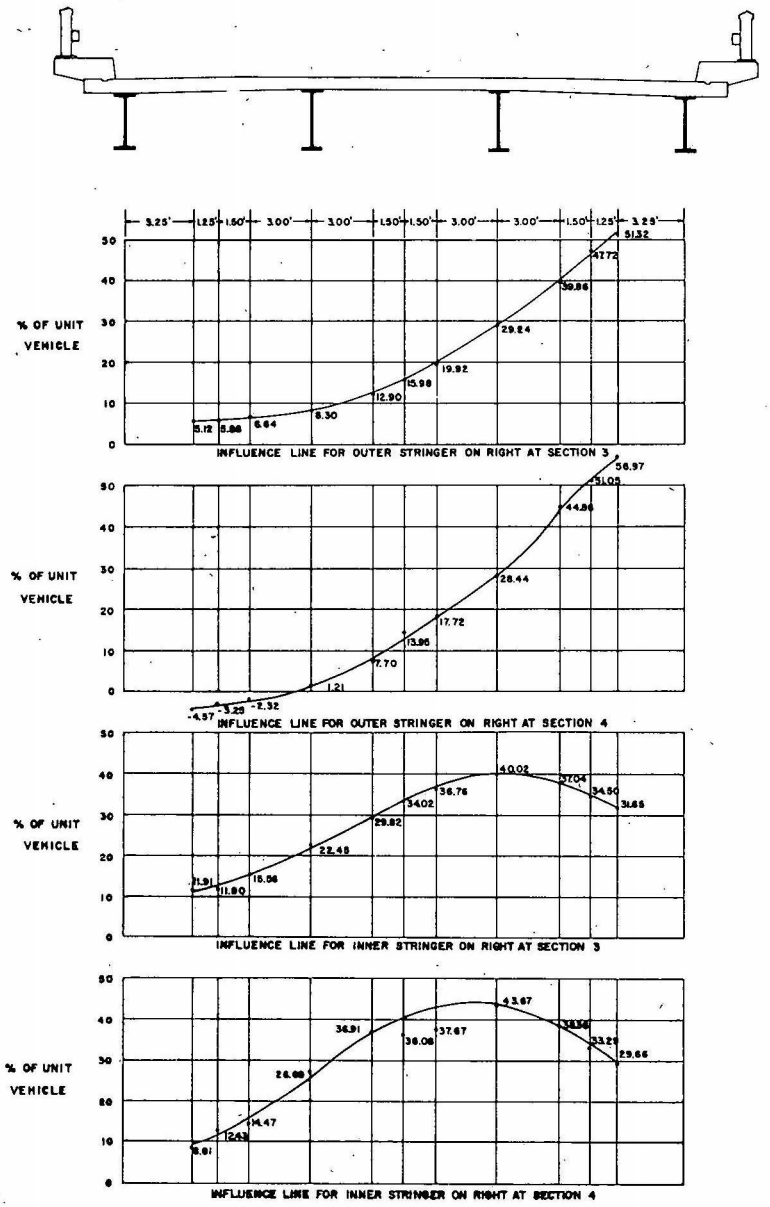

Fig. 55, continued.

ACKNOWLEDGMENTS

Acknowledgment is due to the Iowa Highway Research Board who sponsored this project. Also the cooperation and assistance of Mark Morris, former Director of Highway Research, Neil Welden, Bridge Engineer, and Carl Schach, Engineer of Planning, all of the Iowa Highway Commission, are especially appreciated.

Those undergraduates, especially Dwight Rice and Mel Larsen, who helped in the reduction of more than a mile and a half of experimental strain time records, deserve much praise for their faithful work.

Thanks are also due to Mr. J. N. Dunn, District Manager, of the International Harvester Company and Mr. C. A. Suss, Assistant Manager, for the truck tractor used as a loading vehicle.

SELECTED REFERENCES

1. Biggs, J. M. and Suer, H. S. Vibration measurements of simplespan bridges. Highway Research Board Bulletin 124: 1-15. 1955.
2. Darnley, E. R. The transverse vibrations of beams and the whirling of shafts supported at intermediate points. Lond. Edin. and Dublin Phil. Mag. Ser. 6, 41: 81-96. 1921.
3. Duncan, W. J. Free and forced oscillations of continuous beams: Treatment by the admittance method. Lond. Edin. and Dublin Phil. Mag. Ser. 7, 34: 49-63. 1943.
4. Edgerton, R. C. and Beecroft, G. W. Dynamic studies of two continuous plate-girder bridges. Highway Research Board Bulletin 124: 33-46. 1955.
5. Ford, G. Transverse vibration of a two-span beam under action of a moving constant force. Unpublished Ph. D. Thesis. Stanford, Calif., Stanford University Library. 1950.
6. Foster, G. M. and Oehler, L. T. Vibration and deflection of rolled-beam and plate girder bridges. Highway Research Board Bulletin 124: 79-110. 1955.
7. Goodman, L. E. How we get our present impact specification. (Mimeo.) Illinois Structural Engineering Conference, Urbana, Nov. 12-14, 1952, Proc. 2: 96-107. 1952.
8. Hayes, J. M. and Sbarounis, J. A. Vibration study of three-span continuous I-beam bridge. Highway Research Board Bulletin 124: 47-78. 1955.
9. Hillerborg, A. A study of dynamic influences of moving loads on girders. International Association for Bridge and Structural Engineering Congress. 3: 661-667. 1948.
10. Inglis, C. E. A mathematical treatise on vibration in railway bridges. London, Cambridge University Press. 1934.
11. Jeffcott, H. H. On the vibration of beams under the action of moving loads. Lond. Edin. and Dublin Phil. Mag. Ser. 7, 8: 66-97. 1929.
12. Kryloff, A. N. Über der erzwungen Schwingungen von gleichförmigen elastischen Staben. Mathematische Annalen 61: 211-230. 1905.
13. Looney, T. G. High-speed computer applied to bridge impact. Journal of the Structural Division, Amer. Soc. of Civil Engr. Vol. 84, Paper 1759. September, 1958.
14. Pöschl, T. Über die angenäherte berechnung der schwingzahlen von rahmenträgern. Ingenieur-Archiv 1:469-480. 1929.
15. Prentzas, E. G. Dynamic behavior of two continuous I-beam bridges. Iowa Highway Research Board Bulletin No. 14. August, 1958.
16. Schallenkamp, A. Schwingungen von Tragern bei bewegten lasten. Ingenieur-Archiv 8: 182-198. 1937.
17. Scheffey, C. F. Dynamic load analysis and design of Highway bridges. Highway Research Board Bulletin 124: 16-32. 1955.

Table V. Impact for aluminum stringer bridge at sections I and III for vehicle B.

Run	Velocity (fps)	Impact I_a	Impact $III_{b,e}$	Frequency of vibration (cps)
2W-10	14.1	.094	.198	3.3
2W-20	20.3	.049	.072	4.2
2W-30	35.26	.051	.138	3.3
5W-10	14.98	.10	.11	3.3
5W-12	14.89	.191	.209	3.4
5W-20	25.98	.101	.088	6.0
5W-30	36.2	.169	.102	3.6-8.4
5W-40	37.3	.156	.036	10.0
2E-10	13.42	.054	.202	3.0
2E-20	27.5	.077	.07	5.3
2E-30	42.3	.053	0	4.1
2E-40	45.6	.10	.122	3.5
5E-10	17.05	.05	.179	3.65
5E-20	26.42	.102	.111	6.25
5E-30	39.3	0	.121	3.8
5E-40	49.1	.16	.19	3.3

Table VI. Impact for aluminum stringer bridge at sections II and IV for vehicle B.

Run	Velocity (fps)	Impact II_b	Impact $IV_{b,e}$	Impact $IV_{c,e}$	Frequency of vibration (cps)
2W-10	11.79	0	.091	.025	2.8
2W-20	21.46	.131	.089	.039	5.5
2W-30	34.5	.106	.014	.14	3.7
5W-10	11.59	.03	.041	.042	3.3
5W-20	24.6	.10	.12	.03	5.0
5W-30	35.5	.128	.034	.112	3.8
2E-10	11.38	.058	.072	.025	3.5
2E-20	24.57	.139	.146	.039	5.2
2E-30	34.6	.138	.24	.14	3.2-7.2
5E-10	11.59	.043	.062	.072	2.8
5E-20	22.44	.135	.03	.038	5.0
5E-30	33.9	.032	.106	.088	6.5
5E-40	45.5	.17	.174	.069	3.9

Table VII. Impact for steel stringer bridge at sections I and III for vehicle A.

Run	Velocity (fps)	Impact I_a	Impact III_b	Frequency of vibration (cps)
3N-10	15.3	.092	.008	3.64
3N-20	26.6	.063	.076	6.3
3N-30	41.4	0	.123	3.5
6N-10	14.6	.039	.003	3.8
6N-20	26.6	.015	0	5.9
6N-30	39.8	.04	.003	3.1
6N-40	41.6	0	.061	3.7
3S-10	13.5	.08	.01	3.33
3S-20	26.1	.073	0	5.8
3S-30	39.5	.26	.112	3.3
6S-10	12.4	.018	0	3.7
6S-20	26.1	.052	0	5.6
6S-30	38.0	0	.11	8.6
6S-40	55.5	.04	.118	4.1

Table VIII. Impact for steel stringer bridge at sections II and IV for vehicle A.

Run	Velocity (fps)	Impact II_b	Impact IV_b	Frequency of vibration (cps)
3N-10	14.85	.03	.18	3.7
3N-20	27.66	.045	.102	5.1
3N-30	38.95	.075	.148	4.8
6N-10	13.19	.075	.14	3.85
6N-20	27.19	.039		5.8
6N-30	39.5	.088	.159	3.2
6N-40	51.35	.095	.138	4.1
3S-10	13.44	.058	.056	3.33
3S-20	26.4	.075	.092	7.7
3S-30	38.2	.151	.12	3.2
6S-10	13.25	.021	.125	3.33
6S-20	25.32	.068	.10	6.3
6S-30	41.4	.278	.168	3.45
6S-40	53.3	.443	.228	3.45

Table IX. Impact for steel stringer bridge at sections I and III for vehicle B.

Run	Velocity (fps)	Impact $I_{a,e}$	$I_{a,f}$	$III_{b,e}$	Frequency of vibration (cps)
3N-10	10.2	0	0	0	2.8
3N-20	24.0	.03	.052	.06	5.5
3N-30	33.33	.198	.062	.11	3.3
3N-40	44.1	.056	.087	.145	4.2-2.5
6N-10	11.8	.048	.14	.145	2.9
6N-20	26.54	.049	.042	.058	5.2
6N-30	37.5	.10	.021	.238	3.2
6N-40	43.15	.02	.062	.253	2.1
3S-10	8.51	.0016	0	.041	2.9
3S-20	24.22	.036	.035	.079	5.2
3S-30	42.85	.151	.121	.12	3.1
3S-40	55.55	.123	.083	.152	2.5
6S-10	7.01	.054	.04	.045	2.2
6S-20	23.6	.031	.0375	.05	5.0
6S-30	41.2	.146	.105	.09	3.8
6S-40	51.7	.059	.12	.069	2.3

Table X. Impact for steel stringer bridge at sections II and IV for vehicle B.

Run	Velocity (fps)	Impact $II_{b,e}$	$II_{b,f}$	$IV_{b,e}$	$IV_{b,f}$	Frequency of vibration (cps)
3N-10	15.45	.073	.156	.26	0	3.4
3N-20	26.65	.04	.002			6.7
3N-30	45.0	.039	0	.39	087	3.6
6N-10	12.69	.038	.106	.063	.049	2.8
6N-20	25.0	0	.066	.085	.079	5.5
6N-30	37.5	.095	.088	.19	.003	3.6
3S-10	12.45	0	.038	.122	.10	2.9
3S-20	26.1	.021	.026	.062	.065	5.8
3S-30	40.3	.02	.153	.048	0	3.4
3S-40	55.8	.21	.218	.247	.21	2.5-5.0
6S-10	13.9	.062	.103	.05	.062	3.3
6S-20	25.4	.04	.029	.05	.05	6.2
6S-30	41.0	.096	.115	.062	.135	3.4
6S-40	54.8	.187	.266	.048	.238	2.5

Table XI. Impact for continuous concrete stringer bridge at section I for vehicle A.

Run	Velocity (fps)	Impact I_a	Frequency of vibration (cps)
2N-10	15.83	.018	3.3
2N-20	28.4	.029	8.0-10.0
2N-30	41.4	.048	12.5
5N-10	14.4	.089	3.5
5N-20	29.0	.02	
5N-30	41.4	0	6.4
5N-40	54.0	.03	3.3
2S-10	16.85	.143	3.5
2S-20	28.38	0	5.5
2S-30	40.0	.108	
5S-10	15.9	.058	3.5
5S-20	32.02	.035	4.8
5S-30	41.4	.105	12.0
5S-40	51.15	.006	8.3-12.0

Table XII. Impact for continuous concrete stringer bridge at section II for vehicle A.

Run	Velocity (fps)	Impact II_b	Frequency of vibration (cps)
2N-10	15.0	.131	4.0-9.0
2N-20	26.8	.05	8.0
2N-30	39.4	0	4.5
2N-40	54.5	.10	4.5-9.1
5N-10	14.8	0	4.0-9.0
5N-20	29.6	0	
5N-30	42.0	.054	3.5
5N-40	55.1	.02	4.5-9.0
2S-10	15.4	.109	3.33
2S-20	28.4	.051	
2S-30	38.5	.00	7.7-7.3
2S-40	49.6	.049	4.5-9.0
5S-10	15.75	.10	3.33
5S-20	28.4	.069	8.0
5S-30	41.0	.038	3.8
5S-40	50.0	0	4.5-9.0

Table XIII. Impact for continuous concrete stringer bridge at section III for vehicle A.

Run	Velocity (fps)	Impact III_d	Impact III_b	Frequency of vibration (cps)
2N-10	14.5	.10	.131	4.0-3.33
2N-20	25.56	0	.056	10.0
2N-30	39.1	.119	.078	12.0-17.0
2N-40	51.6	.10	0	9.0-16.7
5N-10	14.6	.046	.091	3.45
5N-20	28.8		.00	
5N-30	41.0	.113	.091	3.8-4.2
5N-40	51.4	.16	0	4.5
2S-10	16.3	.104	.131	
2S-20	24.3		.043	6.1-11.7
2S-30	39.4	0	0	12.0
2S-40	50.4	.122	.10	4.5-9.0
5S-10				
5S-20	30.3	0	0	
5S-30	49.9	.048	.011	4.0-4.5
5S-40	49.68	.071	.011	

Table XIV. Impact for continuous concrete stringer bridge at section IV for vehicle A.

Run	Velocity (fps)	Impact IV_b	Impact IV_c	Frequency of vibration (cps)
2N-10	13.2	0	.02	3.6
2N-20	24.2			3.65
2N-30	42.0	.395	.408	3.75
2N-40	55.0	.51	.50	4.8-8.0
5N-10	12.9	.107	.118	3.7
5N-20	28.8	.088	.093	7.9
5N-30	40.6	.588	.541	3.7
5N-40	54.0	.48	.33	7.8
2S-10	16.5	.02		3.55
2S-20	26.1			3.6
2S-30	39.0	.46	.267	3.7
2S-40	49.6	.29	.243	7.8
5S-10	17.1	.079	.08	3.6
5S-20	29.2	.049		8.3
5S-30	39.4	.559	.437	3.7
5S-40	49.6	.175	.032	7.2